Discovery of New Protein-DNA and Protein-Protein Interactions Associated With Wood Development in *Populus trichocarpa*

Herman Earl Petzold III

Dissertation submitted to the faculty of the Virginia Polytechnic Institute and State University in partial fulfillment of the requirements for the degree of

Doctor of Philosophy

In

Forestry

Amy Brunner, Chair

Eric Beers

Allan Dickerman

Jason Holliday

Gregory Welbaum

September 18th, 2017

Blacksburg, Virginia

Keywords: protein-DNA Interaction, protein-protein interaction, yeast two-hybrid, yeast one-hybrid, secondary cell wall, lignin

Discovery of New Protein-DNA and Protein-Protein Interactions Associated With Wood Development in *Populus trichocarpa*

Herman Earl Petzold III

ABSTRACT

The negative effects from rising carbon levels have created the need to find alternative energy sources that are more carbon neutral. One such alternative energy source is to use the biomass derived from forest trees to fulfill the need for a renewable alternative fuel. Through increased understanding and optimization of regulatory mechanisms that control wood development the potential exists to increase biomass yield. Transcription factors (TFs) are DNA-binding regulatory proteins capable of either activation or repression by binding to a specific region of DNA, normally located in the 5-prime upstream promoter region of the gene. In the first section of this work, six DNA promoters from wood formation-related genes were screened by the Yeast One-Hybrid (Y1H) assay in efforts to identify novel interacting TFs involved in wood formation. The promoters tested belong to genes involved in lignin biosynthesis, programmed cell death, and cambial zone associated TFs. The promoters were screened against a mini-library composed of TFs expressed 4-fold or higher in differentiating xylem vs phloem-cambium. The Y1H results identified PtrRAD1 with interactions involving several of the promoters screened. Further testing of PtrRAD1 by Yeast Two-Hybrid (Y2H) assay identified a protein-protein interaction (PPI) with poplar DIVARACATA RADIALIS INTERACTING FACTOR (DRIF1). PtrDRIF1 was then used in the Y2H assay and formed PPIs with MYB/SANT domain proteins, homeodomain family (HD) TFs, and cytoskeletal-related proteins. In the second section of this work, PPIs involving PtrDRIF1s' interaction partners were further characterized. PtrDRIF1 is composed of two separate domains, an N-terminal MYB/SANT domain that interacted with the MYB/SANT domain containing PtrRAD1 and PtrDIVARICATA-like proteins, and a C-terminal region containing a Domain of Unknown Function 3755 (DUF3755). The DUF3755 domain interacted with HD family members belonging to the ancient WOX clade and Class II KNOX domain TFs. In addition, PtrDRIF1 was able to form a complex between PtrRAD1 and PtrWOX13c in a Y2H bridge assay. PtrDRIF1 may function as a regulatory module linking cambial cell proliferation, lignification, and cell expansion during growth. Combined, these

findings support a role for PtrDRIF1 in regulating aspects of wood formation that may contribute to altering biomass yield.

Discovery of New Protein-DNA and Protein-Protein Interactions Associated with Wood Development in *Populus trichocapa*

Herman Earl Petzold III

GENERAL AUDIENCE ABSTRACT

Trees are unique among plants since they have extremely long life spans and the ability to generate large quantities of woody biomass. The woody biomass derived from forest trees can function to provide renewable energy in the form of biofuels. The process of wood formation is complex and requires coordinated activation of genes involved in multiple metabolic pathways. Transcription factors (TFs) are DNA-binding regulatory proteins capable of either activation or repression by binding to a specific region of DNA. These protein-DNA interactions regulate gene expression during plant growth and development. In this study, new regulators of genes known to be involved in wood formation were identified using the Yeast One-Hybrid (Y1H) assay. One of the proteins identified, PtrRAD1 had not been previously linked to wood formation and was a candidate for further characterization. Further testing of PtrRAD1 by the Yeast Two-Hybrid (Y2H) assay resulted in identification of a protein-protein interaction with *Populus trichocarpa* DIVARICATA RADIALIS INTERACTING FACTOR (DRIF1). PtrDRIF1 was then used in the Y2H assay to identify numerous interacting proteins, in addition to those reported previously in other species. Further characterization of PtrDRIF1, identified an N-terminal region capable of forming interactions with MYB/SANT domain proteins, and C-terminal region that interacted with homeodomain proteins. PtrRAD1, PtrDRIF1, and the homeodomain containing PtrWOX13c were able to form a complex in an Y2H-bridge assay. Combined, these findings support a potential role for PtrDRIF1 in regulating wood polarity, wood formation, and stem cell proliferation.

Acknowledgements

First and foremost, I would like to thank both Dr. Amy Brunner and Dr. Eric Beers for their guidance throughout my research.

I would like to thank my committee members Dr. Allan Dickerman, Dr. Jason Holliday, and Dr. Gregory Welbaum for their support throughout my research.

I would like to express my gratitude to Dr. Chengsong Zhao for his help throughout my research and for his assistance in proofreading my documents. I want to express my gratitiude to Dr. Bidisha Chanda for contributing the confocal microscopy imaging. I want to also thank Stephen Rigoulot for contributing to the confocal microscopy imaging and co-expression data. I would like to also thank Dr. Phoebe Williams her help in formatting my dissertation. I would like to thank Xiaoyan Sheng for her work with poplar transformations and setting up our field trials for poplar transgenics. I would also like to thank Eileen Petzold for her help in proofreading.

I would also like to express my gratitude to the Virginia Tech Department of Forest Resources and Environmental Conservation, and the Translational Plant Sciences program at Virginia Tech for providing a supportive environment to pursue research.

Funding

Chapter II: I would like to thank the Institute for Critical Technology and Applied Sciences (ICTAS) for funding the Yeast One-Hybrid research in Chapter II. This work was also supported by US Department of Energy, grant no. DE-FG02-07ER64449.

Chapter III: This work was supported by US Department of Energy, grant no. DE-FG02-07ER64449.

Attributions

Several colleagues contributed to the writing and research in manuscripts presented in this dissertation.

Chapter II: "Identification of New Protein-DNA Interactions Involved in Wood Development in *Populus trichocarpa*"

The research presented in Chapter II was done by H. Earl Petzold with the contribution of the xylem-cDNA AD-library used in library screens constructed by Dr. Chengsong Zhao.

The Yeast One-Hybrid lignin biosynthesis promoter data and DRIF1 protein-protein interaction network were included as part of the paper "Identification of new protein-protein and protein DNA-interactions linked with wood formation in *Populus trichocarpa*", accepted by Tree Physiology 2017.

The PtrRevoluta promoter Yeast One-Hybrid screen data was published in "The Populus ARBORKNOX1 homeodomain transcription factor regulates woody growth through binding to evolutionarily conserved target genes of diverse function", Published in New Phytologist, 2015.

Chapter III: "DIVARICATA AND RADIALIS INTERACTING FACTOR (DRIF) also interacts with WOX, and KNOX proteins associated with wood formation in *Populus trichocarpa*" submitted to Plant Journal, 2017.

Eric Beers, PhD (Beers Lab, Department of Horticulture Virginia Tech) is current co-principal investigator of the grant that supported this work and contributed editorial comments to the manuscript.

Amy Brunner, PhD (Brunner Lab, Department of Forest Resources and Environmental Conservation, Virginia Tech) is current co-principal investigator of the grant that supported this work and contributed editorial comments to the manuscript.

Bidisha Chanda, PhD (Brunner Lab, Department of Horticulture) is currently working for the USDA and contributed confocal microscopy to the manuscript.

Stephen Rigoulot, (Beers Lab, Department of Horticulture) is a current doctoral student in the Beers laboratory at Virginia Tech, and contributed confocal microscopy and expression data to the manuscript.

Chengsong Zhao, PhD (Beers Lab, Department of Horticulture) is currently a Post-Doctoral Researcher at Virginia Tech in the lab of Dr. Pilot. Dr. Zhao contributed to molecular techniques and vector construction used in the paper.

Table of Content

List of Figures

List of Tables

Table of Abbreviations

AD	Activation Domain
ARK2	ARBORKNOX2
BiFC	Bimolecular Fluorescence Complementation
CCoAOMT	Caffeoyl-CoA O-methyltransferase
DB	DNA Binding Domain
DIV	DIVARICATA
DRIF	DIVARACATA RADIALIS INTERACTING FACTOR
DUF	Domain of Unknown Function
GFP	Green fluorescent protein
GUS	β-Glucoronidase
HCT	Hydroxycinnamoyl-transferase
HD	Homeodomain
KNAT	KNOTTED1-LIKE HOMEOBOX
MYB	Myeloblastosis family
PAL	Phenylalanine ammonia-lyase
PDI	Protein-DNA Interaction
PPI	Protein-Protein Interaction
PCD	Programmed Cell Death
Ptr	*Populus trichocarpa*
RAD	RADIALIS
REV	REVOLUTA
SCW	Secondary Cell Wall
TF	Transcription Factor
Y1H	Yeast One-Hybrid
Y2H	Yeast Two-Hybrid
WOX	WUSCHEL-RELATED HOMEOBOX protein

XCP2	Xylem Cysteine Protease 2

Chapter 1
Literature Review

Wood Formation

Forest Trees are unique among plants since they possess long life spans and the ability to generate large quantities of woody biomass. Secondary growth, also known as wood formation is the radial growth process that occurs in stems after primary (elongating) growth has ceased (Du and Groover 2010). The process of wood formation involves certain sequential developmental events, cell division, cell expansion, secondary cell wall thickening, programmed cell death (PCD), and the formation of heartwood (Plomion et al. 2001; Zhong et al. 2010). Plant vascular tissues mediate the long distance conductance of water and solutes, and provide structural support to plant stems, enabling some trees to grow over 300 feet in height. The vasculature tissues of higher plants consist of xylem, phloem, and the vascular cambium. Xylem and phloem arise from the procambium during primary growth and from the vascular cambium during secondary growth in both stems and roots. The cambium, a lateral meristem located between the xylem and phloem, produces xylem toward the center, and phloem (inner bark) toward the periphery. The cork cambium an additional meristem produces the outer bark (periderm) cells, cork, and phelloderm. Trees utilize xylem for both structural support and the conductance of water. The composition of xylem and the arrangement of cell types determine the physical and structural properties of wood. The xylem consists of vessels for water transport, fibers for support, and parenchyma cells for storage. The two types of water-conducting cells found in xylem are known as tracheids and vessel elements. Together, vessel elements and tracheids are known as tracheary elements (TEs). Tracheary elements lack protoplast at maturity but retain their patterned, thickened secondary cell walls consisting largely of lignin and cellulose (Mauseth 1988). During TE differentiation the cells of the procambium or the vascular cambium become highly active in cellulose and lignin biosynthesis and initiate a cell suicide (PCD) program that ultimately culminates in complete cellular autolysis.

Transcriptional regulation

In order for plant growth and development to occur genes need to be expressed in a specific spatiotemporal manner. Coordinated expression of thousands of genes is required for wood formation to occur. Transcription factors (TFs) are DNA-binding regulatory proteins capable of either activation or repression by binding to a specific region of DNA, normally located in the 5-prime upstream region of the gene. TFs usually contain two distinct domains, the DNA binding domain (DB) and the activation domain (AD). Often TFs are members of larger protein complexes and may lack an AD domain; the activation domain may be contributed by interacting proteins. The DNA binding domain is the region that contains a structural motif that recognizes DNA, usually a specific consensus sequence. The match of the TF to the consensus sequence determines the specificity of binding, and potentially the degree of gene activation. The activation domain is the region of the TF responsible for recruiting the basal transcription machinery, such as RNA polymerase, other TFs and co-activator proteins. Protein-DNA interactions (PDIs) occur between TFs and their target genes, these interactions are the driving force for transcriptional regulation (Vermeirssen et al. 2007). In order for secondary cell wall synthesis to occur coordinated expression between genes making cellulose, xylan, and lignin must take place. In the Arabidopsis genome, approximately 6% of all genes are transcription factors (Riechmann et al. 2000). TFs are divided into families based upon similarities in DB and many of these families have been experimentally linked with cambial activity and wood formation. The NAC, MYB, Homeodomain (HD), and several other TF families are associated with secondary cell wall (SCW) development based on mutant analysis, expressed sequence tags (EST) projects, microarray and RNA-seq data from both Arabidopsis and poplar.

NAC transcription factors

The genome of Arabidopsis contains 105 NAC domain genes, of these 16 are known to be associated with vascular tissue development. (Zhong et al. 2010; Zhong and Ye 2015; Zhou et al. 2014) In *Populus trichocarpa* the NAC family has undergone expansion largely as a result of a whole genome duplication event, resulting in 160 NAC TFs. NAC derives from the No Apical Meristem (NAM) from petunia and the ATAF1/ATAF2 and Cup-shaped Cotyledon (CUC2) from Arabidopsis.(Aida et al. 1997). Reverse genetics experiments utilizing knockouts or ectopic expression of NAC transcription factors have shown this family to be involved in SCW synthesis during wood development in Arabidopsis. Specifically, overexpression of the NAC

transcription factors NST1, NST2 (Mitsuda et al. 2005) and VND7 and VND6 (Kubo et al. 2005) led to ectopic differentiation of TE like cells in Arabidopsis. The ectopic expression of VND7 and NST1 also resulted in expression of associated marker genes for SCW implicating these NACs as regulators of wood development. The results from the aforementioned ectopic expression studies demonstrate SCW synthesis can be manipulated by altering the expression pattern of one or just a few NAC transcription factors. The current view is that NAC TFs function as master regulators activating or in some cases suppressing other TFs, most likely MYBs, thus achieving the regulation of secondary cell wall synthesis (Zhong et al. 2007b).

MYB transcription factors

The MYB gene family is named for the v-MYB oncogene first discovered in chickens, and responsible for avian myeloblastosis (Lipsick 1996). MYB proteins are characterized by an N-terminal highly conserved DNA binding domain consisting of imperfect repeats of an approximately 50-amino acid region. The 50-amino acid repeats yield helix-loop-helix secondary structure that contain three TRP residues, these are responsible for binding to sequence specific regions of target DNA sequences (Lipsick 1996; Wilkins et al. 2009). The C-terminal region often contains the activation domain and is the most highly divergent region among MYB proteins. MYB DNA binding domains contain up to three tandem repeats of the MYB motif, these are designated as R1 (MYB1R), R2 (R2R3-MYB), and R3 (3R-MYB) (Stracke et al. 2001). Most common in plants are the R2R3-MYB genes with Arabidopsis containing 126 while only 5 3R-MYB genes are present. MYB TFs are involved in many plant-specific processes, among these are the regulation of specific types of phenylpropanoid metabolism, such as regulation of flavonoids (Stracke et al. 2007), anthocyanin (Teng et al. 2005), and lignins (Patzlaff et al. 2003a; Patzlaff et al. 2003b). The poplar MYB family of TFs contains almost 300 members and nearly 50% have been associated with secondary growth (Dharmawardhana et al. 2010). NAC and MYB family TFs function as master regulators in SCW development, but reverse genetics experiment have shown the involvement of other TF families. Reviewed by (Demura and Fukuda 2007; Nakano et al. 2015; Du and Groover 2010)

Homeodomain, HD-Zip III, WRKY, bHLH, and bZIP

TFs belonging to several other families have been associated with vascular development, among these are members of the KNOX I and KNOX II classes of HD TFs have been associated with a variety of different SCW- related mutations. The class I KNOX TFs ARBORKNOXI (ARKI)

and ARBORKNOXII (ARKII) are poplar orthologs of SHOOT-MERISTEMLESS (STM) and BREVIPEDICELLUS (BP) respectively from Arabidopsis; both are involved in vascular development (Groover et al. 2006; Du et al. 2009). The class II KNOX TF PotriKNAT7 is a functional homolog of KNAT7 from Arabidopsis. KNAT7 has been found to act as a repressor of lignification, as evidenced from upregulation of lignin associated genes in *knat7* knockout lines, and *irregular xylem phenotypes* (Li et al. 2012a). WUSCHEL-related homeobox (WOX) proteins are known to be involved in numerous developmental processes in plants involving stem cell maintenance in roots and shoots. Ectopic expression of WOX13 in Arabidopsis resulted in decreased lignification in the valve margin and *wox13* loss-of-function yielded an increase in lignin in the valve margin (Romera-Branchat et al. 2013).

The HD-Zip III TFs in Arabidopsis and poplar are a small family of TFs involved in the proper maintenance and development of vascular tissues. HD-Zip III TFs members are regulated by microRNA 165/166 (Zhong and Ye 2007); the mis-expression of these TF's can alter the polarity of the vasculature (fully reviewed by (Du and Wang 2015). Indeed, in the case of POPREVOLUTA (REV) and POPCORONA, a microRNA resistant transcript activates the SCW pathway and in the case of REV produces vascular tissue polarity abnormalities in trees (Robischon et al. 2011a; Du et al. 2011). WRKY TFs are associated with SCW repression based upon ectopic expression of PtrWRKY19 results in an increase in pith parenchyma cells thus inhibiting SCW formation in the pith (Yang et al. 2016). Basic helix-loop-helix (bHLH) TFs in Arabidopsis such as Lonesome Highway (LHW) and Lonesome Highway-like (LHL3) function early in vascular development. LHW and LHL3 are activated downstream of auxin to establish the vasculature in young roots (Ohashi-Ito et al. 2013; Ohashi-Ito and Bergmann 2007).

Lignin synthesis

The secondary cell walls of wood are composed primarily of cellulose and lignin polymers, making it essential to understand the transcriptional regulators controlling wood biosynthesis. Lignin is the second most abundant bio-polymer on earth, and is an important sink for environmental carbon. Lignin synthesis is not only limited to SCW development, but also occurs during stresses such as wounding, pathogen infection, and metabolic stress. Cell wall polysaccharides are protected against microbial degradation by the lignin in the cell walls, and the hydrophobic nature of lignin is necessary for plant cells to conduct water. Consequently, the

recalcitrance of the cell wall due to lignin makes digestion a limiting factor in wood pulping and the conversion of cellulosic biomass for fuels (Stewart et al. 2009; Kumar et al. 2016).

Regulation of lignin biosynthesis has been tied to numerous MYB TFs in several plant lineages. In Arabidopsis AtMYB4 (Jin et al. 2000), AtMYB83 (McCarthy et al. 2009), AtMYB46 (Zhong et al. 2007a), AtMYB58, and AtMYB63 (Fornale et al. 2010) have all been shown to be involved in regulation of enzymes in the lignin biosynthetic pathway. In poplar PttMYB21 (Karpinska et al. 2004), PtrMYB3, and PtrMYB20 (McCarthy et al. 2010) were shown to activate the biosynthetic pathways of cellulose, xylan, and lignin. The loss-of-function phenotype for AtMYB46/AtMYB83 double knockout plants could be rescued by the orthologous poplar proteins PtrMYB3, and PtrMYB20. PtrMYB2 and PtrMYB21 have not been characterized, but potentially these two proteins are also functional orthologs of AtMYB46 and AtMYB83. The Eucalyptus MYBs EgMYB2(Goicoechea et al. 2005) and EgMYB1(Legay et al. 2010) are involved in the lignin biosynthesis pathway and have been shown to interact with *cis* elements known as AC elements. AC elements are those containing concensus motifs with common regions rich in the adenine (A) and cytosine (C) nucleotides. Examples of AC motifs are CCAACC (MYBPZM) and CCACCAACCCCC (ACIIPVPAL2) many of the lignin synthesis promoters in poplar have these or very similar motifs present. (Shi et al. 2010)

Arabidopsis as a model system

Arabidopsis thaliana became the first plant genome sequenced in December 2000 and allowed a fascinating view into the genomic structure of a flowering plant (Arabidopsis Genome 2000). Historically the first Arabidopsis non-taxonomy related research occurred in 1873 but the widespread use as a model plant did not occur until the 1980's (Meyerowitz 2001). Arabidopsis possesses many qualities making it an excellent choice for a model plant, short generation time, small size, small genome, fecundity, and although selfing compatible outcrosses are possible. Numerous investigations on secondary growth and SCW deposition in Arabidopsis have yielded much of our current understanding of the molecular mechanisms at work in wood development (Levyadun 1994; Chaffey et al. 2002; Nieminen et al. 2004). Transcriptional regulation across tissues has also been studied in Arabidopsis and these findings give unique insight into the regulation of SCW deposition- related genes during wood development (Yamaguchi et al. 2011; Zhao et al. 2005).

Poplar as a model system

Despite the many contributions from the herbaceous model plant *Arabidopsis thaliana* towards our current understanding of wood development, a model tree is needed. Although, wood from the Arabidopsis hypocotyl is similar in composition to that found in angiosperm trees, deficiencies in rays and ray parenchyma like cells illustrate that not all aspects of wood formation can be modeled in an herbaceous annual (Zhao et al. 2005; Zhang et al. 2011; Chaffey et al. 2002). These differences combined with the ability to study seasonal growth and dormancy, need for a model tree for research. Members of the genus *Populus* are found worldwide and are comprised of about 30 species that contain aspens, balsam poplars, and cottonwoods. Poplars are widely distributed across the northern hemisphere. The first EST projects were first completed on aspen in 1998 (Sterky et al. 1998) producing 5,692 ESTs, since then interest in poplar research has increased greatly. The selection of *Populus* as the model tree has been due to many factors; relatively small genome size, rapid growth, ease of genetic manipulation, relatively simple transformation with *A. tumafaciens*, readily available quantitative trait loci (QTL) for mapping, ability to be propagated by tissue culture, and the economic importance of wood products derived from poplar (Tuskan et al. 2006). *Populus* and *Arabidopsis* both belong to the Malvidae clade of angiosperm phylogeny making them excellent candidates for comparisons of gene function between species. The poplar genome was the first tree genome to be sequenced in 2006 and a wealth of genetic information was made available (Tuskan et al. 2006) dealing with genome organization, duplication events, and both similarities and differences to Arabidopsis.

Gene expression during the transition from primary to secondary xylem in trees is of great interest for improving wood quality and growth rate (Dharmawardhana et al. 2010). Consequently, the use of microarray data has been instrumental in showing differences in gene expression level. The dataset from the transcriptomics paper by Rogers-Melnick et al., 2012 allows comparisons to be made with the whole-genome NimbleGen oligonucleotide microarray for transcript profiling in poplar tissue types and developmental stages. Fourteen tissue types were profiled, including xylem, phloem-cambium, leaf, root, shoot apex, female catkin, male catkin, and germinating seedling. In *Populus,* genome duplications have resulted in an expansion of gene families involved in wood formation (Tuskan et al. 2006). The synthesis of

cellulose and lignin for secondary cell wall formation requires the coordinated expression of numerous genes, current research in both Arabidopsis and poplar indicate the involvement of both MYB and NAC transcription factors in this process (McCarthy et al. 2010; McCarthy et al. 2009; Kubo et al. 2005). The poplar microarray gene chip data shows 10 NAC TFs and 20 MYB TFs to be expressed 4-fold or higher in xylem versus phloem/cambium, these TFs are potentially involved in regulating important aspects of SCW formation. Representatives from other TF families are also up regulated 4-fold or greater in xylem, including Auxin Response Factors (ARFs), Aux/IAA, B3, Basic Leucine Zipper, Homeodomain, WRKY, and Zinc Finger TFs.
In this dissertation, novel proteins implicated in wood formation were identified through the use of the Yeast One-Hybrid (Y1H) system. TFs interacting with promoters linked to wood formation will be further characterized using the Yeast Two-Hybrid (Y2H) system. Protein-protein interactions (PPIs) that occur between TFs have the potential to lead to a better understanding of the basic mechanisms involved in wood formation. Common reverse genetics techniques were used to alter gene-expression in order to evaluate plant growth and wood quality. Here, a "prey" cDNA library isolated from *P. trichocarpa* in a tissue specific manner was used to screen for interactions using wood formation related genes as "baits".

Yeast Two-Hybrid

The first Y2H system was based on the native GAL4 protein and was developed in 1989 by Fields and Song (Fields and Song 1989) and works for non-trans activating proteins. Since 1989 the Y2H has become the most popular method for identifying protein-protein interactions (PPIs). The Y2H is a vector based system where one vector contains the GAL4 DNA binding domain (DB $^{1\text{-}147}$) from the GAL4 protein in *Saccharomyces cerivisiae* and another vector contains the GAL4 activation domain (AD $^{768\text{-}881}$) from GAL4 in *S. cerivisiae*. Proteins of interest can be cloned as fusion proteins into the DB or AD vector, and if physical interactions were to occur yeast colony growth will result on media lacking essential amino acids. To date, the Y2H has been utilized to identify specific interactions and form interaction networks in a broad range of organisms including *A.thaliana* (Dortay et al. 2008), *C.elegans* (Li et al. 2004), and *H. sapiens* (Rual et al. 2005). Recent advances in cloning using Gateway technology have enabled increased screening of PPIs in Y2H assays using binary matrix type approaches as well as library screens against AD libraries.

Yeast One-Hybrid

The Y1H is a variation on the Y2H, each being based on functional domains of transcription factors arising in eukaryotic organisms. The Y1H enables researchers to identify and characterize proteins that bind to specific *cis* DNA sequences located in the upstream promoter region of genes. The Gateway-Compatible Y1H system allows for integration of the promoter sequence containing *cis* elements into the genome of yeast. DNA baits are fused to the reporter genes, *His3* and *lacZ,* the DNA bait::reporter constructs are then sequentially integrated into the genome of the host yeast strain. DNA baits must be tested for the ability to drive reporter gene expression in the absence of an exogenous prey protein (self-activation). The severity of self-activation can be titrated out by the addition of 3-amino-triazole (3-AT) into the drop-out media, thus allowing for differences in growth between background and interacting "prey" colonies. In our case, the "prey" refers to hybrid proteins from *Populus trichocarpa* xylem tissue fused to a heterologous transcription activation domain. An AD library, mini-library, or specific AD proteins can be screened by this method in a targeted screen. Utilization of the Y1H assay allows for detecting physical interactions between both activators and repressors and their DNA targets. The Y1H system has been successfully utilized in test for transcriptional activators and repressors in numerous species including *C. elegans* (Deplancke et al. 2006a), *A. thaliana* (Brady et al. 2011), and *D. melanogaster* (Kalay et al. 2016).

References

Aida M, Ishida T, Fukaki H, Fujisawa H, Tasaka M (1997) Genes involved in organ separation in Arabidopsis: an analysis of the cup-shaped cotyledon mutant. Plant Cell 9 (6):841-857. doi:10.1105/tpc.9.6.8419/6/841 [pii]

Arabidopsis Genome I (2000) Analysis of the genome sequence of the flowering plant Arabidopsis thaliana. Nature 408 (6814):796-815. doi:10.1038/35048692

Brady SM, Zhang L, Megraw M, Martinez NJ, Jiang E, Yi CS, Liu W, Zeng A, Taylor-Teeples M, Kim D, Ahnert S, Ohler U, Ware D, Walhout AJ, Benfey PN (2011) A stele-enriched gene regulatory network in the Arabidopsis root. Mol Syst Biol 7:459. doi:10.1038/msb.2010.114

Chaffey N, Cholewa E, Regan S, Sundberg B (2002) Secondary xylem development in Arabidopsis: a model for wood formation. Physiol Plant 114 (4):594-600

Demura T, Fukuda H (2007) Transcriptional regulation in wood formation. Trends in plant science 12 (2):64-70. doi:10.1016/j.tplants.2006.12.006

Deplancke B, Mukhopadhyay A, Ao W, Elewa AM, Grove CA, Martinez NJ, Sequerra R, Doucette-Stamm L, Reece-Hoyes JS, Hope IA, Tissenbaum HA, Mango SE, Walhout AJ (2006) A gene-centered C. elegans protein-DNA interaction network. Cell 125 (6):1193-1205. doi:10.1016/j.cell.2006.04.038

Dharmawardhana P, Brunner AM, Strauss SH (2010) Genome-wide transcriptome analysis of the transition from primary to secondary stem development in Populus trichocarpa. Bmc Genomics 11. doi:Artn 15010.1186/1471-2164-11-150

Dortay H, Gruhn N, Pfeifer A, Schwerdtner M, Schmulling T, Heyl A (2008) Toward an interaction map of the two-component signaling pathway of Arabidopsis thaliana. J Proteome Res 7 (9):3649-3660. doi:10.1021/pr0703831

Du J, Groover A (2010) Transcriptional regulation of secondary growth and wood formation. J Integr Plant Biol 52 (1):17-27. doi:10.1111/j.1744-7909.2010.00901.x

Du J, Mansfield SD, Groover AT (2009) The Populus homeobox gene ARBORKNOX2 regulates cell differentiation during secondary growth. Plant J 60 (6):1000-1014. doi:10.1111/j.1365-313X.2009.04017.x

Du J, Miura E, Robischon M, Martinez C, Groover A (2011) The Populus Class III HD ZIP transcription factor POPCORONA affects cell differentiation during secondary growth of woody stems. PLoS One 6 (2):e17458. doi:10.1371/journal.pone.0017458

Du Q, Wang H (2015) The role of HD-ZIP III transcription factors and miR165/166 in vascular development and secondary cell wall formation. Plant Signal Behav 10 (10):e1078955. doi:10.1080/15592324.2015.1078955

Fields S, Song O (1989) A novel genetic system to detect protein-protein interactions. Nature 340 (6230):245-246. doi:10.1038/340245a0

Fornale S, Shi X, Chai C, Encina A, Irar S, Capellades M, Fuguet E, Torres JL, Rovira P, Puigdomenech P, Rigau J, Grotewold E, Gray J, Caparros-Ruiz D (2010) ZmMYB31 directly represses maize lignin genes and redirects the phenylpropanoid metabolic flux. Plant J 64 (4):633-644. doi:10.1111/j.1365-313X.2010.04363.x

Goicoechea M, Lacombe E, Legay S, Mihaljevic S, Rech P, Jauneau A, Lapierre C, Pollet B, Verhaegen D, Chaubet-Gigot N, Grima-Pettenati J (2005) EgMYB2, a new transcriptional activator from Eucalyptus xylem, regulates secondary cell wall formation and lignin biosynthesis. Plant J 43 (4):553-567. doi:TPJ2480 [pii]10.1111/j.1365-313X.2005.02480.x

Groover AT, Mansfield SD, DiFazio SP, Dupper G, Fontana JR, Millar R, Wang Y (2006) The Populus homeobox gene ARBORKNOX1 reveals overlapping mechanisms regulating the shoot apical meristem and the vascular cambium. Plant Mol Biol 61 (6):917-932. doi:10.1007/s11103-006-0059-y

Jin H, Cominelli E, Bailey P, Parr A, Mehrtens F, Jones J, Tonelli C, Weisshaar B, Martin C (2000) Transcriptional repression by AtMYB4 controls production of UV-protecting sunscreens in Arabidopsis. EMBO J 19 (22):6150-6161. doi:10.1093/emboj/19.22.6150

Kalay G, Lusk R, Dome M, Hens K, Deplancke B, Wittkopp PJ (2016) Potential Direct Regulators of the Drosophila yellow Gene Identified by Yeast One-Hybrid and RNAi Screens. G3 (Bethesda) 6 (10):3419-3430. doi:10.1534/g3.116.032607

Karpinska B, Karlsson M, Srivastava M, Stenberg A, Schrader J, Sterky F, Bhalerao R, Wingsle G (2004) MYB transcription factors are differentially expressed and regulated during secondary vascular tissue development in hybrid aspen. Plant Mol Biol 56 (2):255-270. doi:DO00003354 [pii]10.1007/s11103-004-3354-5

Kubo M, Udagawa M, Nishikubo N, Horiguchi G, Yamaguchi M, Ito J, Mimura T, Fukuda H, Demura T (2005) Transcription switches for protoxylem and metaxylem vessel formation. Genes Dev 19 (16):1855-1860. doi:19/16/1855 [pii]10.1101/gad.1331305

Kumar M, Campbell L, Turner S (2016) Secondary cell walls: biosynthesis and manipulation. J Exp Bot 67 (2):515-531. doi:10.1093/jxb/erv533

Legay S, Sivadon P, Blervacq AS, Pavy N, Baghdady A, Tremblay L, Levasseur C, Ladouce N, Lapierre C, Seguin A, Hawkins S, Mackay J, Grima-Pettenati J (2010) EgMYB1, an R2R3 MYB transcription factor from eucalyptus negatively regulates secondary cell wall formation in Arabidopsis and poplar. New Phytol 188 (3):774-786. doi:10.1111/j.1469-8137.2010.03432.x

Levyadun S (1994) Induction of Sclereid Differentiation in the Pith of Arabidopsis-Thaliana (L) Heynh. J Exp Bot 45 (281):1845-1849. doi:DOI 10.1093/jxb/45.12.1845

Li E, Bhargava A, Qiang W, Friedmann MC, Forneris N, Savidge RA, Johnson LA, Mansfield SD, Ellis BE, Douglas CJ (2012) The Class II KNOX gene KNAT7 negatively regulates secondary wall formation in Arabidopsis and is functionally conserved in Populus. The New phytologist 194 (1):102-115. doi:10.1111/j.1469-8137.2011.04016.x

Li S, Armstrong CM, Bertin N, Ge H, Milstein S, Boxem M, Vidalain PO, Han JD, Chesneau A, Hao T, Goldberg DS, Li N, Martinez M, Rual JF, Lamesch P, Xu L, Tewari M, Wong SL, Zhang LV, Berriz GF, Jacotot L, Vaglio P, Reboul J, Hirozane-Kishikawa T, Li Q, Gabel HW, Elewa A, Baumgartner B, Rose DJ, Yu H, Bosak S, Sequerra R, Fraser A, Mango SE, Saxton WM, Strome S, Van Den Heuvel S, Piano F, Vandenhaute J, Sardet C, Gerstein M, Doucette-Stamm L, Gunsalus KC, Harper JW, Cusick ME, Roth FP, Hill DE, Vidal M (2004) A map of the interactome network of the metazoan C. elegans. Science 303 (5657):540-543. doi:10.1126/science.1091403

Lipsick JS (1996) One billion years of Myb. Oncogene 13 (2):223-235

Mauseth J (1988) Plant Anatomy. The Benjamin/Cummings Publish Company Menlo Park, CA

McCarthy RL, Zhong R, Fowler S, Lyskowski D, Piyasena H, Carleton K, Spicer C, Ye ZH (2010) The poplar MYB transcription factors, PtrMYB3 and PtrMYB20, are involved in the regulation of secondary wall biosynthesis. Plant & cell physiology 51 (6):1084-1090. doi:10.1093/pcp/pcq064

McCarthy RL, Zhong R, Ye ZH (2009) MYB83 is a direct target of SND1 and acts redundantly with MYB46 in the regulation of secondary cell wall biosynthesis in Arabidopsis. Plant & cell physiology 50 (11):1950-1964. doi:10.1093/pcp/pcp139

Meyerowitz EM (2001) Prehistory and history of Arabidopsis research. Plant physiology 125 (1):15-19

Mitsuda N, Seki M, Shinozaki K, Ohme-Takagi M (2005) The NAC transcription factors NST1 and NST2 of Arabidopsis regulate secondary wall thickenings and are required for anther dehiscence. Plant Cell 17 (11):2993-3006. doi:10.1105/tpc.105.036004

Nakano Y, Yamaguchi M, Endo H, Rejab NA, Ohtani M (2015) NAC-MYB-based transcriptional regulation of secondary cell wall biosynthesis in land plants. Front Plant Sci 6:288. doi:10.3389/fpls.2015.00288

Nieminen KM, Kauppinen L, Helariutta Y (2004) A weed for wood? Arabidopsis as a genetic model for xylem development. Plant physiology 135 (2):653-659. doi:10.1104/pp.104.040212

Ohashi-Ito K, Bergmann DC (2007) Regulation of the Arabidopsis root vascular initial population by LONESOME HIGHWAY. Development 134 (16):2959-2968. doi:10.1242/dev.006296

Ohashi-Ito K, Matsukawa M, Fukuda H (2013) An atypical bHLH transcription factor regulates early xylem development downstream of auxin. Plant Cell Physiol 54 (3):398-405. doi:10.1093/pcp/pct013

Patzlaff A, McInnis S, Courtenay A, Surman C, Newman LJ, Smith C, Bevan MW, Mansfield S, Whetten RW, Sederoff RR, Campbell MM (2003a) Characterisation of a pine MYB that regulates lignification. Plant J 36 (6):743-754. doi:1916 [pii]

Patzlaff A, Newman LJ, Dubos C, Whetten RW, Smith C, McInnis S, Bevan MW, Sederoff RR, Campbell MM (2003b) Characterisation of Pt MYB1, an R2R3-MYB from pine xylem. Plant Mol Biol 53 (4):597-608. doi:10.1023/B:PLAN.0000019066.07933.d65255410 [pii]

Plomion C, Leprovost G, Stokes A (2001) Wood formation in trees. Plant Physiol 127 (4):1513-1523

Riechmann JL, Heard J, Martin G, Reuber L, Jiang C, Keddie J, Adam L, Pineda O, Ratcliffe OJ, Samaha RR, Creelman R, Pilgrim M, Broun P, Zhang JZ, Ghandehari D, Sherman BK, Yu G (2000) Arabidopsis transcription factors: genome-wide comparative analysis among eukaryotes. Science 290 (5499):2105-2110. doi:9054 [pii]

Robischon M, Du J, Miura E, Groover A (2011) The Populus class III HD ZIP, popREVOLUTA, influences cambium initiation and patterning of woody stems. Plant physiology 155 (3):1214-1225. doi:10.1104/pp.110.167007

Romera-Branchat M, Ripoll JJ, Yanofsky MF, Pelaz S (2013) The WOX13 homeobox gene promotes replum formation in the Arabidopsis thaliana fruit. Plant J 73 (1):37-49. doi:10.1111/tpj.12010

Rual JF, Venkatesan K, Hao T, Hirozane-Kishikawa T, Dricot A, Li N, Berriz GF, Gibbons FD, Dreze M, Ayivi-Guedehoussou N, Klitgord N, Simon C, Boxem M, Milstein S, Rosenberg J, Goldberg DS, Zhang LV, Wong SL, Franklin G, Li S, Albala JS, Lim J, Fraughton C, Llamosas E, Cevik S, Bex C, Lamesch P, Sikorski RS, Vandenhaute J, Zoghbi HY, Smolyar A, Bosak S, Sequerra R, Doucette-Stamm L, Cusick ME, Hill DE, Roth FP, Vidal M (2005) Towards a proteome-scale map of the human protein-protein interaction network. Nature 437 (7062):1173-1178. doi:10.1038/nature04209

Shi R, Sun YH, Li Q, Heber S, Sederoff R, Chiang VL (2010) Towards a systems approach for lignin biosynthesis in Populus trichocarpa: transcript abundance and specificity of the monolignol biosynthetic genes. Plant Cell Physiol 51 (1):144-163. doi:pcp175 [pii] 10.1093/pcp/pcp175

Sterky F, Regan S, Karlsson J, Hertzberg M, Rohde A, Holmberg A, Amini B, Bhalerao R, Larsson M, Villarroel R, Van Montagu M, Sandberg G, Olsson O, Teeri TT, Boerjan W, Gustafsson P, Uhlen M, Sundberg B, Lundeberg J (1998) Gene discovery in the wood-forming tissues of poplar: Analysis of 5,692 expressed sequence tags. P Natl Acad Sci USA 95 (22):13330-13335. doi:DOI 10.1073/pnas.95.22.13330

Stewart JJ, Akiyama T, Chapple C, Ralph J, Mansfield SD (2009) The effects on lignin structure of overexpression of ferulate 5-hydroxylase in hybrid poplar. Plant physiology 150 (2):621-635. doi:10.1104/pp.109.137059

Stracke R, Ishihara H, Huep G, Barsch A, Mehrtens F, Niehaus K, Weisshaar B (2007) Differential regulation of closely related R2R3-MYB transcription factors controls flavonol accumulation in different parts of the Arabidopsis thaliana seedling. Plant J 50 (4):660-677. doi:TPJ3078 [pii] 10.1111/j.1365-313X.2007.03078.x

Stracke R, Werber M, Weisshaar B (2001) The R2R3-MYB gene family in Arabidopsis thaliana. Curr Opin Plant Biol 4 (5):447-456. doi:S1369-5266(00)00199-0 [pii]

Teng S, Keurentjes J, Bentsink L, Koornneef M, Smeekens S (2005) Sucrose-specific induction of anthocyanin biosynthesis in Arabidopsis requires the MYB75/PAP1 gene. Plant Physiol 139 (4):1840-1852. doi:pp.105.066688 [pii] 10.1104/pp.105.066688

Tuskan GA, Difazio S, Jansson S, Bohlmann J, Grigoriev I, Hellsten U, Putnam N, Ralph S, Rombauts S, Salamov A, Schein J, Sterck L, Aerts A, Bhalerao RR, Bhalerao RP, Blaudez D, Boerjan W, Brun A, Brunner A, Busov V, Campbell M, Carlson J, Chalot M, Chapman J, Chen GL, Cooper D, Coutinho PM, Couturier J, Covert S, Cronk Q, Cunningham R, Davis J, Degroeve S, Dejardin A, Depamphilis C, Detter J, Dirks B, Dubchak I, Duplessis S, Ehlting J, Ellis B, Gendler K, Goodstein D, Gribskov M, Grimwood J, Groover A, Gunter L, Hamberger B, Heinze B, Helariutta Y, Henrissat B, Holligan D, Holt R, Huang W, Islam-Faridi N, Jones S, Jones-Rhoades M, Jorgensen R, Joshi C, Kangasjarvi J, Karlsson J, Kelleher C, Kirkpatrick R, Kirst M, Kohler A, Kalluri U, Larimer F, Leebens-Mack J, Leple JC, Locascio P, Lou Y, Lucas S, Martin F, Montanini B, Napoli C, Nelson DR, Nelson C, Nieminen K, Nilsson O, Pereda V, Peter G, Philippe R, Pilate G, Poliakov A, Razumovskaya J, Richardson P, Rinaldi C, Ritland K, Rouze P, Ryaboy D, Schmutz J, Schrader J, Segerman B, Shin H, Siddiqui A, Sterky F, Terry A, Tsai CJ, Uberbacher E, Unneberg P, Vahala J, Wall K, Wessler S, Yang G, Yin T, Douglas C, Marra M, Sandberg G, Van de Peer Y, Rokhsar D (2006) The genome of black cottonwood, Populus trichocarpa (Torr. & Gray). Science 313 (5793):1596-1604. doi:10.1126/science.1128691

Vermeirssen V, Barrasa MI, Hidalgo CA, Babon JA, Sequerra R, Doucette-Stamm L, Barabasi AL, Walhout AJ (2007) Transcription factor modularity in a gene-centered C. elegans core neuronal protein-DNA interaction network. Genome research 17 (7):1061-1071. doi:10.1101/gr.6148107

Wilkins O, Nahal H, Foong J, Provart NJ, Campbell MM (2009) Expansion and diversification of the Populus R2R3-MYB family of transcription factors. Plant Physiol 149 (2):981-993. doi:pp.108.132795 [pii] 10.1104/pp.108.132795

Yamaguchi M, Mitsuda N, Ohtani M, Ohme-Takagi M, Kato K, Demura T (2011) VASCULAR-RELATED NAC-DOMAIN7 directly regulates the expression of a broad range of genes for xylem vessel formation. Plant J 66 (4):579-590. doi:10.1111/j.1365-313X.2011.04514.x

Yang L, Zhao X, Yang F, Fan D, Jiang Y, Luo K (2016) PtrWRKY19, a novel WRKY transcription factor, contributes to the regulation of pith secondary wall formation in Populus trichocarpa. Sci Rep 6:18643. doi:10.1038/srep18643

Zhang J, Elo A, Helariutta Y (2011) Arabidopsis as a model for wood formation. Curr Opin Biotechnol 22 (2):293-299. doi:10.1016/j.copbio.2010.11.008

Zhao C, Avci U, Grant EH, Haigler CH, Beers EP (2008) XND1, a member of the NAC domain family in Arabidopsis thaliana, negatively regulates lignocellulose synthesis and programmed cell death in xylem. Plant J 53 (3):425-436. doi:TPJ3350 [pii] 10.1111/j.1365-313X.2007.03350.x

Zhao C, Craig JC, Petzold HE, Dickerman AW, Beers EP (2005a) The xylem and phloem transcriptomes from secondary tissues of the Arabidopsis root-hypocotyl. Plant Physiol 138 (2):803-818. doi:pp.105.060202 [pii]10.1104/pp.105.060202

Zhong R, Lee C, Ye ZH (2010) Functional characterization of poplar wood-associated NAC domain transcription factors. Plant physiology 152 (2):1044-1055. doi:10.1104/pp.109.148270

Zhong R, Richardson EA, Ye ZH (2007a) The MYB46 transcription factor is a direct target of SND1 and regulates secondary wall biosynthesis in Arabidopsis. The Plant cell 19 (9):2776-2792. doi:10.1105/tpc.107.053678

Zhong R, Richardson EA, Ye ZH (2007b) Two NAC domain transcription factors, SND1 and NST1, function redundantly in regulation of secondary wall synthesis in fibers of Arabidopsis. Planta 225 (6):1603-1611. doi:10.1007/s00425-007-0498-y

Zhong R, Ye ZH (2007) Regulation of HD-ZIP III Genes by MicroRNA 165. Plant Signal Behav 2 (5):351-353

Chapter 2

Identification of new protein-DNA interactions linked to wood development in *Populus trichocarpa*

Abstract

Trees are unique among plants since they have extremely long life spans and the ability to generate large quantities of woody biomass resulting from the formation of secondary xylem formed by the vascular cambium. Transcription factors (TFs) are DNA-binding regulatory proteins capable of activation or repression by binding to a specific region of DNA, normally located in the 5-prime upstream region of the gene. These Protein-DNA interactions (PDIs) are responsible for developmental gene expression during plant growth and development. By using data from tissue specific *Populus trichocarpa* microarray studies, TFs expressed 4-fold or higher in a xylem-biased manner were used to screen for interactions with specific promoter sequences. The promoters of the *Populus trichocarpa* lignin biosynthetic pathway enzymes phenylalanine ammonia-lyase (PAL), *p*-hydroxycinnamoyl-transferase (HCT), and caffeoyl-CoA O-methyltransferase (CCoAOMT) were used as baits in Yeast One-Hybrid (Y1H) screens. In addition to these lignin biosynthesis enzymes, the promoters from two cambial zone associated TFs PtrARBORKNOX2 (ARK2) and PtrREVOLUTA (REV) were used as baits in the Y1H screen, *ark2* and *rev* have been previously shown to alter lignin content and secondary cell wall (SCW) development. The Y1H results are in agreement with previous work from Arabidopsis that indicate transcriptional regulation by TFs from the MYB family plays a central role in SCW development. Despite the similarities with prior work from Arabidopsis, novel PDIs were identified; belonging to the C2H2 type zinc-finger (C2H2ZF2), Bell-like homeodomain, B-box zinc-finger, Homeodomain (HD), and MYB/SANT families capable of driving reporter expression in the Y1H.

Introduction

Wood is a natural resource of great economic importance worldwide. In addition to its importance in the construction and paper industries, wood also functions as a sink for sequestering excess CO_2 from the atmosphere (Ter-Mikaelian et al. 2015; Bonan 2008). Wood or secondary xylem is composed of cellulose, hemicelluloses, and lignin (Plomion et al. 2001). In trees, wood is formed by the radial growth of stems occurring after the cessation of elongating growth (Du and Groover 2010). Secondary xylem and phloem are formed by the vascular cambium, a lateral meristem functioning to generate a continuous supply of cells for vascular development. Xylem is composed of tracheary elements and fibres that have undergone the cell death program known as xylogenesis. Xylogenesis normally proceeds by cells undergoing division and enlargement, cell wall thickening, lignification, and programmed cell death (PCD) (Fukuda et al. 1998; Roberts and McCann 2000) . The process of xylem development is complex and involves the coordinated spatio-temporal expression of numerous genes involved in the biosynthetic pathways for formation of the SCW. The final steps in SCW formation involve the emergence of the characteristic thick lignified secondary cell walls of xylem followed by total collapse of the living xylem cells by autolysis (Fukuda 1996).

Lignin is the second most abundant bio-polymer on Earth, functioning to give wood its structural strength and prevent biodegradation. The unfortunate consequence of the presence of lignin in the SCW is that difficulties in removal arise in the pulp industry and lignin inhibits access to sugars for enzymatic biofuel production (Vermaas et al. 2015; Li et al. 2003). In trees, the percentage of lignin present in wood has been linked to a negative correlation with biomass production (Novaes et al. 2010). This, negative correlation in biomass production with lignin content highlights the importance of understanding the mechanisms involved in SCW development. Mutant analysis and transcriptome profiling experiments from the model organisms Zinnia (Demura et al. 2002) and Arabidopsis (Zhao et al. 2005) have revealed many genes involved in SCW development, but many regulatory factors remain to be identified. Indeed, transcript profiling experiments in poplar show many of the previously identified lignin pathway enzymes and other SCW associated proteins are up-regulated during the transition from primary to secondary growth (Dharmawardhana et al. 2010; Rodgers-Melnick et al. 2012b). One

option to identify regulators of SCW development is to identify TFs involved in activation of genes known to function in wood development.

Protein-DNA interactions (PDIs), those occurring between *cis* regulatory regions usually found in the promoter regions of genes and their targeting TFs, are of great importance for transcriptional regulation (Deplancke et al. 2006b). The Gateway compatible Yeast One-Hybrid (Y1H) system utilizes the promoter sequence of a target gene as a starting point to locate PDIs. Promoter reporter combinations for *His3* and *LacZ* are directly integrated into the yeast genome by recombination allowing for a more streamlined procedure compared to multiple vector based Y1H "bait" systems. DNA baits are screened against a cDNA activation domain (AD) "prey" library or in some cases mini-libraries. The AD "prey" containing protein upon interaction with the "bait" will activate reporter gene expression enabling growth on minimal media. The Y1H assay enables TFs that function as activators or repressors protein to be identified.

Here, the Gateway-Compatible (Y1H) assay was utilized to screen 4 promoters as baits from *Populus trichocarpa (Ptr)* involved in xylem formation and 2 promoters from TFs involved in cambial zone proliferation and patterning. The promoters of the lignin biosynthetic pathway enzymes phenylalanine ammonia-lyase (PAL), *p*-hydroxycinnamoyl-transferase (HCT), and caffeoyl-CoA O-methyltransferase (CCoAOMT) were used as baits in Y1H screens. PAL, HCT, and CCoAOMT are well characterized enzymes involved in lignin biosynthesis and were chosen in an effort to find novel interacting transcription factors involved in SCW formation in poplar. Poplar Xylem Cysteine Protease 2 (XCP2) is a homolog of a protease involved in the micro-autolysis step of programmed cell death (PCD) during tracheary element development in Arabidopsis (Avci et al. 2008). The final two promoters screened belonged to *PtrREVOLUTA* (*REV*), a transcription factor involved in cambium polarity and patterning (Robischon et al. 2011b), and *PtrARBORKNOX2* (*ARK2*), a poplar homolog of *Brevipedicellus (BP)* from Arabidopsis associated with cambial zone development and terminal cell differentiation during secondary growth, *ARK2* was previously shown to be involved in the negative regulation of genes involved in SCW development (Du et al. 2009).

Materials and Methods:

Cloning

The Qiagen DNAeasy Plant Mini Kit (Qiagen) was used to isolate genomic DNA from *Populus trichocarpa*. Primers used to amplify promoters for testing by Y1H are listed in **Table 2.S1**. Following PCR amplification promoters were cloned and sequenced in pGEM-T-Easy vector system (Promega). The pGEM-T-Easy clones were then subject to subsequent restriction site based cloning using digestion by Kpn I and Spe I, followed by ligation into Vector 476 MCS-P5E, a gift from Nathan Lawson (Addgene # 26029). The promoter in vector 476 MCS-P5E was recombined using LR clonase (Invitrogen) into both PMW2 and PMW3, then integrated into the yeast genome by homologous recombination.

Poplar TFs were cloned from *Populus trichocarpa* cDNA using the primers listed in Supplemental **Table 2.S1** into pENTR^{TM}/D-TOPO (Invitrogen) as per the method indicated in the Invitrogen manual (25-0434). Subsequent recombination into pAD-Dest and pDB-Dest vectors was conducted using LR clonase (Invitrogen) according to manufacturers' instruction. Promoter::GUS constructs were made using the pENTR/D-TOPO cloning system (Invitrogen) followed by LR clonase (Invitrogen) recombination into Gateway compatible vector pKGWFS7 (Karimi et al. 2005).

Ectopic expression vectors were constructed by recombination of previously cloned TFs into Gateway compatible vector pB2GW7.0 (Karimi et al. 2005) using LR clonase based recombination for BAR selection. Constructs for poplar transformation utilized the same procedure except vector pK2GW7.0 was used for kanamycin selection.

promLMX5 Vector Construction

Plasmid DNA from pFGC5941 was digested with Hind III/BamHI, releasing two fragments. The smaller one containing *Tocs* was ligated with PBI121 previously digested with HindIII/BamHI, replacing *CaMV 35S* promoter with *Tocs* and bringing the SpeI, XmaI, PacI, XbaI, AvrII, and BamHI portion of the multiple cloning site. The new vector is named pBI121.1
Vector *promLMX5*::pBI121.1 was constructed using the primers LMX5s and LMX5as as listed in **Table 2.S1** to amplify and clone 1.7 kb of the upstream promoter of *LMX5* from 717 genomic DNA, into pGEM-t-easy (Promega) for use as a shuttle vector. Vector PBI121.1 was digested

with Hind III and Pac I allowing for insertion of 1.7 kb *LMX5* promoter into PBI121.1 to create vector *promLMX5*::PBI121.1. *LMX5::DIV4:SRDX* was constructed by amplifying from *DIV4* from cDNA using primers DIV4s and DIV4as followed by using the Avr II and Sac I sites on vector *promLMX5*::pBI121.1 for insertion into *promLMX5*::pBI121.1 vector to create *promLMX5::DIV4:SRDX*.

Cloning strategies for amiRNAs all followed the procedure described previously by Shi et al, (2010) and utilized the native *Populus trichocarpa* encoding miRNA408 (Lu et al. 2005) , primers for all amiRNAs are listed in primer **Table 2.S1**.

Mini-Library preparation

TF cloning was done using pENTR^{TM}/D-TOPO (Invitrogen) as per the method indicated in the Invitrogen manual (25-0434). Subsequent recombination into pAD Dest vector (a gift from the Vidal lab) was conducted using LR clonase (Invitrogen) according to manufacturers' instruction. The previously cloned TFs were combined into a mini-library by adding 235 ng of each TF::AD Dest vector to give a final concentration of 10 ug/60 µl for mini-library concentration. Positive TFs were retested by (Y1H) using 235 ng of individual TF::AD Dest.

Xylem-biased AD Library Preparation

Developing secondary xylem was harvested directly into liquid nitrogen from the stems (below internode 10) of *Populus trichocarpa* after bark had been peeled. Total RNA was isolated by using the RNeasy Mini Kit (Qiagen) with a modified protocol (Brunner et al. 2004). mRNA was isolated by using the PolyATtract mRNA Isolation System (Promega, Madison, WI). A standard cDNA library was constructed by using CloneMiner II cDNA library construction Kit (Invitrogen, Carlsbad, CA) and the cDNA library was transferred into Gateway compatible destination vector pAD Dest(a gift from Vidal lab) using LR Clonase (Invitrogen) according to manufacturers' instruction. The xylem-biased AD Dest library was utilized for the *PtrXCP2p* Y1H, PtrRAD1, and PtrDRIF1 Yeast Two-Hybrid (Y2H).

Yeast One-Hybrid

The protocol of Walhout and Deplanke was used for our Y1H (Deplancke et al. 2006b) with the following exceptions. Vector 476-P5E MCS (Addgene #26029) a gift from Nathan Lawson was used in place of pDONR-P4-P1R. Retesting was accomplished by using individual TF-AD Dest

at 250 ng compared to an AD-Dest vector control in the Y1H. Only those TFs that retested as positive are reported.

Yeast Two-Hybrid

The protocol of Walhout and Vidal 2001 was followed for our (Y2H), with the exceptions listed in Petzold and Rigoulot et al., 2017. The PtrRAD1 Y2H used 3 μM 3-AT MaV203 MATα , the PtrDRIF1 Y2H used 20 uM 3AT in yeast strain Y8800 MATa.

Transient Assays in Nicotiana benthamiana

The method outlined by (Yang et al. 2000) was followed for transient expression in *Nicotiana benthamiana* but with the following changes. Two different transgenic cultures of *Agrobacterium tumefaciens* strain GV3101 were used. The first culture contained the promoter region of interest fused to the GUS reporter, while the second culture contained an estradiol induced fusion protein in vector pMDC7. Vector pMDC7 contained the XVE (LexA-VP16-ER) inducible system for plants (Zuo et al. 2000). Induction was performed by spraying 17D-beta-estradiol at a concentration of 10 μM onto the inoculated plants 3 hours and 16 hours post inoculation. Leaves were harvested and GUS stained a minimum of 8 hours following the second induction with estradiol. Negative control samples contained the promoter::GUS vector construct with a different estradiol fusion protein than the tested effector.

Analysis of GUS Activity

Leaf disc from transiently expressed plants were collected and analyzed for GUS activity by placing them in GUS histochemical staining buffer (100 mM Na_2HPO_4, pH 7.0, 10 mM EDTA, 0.5 mM $K_4Fe(CN)_6$, 0.5 mM $K_3Fe(CN)_6$, 0.1% Triton X-100), 1mM filter-sterilized X-Glu (Oono et al. 1998). The staining buffer was infiltrated by vacuum for 5 minutes at room temperature and incubated overnight at 37^{o}C. Samples were de-greened by two brief 70% ethanol washes followed by overnight fixing in 95% ethanol. The tissue and cell-type specific GUS localization were detected by using a light microscope if needed. TF Constructs were tested a minimum of three times.

Arabidopsis transformations

Arabidopsis transformations followed the floral dip method of (Clough and Bent 1998) using *Agrobacterium tumafaciens* strain GV3101, and were plated with appropriate antibiotics. Colonies carrying the antibiotic resistant construct were grown overnight in 2XTY media,

pelleted and resuspended in infiltration buffer (5% Sucrose, 0.03% Silwet L-77), followed by dipping infloresences in infiltration buffer for 5 minutes. Transformed plants were then selected by application of herbicide or selection on GM media plates containing antibiotics.

Poplar transformations

The Agrobacterium-mediated tissue culture based procedure was used for our transformations, explants utilizing 6-week old hybrid poplar clone 717 (*P. alba* x *P. tremula*) leaf disc were used for co-culture (Meilan and Ma 2006). Candidate transformed plants were verified using vector specific and transgene specific primers prior to propagation and planting in the field.

Results

PtrXCP2 promoter library screen

1100-bp of *PtrXCP2promoter (PtrXCP2p,* Potri.002G005700) upstream of the initiation start site was integrated into the genome of yeast and used as bait in an Y1H screen against a poplar xylem cDNA-AD "prey" library. The reporters for both *His3* and *LacZ* were activated for 50 colonies as demonstrated by growth on minimal media and activation of *LacZ*. From these colonies, only one resulted in an in-frame fusion with a TF; it was a small MYB/SANT domain containing TF most similar to RADIALIS (RAD) from snapdragon. Due to the large number of colonies yielding results that were ribosomal proteins or out-of-frame products instead of TFs, the decision was made to proceed by a targeted approach that enriched for interactions with TFs in future Y1H screens. This approach was achieved by expanding previously cloned poplar TFs to create a TF-AD mini-library for future use in Y1H screens.

Mini-library preparation

Based upon previous experiments using a full AD-TF "prey" library screen for *PtrXCP2p* the TF mini-library was made (**Figure 2.2**). The 43 TFs in the mini-library were cloned from *Populus trichocarpa* based upon either xylem-biased expression at 4-fold or higher in poplar (Dharmawardhana et al. 2010; Rodgers-Melnick et al. 2012b), or known regulators of cambial zone formation in poplar and Arabidopsis, as is the case with the Lateral Organ Boundaries Domain (LBD), Homeodomain-Zip III (HD-Zip III), and the HD domain containing proteins ARK1 and ARK2. Based upon the identification of the RAD-like protein in our first *PtrXCP2p* Y1H screen, PtrRAD1 and four PtrDIVARICATA (DIV)-like TFs were added to the mini-library. The competition between RAD and DIV TFs has been well documented due to their involvement in organ polarity and differential cell growth in both snapdragon (Baxter et al. 2007; Raimundo et al. 2013) and tomato (Machemer et al. 2011).

Lignin biosynthesis and cambial zone promoter screens

The first enzyme of the general phenylpropanoid pathway is PAL, whose function is to convert L-phenylalanine into trans-cinnamic acid, and is the precursor for lignins, flavanoids, and coumarins. The enzymes HCT and CCoAOMT are both upstream of the production of coniferaldehyde and are necessary for the production of the S and G units of lignin. Promoters for other lignin pathway enzymes from poplar were cloned but due to auto-activation were unable to be used in the Y1H assay. The upstream promoters 1011-bp PAL4 (*PtrPALp*), 1589-bp

HCT (*PtrHCTp*), 1716-bp CCoAOMT (*PtrCCoAOMTp*), 1500-bp PtrRevoluta (*PtrREVp*), and 1600-bp PtrARK2 (*PtrARK2p*) were each cloned and integrated into the yeast genome for use as baits in the Y1H with low auto-activation. The difference in promoter sizes used in the assay is due to the presence of restriction endonuclease recognition sites in the promoters of interest limits the ability to clone larger fragments. **Figure 2.1** shows a force-integrated Cytoscape network for all PDIs identified in our Y1H screens using the lignin biosynthesis promoters and the cambial zone promoters as bait. **Figure 2.2** shows the results for the Y1H screen for the lignin biosynthetic pathway and cambial zone promoter screens combined with the biweight midcorrelation scores for all PDI (Song, Langfelder, & Horvath). The bicor scores range from -1 (negative correlation) to 1 (positively correlated). **Figure 2.3** shows the Y1H results combined with the number of colonies identified that correspond to each PDI.

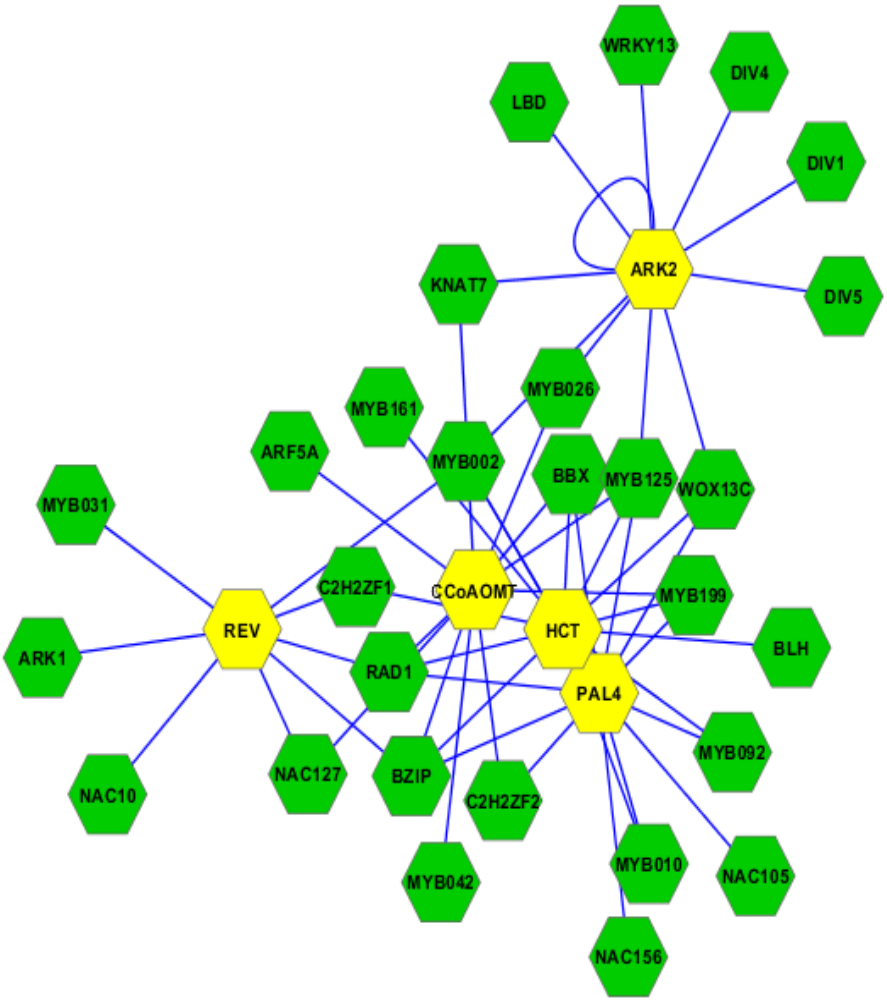

Figure 2.1. Cytoscape network of Yeast One-Hybrid mini-library screens showing protein-DNA interactions.

Nodes for transcription factors are colored in green, Nodes for promoters are colored in yellow, edges are colored in blue. The force-directed algorithm setting on Cytoscape 2.8.3 was used to generate the network.

				Lignin Biosynthesis Promoters			Cambial Zone Promoters	
Arabidopsis thaliana		*Populus trichocarpa*		PAL4	HCT	CCoAOMT	ARK2	REV
At1g19850	ARF5	Potri.002G024700	**ARF5a**					
At4g15248	BBX30	Potri.007G121100	**BBX**		0.943	0.594		
At2g23760	BLH4	Potri.007G032700	**BLH**					
At5g02030	BLH9	Potri.010G197300	**BLH**					
At5g04840	bZIP	Potri.008G018400	**BZIP**		0.897			
At2g28710	C2H2-ZF	Potri.010G209400	**C2H2ZF1**					
At1g02040	C2H2-ZF	Potri.014G066200	**C2H2ZF2**	0.669		0.756		
At2g38090	DIV	Potri.016G112300	**DIV1**					
At5g58900	DIV	Potri.009G042600	**DIV4**					
At5g05790	DIV	Potri.010G193000	**DIV5**					
At5g05790	DIV	Potri.008G064200	**DIV6**					
At3g28920	HB34	Potri.017G082900	**HDZF**					
At4g32280	IAA29	Potri.018G127800	**IAA**					
At1g62990	KNAT7	Potri.001G112200	**KNAT7**		0.953	0.610	-0.672	
At1g22640	MYB3	Potri.019G081500	**MYB168**					
At5g12870	MYB46	Potri.001G258700	**MYB002**	0.677	0.892		-0.686	
At1g57560	MYB50	Potri.010G004300	**MYB042**			0.674		
At1g17950	MYB52	Potri.015G033600	**MYB90**					
At1g17950	MYB52	Potri.007G134500	**MYB161**		0.952			
At4g33450	MYB69	Potri.005G063200	**MYB026**			0.716		-0.679
At4g33450	MYB85	Potri.007G106100	**MYB031**					
At4g22680	MYB85	Potri.015G129100	**MYB85-L**					
At4g22680	MYB85	Potri.001G118800	**MYB092**					
At4g22680	MYB85	Potri.003G114100	**MYB125**	0.960		0.796		
At4g22680	MYB85	Potri.012G127700	**MYB199**	0.712		0.950		
At1g63910	MYB103	Potri.001G099800	**MYB010**		0.950	0.635		
At4g29230	NAC075	Potri.018G068700	**NAC127**			0.799		
At2g46770	NST1	Potri.002G178700	**NAC061**					
At1g75250	RAD/L6	Potri.002G260000	**RAD1**					
At4g28500	SND2	Potri.011G058400	**NAC105**		0.873			
At4g28500	SND2	Potri.007G135300	**NAC156**	0.861				
At4g28500	SND2	Potri.004G049300	**NAC154**					-0.670
At1g71930	VND7	Potri.013G113100	**NAC055**					
At4g35550	WOX13	Potri.002G008800	**WOX13**	0.723				
At2g44745	WRKY12	Potri.002G138900	**WRKY12**					
At4g39410	WRKY13	Potri.007G078200	**WRKY13**					
At5g64530	XND1	Potri.003G022800	**NAC118**					
At5g64530	XND1	Potri.007G105000	**NAC104**					
AT1G62360	BUM1/STM	Potri.011G011100	**ARK1**					0.796
AT4G08150	BP/KNAT1	Potri.002G113300	**ARK2**				1.000	
At1g52150	CORONA	Potri.001G188800	**CORONA**					
At2g28500	LBD11	Potri.010G217700	**LBD**				0.680	

Figure 2.2. Protein-DNA interactions for promoters screened by Yeast One-hybrid.

Columns (1-4) Poplar transcription factors cloned and pooled in the xylem-biased mini-library showing Arabidopsis homolog gene ID and protein name, poplar gene ID and protein names when available. Column (5) PDIs for *PtrPAL4p* (Potri.010G224100); Column (6) PDIs for *PtrHCTp* (Potri.001G042900); Column (7) PDIs for *PtrCCoAOMTp* (Potri.009G099800); Column (8), PDIs for *PtrARK2p* (Potri002G11300); Column (9) PDIs *PtrREVp* (Potri004G211300). Cells shaded in red interactions activating both *His3* and *LacZ* reporters in Yeast, cells shaded in grey activate *His3* reporter, clear cells TFs failed to activate reports. Significant bi-weight mid-correlation scores ($p \leq 0.05$) are displayed in cells with positive reporter output.

		Lignin Biosynthesis Promoters			Cambial Zone Promoters	
Populus trichocarpa		PAL4	HCT	CCoAOMT	ARK2	REV
Potri.002G024700	**ARF5a**			1		
Potri.007G121100	**BBX**	1	2	2		
Potri.007G032700	**BLH**					1
Potri.010G197300	**BLH**	1	3			1
Potri.008G018400	**BZIP**	1	2	1		
Potri.010G209400	**C2H2ZF1**		3			
Potri.014G066200	**C2H2ZF2**	2		6		
Potri.016G112300	**DIV1**				1	
Potri.009G042600	**DIV4**				4	
Potri.010G193000	**DIV5**				1	
Potri.008G064200	**DIV6**					1
Potri.017G082900	**HDZF**					
Potri.018G127800	**IAA**					1
Potri.001G112200	**KNAT7**		2	1	5	
Potri.019G081500	**MYB168**					
Potri.001G258700	**MYB002**	2	2		1	
Potri.010G004300	**MYB042**			3		
Potri.015G033600	**MYB90**					
Potri.007G134500	**MYB161**	1	2	5		
Potri.005G063200	**MYB026**			3	1	3
Potri.007G106100	**MYB031**					
Potri.015G129100	**MYB85-L**					
Potri.001G118800	**MYB092**	5	2			
Potri.003G114100	**MYB125**	3	5	1	2	
Potri.012G127700	**MYB199**	2	1	1		
Potri.001G099800	**MYB010**	3	6	3		
Potri.018G068700	**NAC127**			1		
Potri.002G178700	**NAC061**					
Potri.002G260000	**RAD1**	1	2	1		2
Potri.011G058400	**NAC105**		1			
Potri.007G135300	**NAC156**	2				2
Potri.004G049300	**NAC154**					6
Potri.013G113100	**NAC055**					2
Potri.002G008800	**WOX13**	1	5		1	
Potri.002G138900	**WRKY12**					
Potri.007G078200	**WRKY13**				4	1
Potri.003G022800	**NAC118**					
Potri.007G105000	**NAC104**					
Potri.011G011100	**ARK1**					2
Potri.002G113300	**ARK2**				1	
Potri.001G188800	**CORONA**					1
Potri.010G217700	**LBD**				1	
	Total Colonies	**25**	**38**	**30**	**22**	**23**

Figure 2.3. Protein-DNA interactions showing number of colonies identified for each interaction.

Column 1-2) Poplar gene ID and protein name when available for each TF in the mini-library. Column 3) *PtrPAL4p* (Potri.010G224100); Column 4) PDIs for *PtrHCTp* (Potri.001G042900); Column 5) PDIs for *PtrCCoAOMTp* (Potri.009G099800); Column 6) PDIs for *PtrARK2p* (Potri002G11300); Column 7) PDIs for *PtrREVp (*Potri004G211300); Cells shaded in red are interactions activating both *His3* and *LacZ* reporters in yeast, Cells shaded in grey only activate *His3* reporter, no interaction occurred for clear cells. Numbers in each cell show the number of colonies identified for each TF using the same mini-library, same number of plates and same starting OD of yeast cells.

Promoter GUS reporter fusion

In order to verify a subset of the Y1H interactions, promoter GUS fusion constructs were made prior to proceeding with functional analysis of TFs of interest. Transient co-expression in *Nicotiana benthamiana* was used to confirm reliability of PDIs, the *XVE* (LexA-VP16-ER) inducible system for plants was used (Zuo et al. 2000). Cotransfection of the reporter plasmid containing 1100-bp upstream of the initiation start codon of *PtrXCP2p*::*GUS* showed strong activation post estradiol induction using vector *XVE*::*PtrRAD* (**Figure 2.4**), although some leaf-to-leaf variation occurred, the results were consistently greater than background observed with the estradiol induced negative control *XVE*::*PtrXND1*. The Y1H using *PtrCCoAOMTp* as bait (**Figure 2.3**) resulted in numerous colonies with strong interactions involving a previously uncharacterized C2H2 Zinc-finger TF (Potri.014g066200). The estradiol inducible system was used to test Potri.014g066200 and Potri.007G134500 (MYB 161) based upon strength of interaction in the Y1H, as evidenced by reporter output and colony number, results are shown in (**Figure 2.5**). Both Potri.014g066200 and Potri.007G134500 (MYB161) showed transactivation greater than background when co-expressed in *N.benthamiana* with *PtrCCoAOMTp*::*GUS*, estradiol induced *XVE*::*PtrXND1*was used in this assay as the negative control and results were consistently greater than background. The results for all promoter::GUS constructs tested are listed in **Table 2.1**.

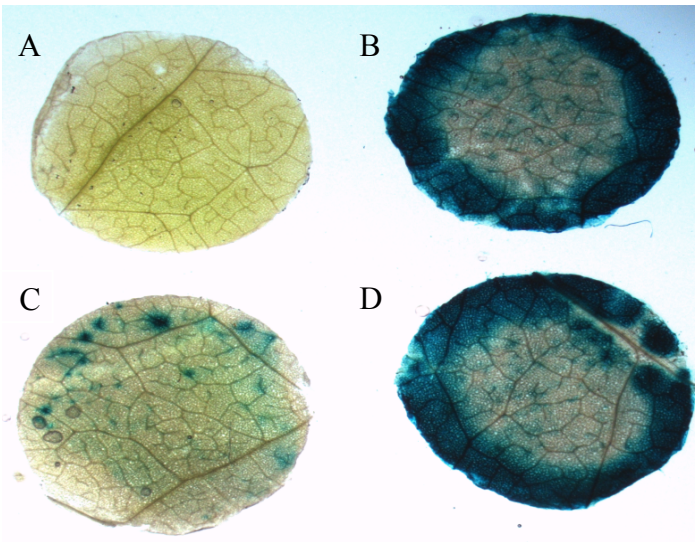

Figure 2.4. 1100-bp *PtrXCP2p::GUS* reporter is activated by transient expression when co-transformed with *XVE*::*PtrRAD* post estradiol induction.

A) Co-transformed negative control estradiol induced *XVE::PtrXND1* and *PtrXCP2p::GUS*; B) Co-transformed estradiol induced *XVE*::*PtrRAD* and *PtrXCP2p*::*GUS*; C) Co-transformed Negative control estradiol induced *XVE*::*PtrXND1* and *PtrXCP2p::GUS*; D) Co-transformed estradiol induced *XVE::PtrRAD* and *PtrXCP2p*::*GUS*. Each column is a replicate from different 3-4 week old *N. benthamiana*.

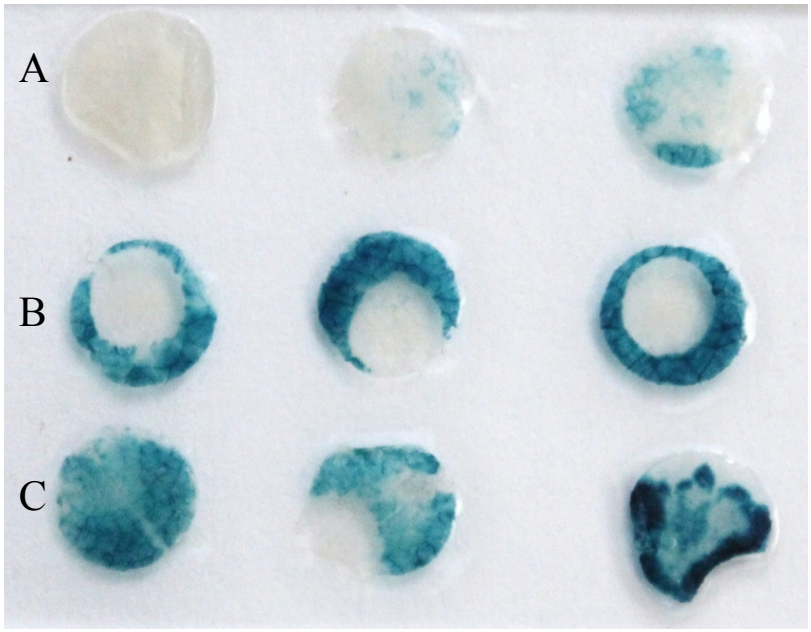

Figure 2.5. Co-transformed *PtrCCoAOMTp*::*GUS* reporter is transiently activated post estradiol induction by *XVE*::*Potri.014g066200* (C2H2ZF2) and *XVE*::Potri.007G134500 (MYB161) in *N. benthamiana*.

A) Negative control co-transformed estradiol induced *XVE*::*PtrXND1* and *PtrCCoAOMTp*::*GUS*; B) Co-transformed estradiol induced *XVE::Potri.014g066200* (C2H2ZF2) and *PtrCCoAOMTp*::GUS; C) Co-transformed estradiol induced *XVE:: Potri.007G134500* (MYB 161) and *PtrCCoAOMTp*::*GUS* . Each column is a biological replicate from different 3-4 week old *N. benthamiana*.

Table 2.1. Results for co-transformed promoter GUS fusion constructs with TFs identified by Yeast One-Hybrid.

Column 1) Poplar gene ID; Column 2) Poplar protein name; Column 3) 1011-bp *PtrPAL4p* (*Potri.010G224100)::GUS* results; Column 4) 1589-bp *PtrHCTp (Potri.001G04290)::GUS* results; Column 5) 1716-bp *PtrCCoAOMTp* (*Potri.009G099800)::GUS* results; Column 6) 1100-bp *PtrXCP2p*:*:GUS*. Clear cells were not tested in this assay. Three independent biological replicates expressed GUS greater than background to be considered positive.

Populus trichocarpa		***PAL4p* ::GUS**	***HCTp* ::GUS**	***CCoAOMTp* :: GUS**	***XCP2p* ::GUS**
Potri.010G209400	**C2H2ZF1**	Negative	Positive	Negative	
Potri.014G066200	**C2H2ZF2**	Positive		Positive	
Potri.008G018400	**BZIP**	Positive	Positive	Positive	
Potri.001G258700	**MYB002**	Positive	Positive		
Potri.007G134500	**MYB161**	Positive	Positive	Positive	
Potri.001G099800	**MYB010**	Positive	Positive	Positive	
Potri.002G260000	**RAD1**			Positive	Positive
Potri.003G022800	**XND1-like**	Negative	Negative	Negative	Negative

Based upon the results from the Y1H and agreement with promoter GUS reporter assays, constructs were made utilizing common reverse genetics methods in both poplar and Arabidopsis (**Table 2.2**). The involvement of PtrRAD1 in PDIs occurring with multiple promoters in theY1H assays made PtrRAD1 a candidate for investigation by ectopic expression and amiRNA mediated gene silencing. DIV4 contained the highest xylem-biased expression level of any of the DIVs cloned in our mini-library, making it a candidate for further investigation using ectopic expression of an in-frame fusion with the SRDX repression domain (Hiratsu et al. 2003). The RAD1 and DIV4 constructs in Arabidopsis failed to result in detectable phenotypes, the poplar constructs are in the process of being evaluated for changes in wood quality, biomass, and wood chemistry. The LMX5 cambial zone-specific promoter (Love et al. 2009) was used to construct *LMX5::DIV4::SRDX* plants. Utilizing the *LMX5* promoter in field trials resulted in *LMX5::DIV4::SRDX* plants that have a horizontal/curving branch phenotype and these plants are undergoing additional characterization. The *35s::C2H2ZF2* construct in Arabidopsis showed a phenotype of dwarf plants with wrinkled leaves, but failed to yield any transformed plants in poplar (**Figure 2.6**).

Figure 2.6. Five-week old *Arabidopsis thaliana* transformed with *35s*::*PtrC2H2ZF2*.

Ectopic expression of *PtrC2H2ZF2* (Potri.014G066200) in Arabidopsis resulted in dwarf plants that were growth-arrested with a wrinkled leaf phenotype.

Table 2.2. Constructs used to make transgenic plants for functional analysis.

Column 1) Constructs; Column 2) *Arabidopsis thaliana* transgenic plants and phenotype when available; Column 3) *Populus tremula X Populus alba* clone 717 background and phenotype when available.

Constructs	***Arabidopsis thaliana***	***Populus tremula X Populus alba* clone 717**
35s ::PtrRAD1	No visible phenotype	under evaluation
LMX5 ::PtrDIV4::SRDX	No visible phenotype	visible phenotype in poplar
35s ::PtrWOX13	No visible phenotype	under evaluation
35s ::PtrC2H2ZF2	Growth-arrested plants	failed to yield transformants
amiRNA::PtrRAD1	N/A	under evaluation
amiRNA::PtrDRIF1	N/A	under evaluation
amiRNA::PtrC2H2ZF2	N/A	under evaluation

Interactome walking utilizing PtrRAD1

As part of ongoing efforts to study genes involved in wood development and biomass production, *PtrRAD1*was added as a candidate gene for screening by Y2H. *PtrRAD1* was screened for interactions based upon its xylem-biased expression and PDIs with the SCW-related promoters from the Y1H assays. The open reading frame of *PtrRAD1*was cloned and screened as a DB fusion against the xylem-biased AD library and a protein-protein interaction (PPI) with PtrDRIF1 was discovered and confirmed by re-testing in binary screens. Following conformation of the DRIF1/RAD1 PPI, PtrDRIF1 was used in a subsequent Y2H library screen as a DB fusion and identified the PPI network shown in **Figure 2.7**. The initial library screen only identified PtrDIV4 as an interaction but 3 more PtrDIVs were cloned and screened resulting in positive interactions. Based upon the unique finding of a PPI occurring between the homeodomain (HD) containing protein PtrWOX13c and PtrDRIF1, several additional HD proteins were screened in the Y2H resulting in identification of PtrDRIF1/PtrKNAT7 as an interaction.

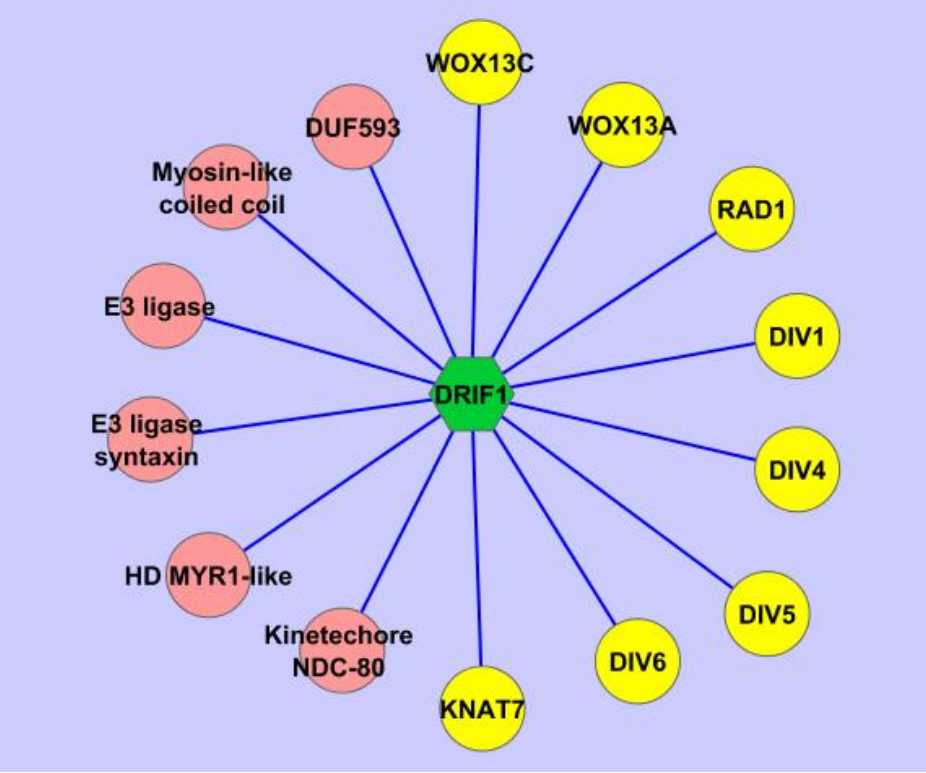

Figure 2.7. Cytoscape generated PtrDRIF1 Protein-Protein interaction network for *Populus trichocarpa*.

Node for DRIF is colored in green, nodes for transcription factors re-tested and confirmed as positive interactions are colored in yellow, nodes for interactions not confirmed by re-test are colored in pink, edges are colored in blue. Cytoscape 2.8.3 was used to generate this figure.

Discussion

The PDIs identified in the Y1H mini-library screens are consistent with prior data obtained from Arabidopsis homologs involved in lignin biosynthesis (Taylor-Teeples et al. 2015) and from promoter-reporter binding assays involving PtrMYB002 and PtrMYB92 (Zhong et al. 2013; Li et al. 2015). In these experiments, promoter::GUS reporter assays were used to verify some of the TFs identified in PDIs were capable of transactivation of the promoters screened in the Y1H. Although, the transactivation reporter GUS assays are not a direct test of the PDIs, they show the TFs identified as interactions by the Y1H are capable of activating the SCW development pathways. The correlation scores in **Figure 2.2** show high expression correlation occurs between the interacting TFs and the expression of the lignin pathway enzymes, indicative of the TF being present when the gene-product is expressed. The lignin biosynthesis gene promoters *PtrPAL4p*, *PtrHCTp*, and *PtrCCoAOMTp* used as baits interacted with a core group of MYB TFs similar to previously published PDIs from Arabidopsis involving MYB85, MYB103, MYB46, MB69, and KNAT7 (Ohman et al. 2013; Li et al. 2012b; Kim et al. 2014; Ko et al. 2014; Zhong et al. 2008; Taylor-Teeples et al. 2015). Exceptions include, MYB52 that has not been previously reported to activate a specific lignin pathway promoter but ectopic MYB52 expression resulted in hyperlignified SCW (Cassan-Wang et al. 2014) and the interaction of a MYB85 homolog with a PAL promoter has not been previously reported. The presence of distinct AC motifs in the promoters tested likely contributed to the interactions with the large number of MYB TFs.

The NAC family was well represented with 9 TFs constituting the second largest family in the mini-library, but results from the lignin pathway promoter screens only showed 3 interactions with NAC TFs, out of a total of 40 PDIs. In contrast, 18 PDIs involved MYB TFs, consistent with the current view that the NAC TFs VND7, VND6, NST1, NST2, and SND1 function as master regulators of SCW development in various cell types by activating other TFs, most likely MYBs, to regulate SCW development (Mitsuda et al. 2007; Mitsuda et al. 2005; Yamaguchi et al. 2011). In these five Y1H mini-library screens three of the 4 SND2 or NAC075 homologs interacted with the promoters tested. In poplar, ectopic expression of SND2 co-ortholog PtrNAC154 resulted in deviations in bark ratio to xylem and reduced height (Grant et al. 2010). New TF's identified to form PDIs with lignin pathway promoters include RAD1, two C2H2-ZF

TFs, bZIP, BBX, BLH, and a homeodomain (HD) family member WOX13c. WOX13 was known primarily for involvement in replum formation in Arabidopsis (Romera-Branchat et al. 2013). Both the similarities and differences found between PDIs in these screens with previous data demonstrate the utility of the Y1H in identifying novel regulators of SCW development in poplar **Figure 2.1**.

Although, ARK2 and REV have been associated with SCW-related phenotypes (Du et al. 2009; Robischon et al. 2011b), the PDIs involving poplar *PtrARK2*p and *PtrREV*p differed substantially from the lignin biosynthesis group as seen in **Figure 2.1** and **Figure 2.2**. The co-expression values generated for these PDIs with the gene products with TFs were mostly negatively correlated except for ARK2 with *PtrARK2p*. The Cytoscape generated network in **Figure 2.1** demonstrates the close interconnectedness of the PDIs involving *PtrPAL4*p, *PtrHCT*p, and *PtrCCoAOMT*p. The interactions of *PtrARK2p* with WOX13, MYB002, MYB026, and KNAT7 were the only shared interactions with any of the three promoters screened from the lignin biosynthetic pathway and differences include interactions involving LBD, and three DIV TFs. The interactions involving the DIV TFs were strong, as evidenced by reporter activation, and large number of colonies identified that contained DIV TFs (**Figure 2.3**). The Y1H is not a quantitative assay, but the percentage of colonies is worth noting for the DIV TFs. DIV family TFs have not been previously shown to interact with *PtrARK2*p and although widely expressed in poplar failed to show a significant co-expression value with ARK2. The Y1H for *PtrREVp* identified NAC156, MYB026, MYB002, RAD1, and BLH TFs in common with the lignin biosynthesis promoter Y1H screens but differed by identifying interactions involving DIV6, IAA, VND7, WRKY13, ARK1, and CORONA.

The Cytosocape network (**Figure 2.1**) shows the lignin biosynthesis proteins are under similar transcriptional regulation as would be expected for a group of enzymes in the same biosynthetic pathway, and the two cambial zone-related TFs share some of the same PDIs with the lignin pathway promoters, but differ substantially in the interacting TFs involved in their regulation. The MYB/SANT domain TFs that were included in the mini-library interacted with all of the promoters screened, identifying them as potential novel regulators of wood development. Previous research involving DIVs in snapdragon (Raimundo et al. 2013) and tomato (Machemer

et al. 2011) have shown phenotypes with altered cell differentiation and tissue polarity. The ability of the MYB/SANT TFs to form PDIs with *PtrARK2p* and *PtrREVp* is interesting because mis-expression of ARK2 resulted in phenotypes with altered vascular differentiation, while mis-expression of REV resulted in altered cambial polarity. The DIV PDIs with *PtrARK2p* and *PtrREVp* raise the possibility that these proteins may function in trees to regulate cambial polarity or differential cell development in vascular tissues (Du et al. 2009; Robischon et al. 2011b).

The results from the PDIs combined with xylem-biased expression of PtrRAD1 led to the discovery of the PtrRAD1/PtrDRIF interaction. PtrDRIF1, interacted with numerous proteins, and had previously not been linked to wood development. Previous DRIF interactions had only involved the MYB/SANT containing RAD and DIV proteins from Antirrhinum (Raimundo et al. 2013) and tomato (McCarthy et al. 2010). Among these new interactions are the HD proteins PtrWOX13c and PtrKNAT7, and the three cytoskeletal-related proteins Nuclear Division Cycle 80 (NDC80), Myosin Binding B (MyoB), and microtubule polymerization protein (Kin7a).

Conclusions

The basic mechanisms controlling wood formation are of great importance to meet future energy demands for biofuels and to help decrease the production of greenhouse gases. Here, several TFs that have not been previously associated with SCW development have been identified. Based upon agreement with previous Y1H data and promoter reporter fusion data from model organisms showing the involvement of MYB TFs in wood development; the consistency of the results for the lignin biosynthesis promoters would imply support to the relevance of the novel interactions. In this study, TFs were identified belonging to the RAD and DIV family interacted with promoters from the lignin pathway and cambial zone, these TFs had not been previously linked to wood development. The exact function of RAD and DIV-like proteins in these tissues is not currently known but based upon gene expression data (Rodgers-Melnick et al. 2012b) they are expressed in varying amounts across multiple tissues. The PDIs also identified a HD protein PtrWOX13c that is highly expressed in xylem and interacted with both *PAL4* and *HCT* promoters, PtrWOX13c has not been previously found to specifically interact with promoters involved in SCW development.

The C2H2 Zinc-finger TFs identified to interact with the lignin pathway promoters are interesting candidates for future study based upon high expression level in xylem (Rodgers-Melnick et al. 2012b), and ectopic expression of Potri.014g066200 resulted in a growth-arrest phenotype in Arabidopsis (**Figure 2.6**) but failed to give any transformants in poplar. The failure to yield transformants in poplar could be due to ectopic expression interfering with a key aspect of tissue culture-based transformation. The amiRNA trees for Potri.014g066200 are currently under evaluation for wood quality, biomass accumulation, and wood cell wall morphology.

References

Arabidopsis Genome I (2000) Analysis of the genome sequence of the flowering plant Arabidopsis thaliana. Nature 408 (6814):796-815. doi:10.1038/35048692

Avci U, Petzold HE, Ismail IO, Beers EP, Haigler CH (2008) Cysteine proteases XCP1 and XCP2 aid micro-autolysis within the intact central vacuole during xylogenesis in Arabidopsis roots. Plant J 56 (2):303-315. doi:10.1111/j.1365-313X.2008.03592.x

Baxter CE, Costa MM, Coen ES (2007) Diversification and co-option of RAD-like genes in the evolution of floral asymmetry. Plant J 52 (1):105-113. doi:10.1111/j.1365-313X.2007.03222.x

Bonan GB (2008) Forests and climate change: forcings, feedbacks, and the climate benefits of forests. Science 320 (5882):1444-1449. doi:10.1126/science.1155121

Brunner AM, Yakovlev IA, Strauss SH (2004) Validating internal controls for quantitative plant gene expression studies. BMC Plant Biol 4:14. doi:10.1186/1471-2229-4-14

Cassan-Wang H, Goue N, Saidi MN, Legay S, Sivadon P, Goffner D, Grima-Pettenati J (2014) Identification of novel transcription factors regulating secondary cell wall formation in Arabidopsis (vol 4, 189, 2013). Front Plant Sci 5. doi:ARTN 24610.3389/fpls.2014.00246

Clough SJ, Bent AF (1998) Floral dip: a simplified method for Agrobacterium-mediated transformation of Arabidopsis thaliana. Plant Journal 16 (6):735-743. doi:DOI 10.1046/j.1365-313x.1998.00343.x

Demura T, Tashiro G, Horiguchi G, Kishimoto N, Kubo M, Matsuoka N, Minami A, Nagata-Hiwatashi M, Nakamura K, Okamura Y, Sassa N, Suzuki S, Yazaki J, Kikuchi S, Fukuda H (2002) Visualization by comprehensive microarray analysis of gene expression programs during transdifferentiation of mesophyll cells into xylem cells. Proc Natl Acad Sci U S A 99 (24):15794-15799. doi:10.1073/pnas.232590499

Deplancke B, Vermeirssen V, Arda HE, Martinez NJ, Walhout AJ (2006) Gateway-compatible yeast one-hybrid screens. CSH Protoc 2006 (5). doi:10.1101/pdb.prot4590

Deveaux Y, Toffano-Nioche C, Claisse G, Thareau V, Morin H, Laufs P, Moreau H, Kreis M, Lecharny A (2008) Genes of the most conserved WOX clade in plants affect root and flower development in Arabidopsis. BMC Evol Biol 8:291. doi:10.1186/1471-2148-8-291

Dharmawardhana P, Brunner AM, Strauss SH (2010) Genome-wide transcriptome analysis of the transition from primary to secondary stem development in Populus trichocarpa. Bmc Genomics 11. doi:Artn 150 10.1186/1471-2164-11-150

Du J, Groover A (2010) Transcriptional regulation of secondary growth and wood formation. J Integr Plant Biol 52 (1):17-27. doi:10.1111/j.1744-7909.2010.00901.x

Du J, Mansfield SD, Groover AT (2009) The Populus homeobox gene ARBORKNOX2 regulates cell differentiation during secondary growth. Plant J 60 (6):1000-1014. doi:10.1111/j.1365-313X.2009.04017.x

Fukuda H (1996) Xylogenesis: Initiation, Progression, and Cell Death. Annu Rev Plant Physiol Plant Mol Biol 47:299-325. doi:10.1146/annurev.arplant.47.1.299

Fukuda H, Watanabe Y, Kuriyama H, Aoyagi S, Sugiyama M, Yamamoto R, Demura T, Minami A (1998) Programming of cell death during xylogenesis. J Plant Res 111 (1102):253-256. doi:Doi 10.1007/Bf02512179

Grant EH, Fujino T, Beers EP, Brunner AM (2010) Characterization of NAC domain transcription factors implicated in control of vascular cell differentiation in Arabidopsis and Populus. Planta 232 (2):337-352. doi:10.1007/s00425-010-1181-2

Hiratsu K, Matsui K, Koyama T, Ohme-Takagi M (2003) Dominant repression of target genes by chimeric repressors that include the EAR motif, a repression domain, in Arabidopsis. Plant J 34 (5):733-739

Karimi M, De Meyer B, Hilson P (2005) Modular cloning in plant cells. Trends Plant Sci 10 (3):103-105. doi:10.1016/j.tplants.2005.01.008

Kim WC, Kim JY, Ko JH, Kang H, Han KH (2014) Identification of direct targets of transcription factor MYB46 provides insights into the transcriptional regulation of secondary wall biosynthesis. Plant Mol Biol 85 (6):589-599. doi:10.1007/s11103-014-0205-x

Ko JH, Jeon HW, Kim WC, Kim JY, Han KH (2014) The MYB46/MYB83-mediated transcriptional regulatory programme is a gatekeeper of secondary wall biosynthesis. Ann Bot 114 (6):1099-1107. doi:10.1093/aob/mcu126

Love J, Bjorklund S, Vahala J, Hertzberg M, Kangasjarvi J, Sundberg B (2009) Ethylene is an endogenous stimulator of cell division in the cambial meristem of Populus. Proc Natl Acad Sci U S A 106 (14):5984-5989. doi:10.1073/pnas.0811660106

Li C, Wang X, Ran L, Tian Q, Fan D, Luo K (2015) PtoMYB92 is a Transcriptional Activator of the Lignin Biosynthetic Pathway During Secondary Cell Wall Formation in Populus tomentosa. Plant Cell Physiol 56 (12):2436-2446. doi:10.1093/pcp/pcv157

Li EY, Bhargava A, Qiang WY, Friedmann MC, Forneris N, Savidge RA, Johnson LA, Mansfield SD, Ellis BE, Douglas CJ (2012) The Class II KNOX gene KNAT7 negatively regulates secondary wall formation in Arabidopsis and is functionally conserved in Populus. New Phytologist 194 (1):102-115. doi:10.1111/j.1469-8137.2011.04016.x

Li L, Zhou Y, Cheng X, Sun J, Marita JM, Ralph J, Chiang VL (2003) Combinatorial modification of multiple lignin traits in trees through multigene cotransformation. Proc Natl Acad Sci U S A 100 (8):4939-4944. doi:10.1073/pnas.0831166100

Lu S, Sun YH, Shi R, Clark C, Li L, Chiang VL (2005) Novel and mechanical stress-responsive MicroRNAs in Populus trichocarpa that are absent from Arabidopsis. Plant Cell 17 (8):2186-2203. doi:10.1105/tpc.105.033456

Machemer K, Shaiman O, Salts Y, Shabtai S, Sobolev I, Belausov E, Grotewold E, Barg R (2011) Interplay of MYB factors in differential cell expansion, and consequences for tomato fruit development. Plant J 68 (2):337-350. doi:10.1111/j.1365-313X.2011.04690.x

McCarthy RL, Zhong R, Fowler S, Lyskowski D, Piyasena H, Carleton K, Spicer C, Ye ZH (2010) The poplar MYB transcription factors, PtrMYB3 and PtrMYB20, are involved in the regulation of secondary wall biosynthesis. Plant Cell Physiol 51 (6):1084-1090. doi:10.1093/pcp/pcq064

Meilan R, Ma C (2006) Poplar (Populus spp.). Methods Mol Biol 344:143-151. doi:10.1385/1-59745-131-2:143

Mitsuda N, Iwase A, Yamamoto H, Yoshida M, Seki M, Shinozaki K, Ohme-Takagi M (2007) NAC transcription factors, NST1 and NST3, are key regulators of the formation of secondary walls in woody tissues of Arabidopsis. Plant Cell 19 (1):270-280. doi:10.1105/tpc.106.047043

Mitsuda N, Seki M, Shinozaki K, Ohme-Takagi M (2005) The NAC transcription factors NST1 and NST2 of Arabidopsis regulate secondary wall thickenings and are required for anther dehiscence. Plant Cell 17 (11):2993-3006. doi:10.1105/tpc.105.036004

Novaes E, Kirst M, Chiang V, Winter-Sederoff H, Sederoff R (2010) Lignin and biomass: a negative correlation for wood formation and lignin content in trees. Plant Physiol 154 (2):555-561. doi:10.1104/pp.110.161281

Ohman D, Demedts B, Kumar M, Gerber L, Gorzsas A, Goeminne G, Hedenstrom M, Ellis B, Boerjan W, Sundberg B (2013) MYB103 is required for FERULATE-5-HYDROXYLASE expression and syringyl lignin biosynthesis in Arabidopsis stems. Plant Journal 73 (1):63-76. doi:10.1111/tpj.12018

Oono Y, Chen QG, Overvoorde PJ, Kohler C, Theologis A (1998) age Mutants of Arabidopsis exhibit altered auxin-regulated gene expression. The Plant cell 10 (10):1649-1662

Plomion C, Leprovost G, Stokes A (2001) Wood formation in trees. Plant Physiol 127 (4):1513-1523

Raimundo J, Sobral R, Bailey P, Azevedo H, Galego L, Almeida J, Coen E, Costa MM (2013) A subcellular tug of war involving three MYB-like proteins underlies a molecular antagonism in Antirrhinum flower asymmetry. Plant J 75 (4):527-538. doi:10.1111/tpj.12225

Roberts K, McCann MC (2000) Xylogenesis: the birth of a corpse. Curr Opin Plant Biol 3 (6):517-522

Robischon M, Du JA, Miura E, Groover A (2011) The Populus Class III HD ZIP, popREVOLUTA, Influences Cambium Initiation and Patterning of Woody Stems. Plant Physiol 155 (3):1214-1225. doi:10.1104/pp.110.167007

Rodgers-Melnick E, Mane SP, Dharmawardhana P, Slavov GT, Crasta OR, Strauss SH, Brunner AM, Difazio SP (2012) Contrasting patterns of evolution following whole genome versus tandem duplication events in Populus. Genome research 22 (1):95-105. doi:10.1101/gr.125146.111

Taylor-Teeples M, Lin L, de Lucas M, Turco G, Toal TW, Gaudinier A, Young NF, Trabucco GM, Veling MT, Lamothe R, Handakumbura PP, Xiong G, Wang C, Corwin J, Tsoukalas A, Zhang L, Ware D, Pauly M, Kliebenstein DJ, Dehesh K, Tagkopoulos I, Breton G, Pruneda-Paz JL, Ahnert SE, Kay SA, Hazen SP, Brady SM (2015) An Arabidopsis gene regulatory network for secondary cell wall synthesis. Nature 517 (7536):571-575. doi:10.1038/nature14099

Ter-Mikaelian MT, Colombo SJ, Lovekin D, McKechnie J, Reynolds R, Titus B, Laurin E, Chapman AM, Chen JX, MacLean HL (2015) Carbon debt repayment or carbon sequestration parity? Lessons from a forest bioenergy case study in Ontario, Canada. Gcb Bioenergy 7 (4):704-716. doi:10.1111/gcbb.12198

Vermaas JV, Petridis L, Qi XH, Schulz R, Lindner B, Smith JC (2015) Mechanism of lignin inhibition of enzymatic biomass deconstruction. Biotechnol Biofuels 8. doi:ARTN 217 10.1186/s13068-015-0379-8

Yamaguchi M, Mitsuda N, Ohtani M, Ohme-Takagi M, Kato K, Demura T (2011) VASCULAR-RELATED NAC-DOMAIN7 directly regulates the expression of a broad range of genes for xylem vessel formation. Plant J 66 (4):579-590. doi:10.1111/j.1365-313X.2011.04514.x

Yang Y, Li R, Qi M (2000) In vivo analysis of plant promoters and transcription factors by agroinfiltration of tobacco leaves. Plant J 22 (6):543-551. doi:tpj760 [pii]

Zhao CS, Craig JC, Petzold HE, Dickerman AW, Beers EP (2005) The xylem and phloem transcriptomes from secondary tissues of the Arabidopsis root-hypocotyl. Plant Physiol 138 (2):803-818. doi:10.1104/pp.105.060202

Zhong R, Lee C, Zhou J, McCarthy RL, Ye ZH (2008) A battery of transcription factors involved in the regulation of secondary cell wall biosynthesis in Arabidopsis. Plant Cell 20 (10):2763-2782. doi:10.1105/tpc.108.061325

Zhong R, McCarthy RL, Haghighat M, Ye ZH (2013) The poplar MYB master switches bind to the SMRE site and activate the secondary wall biosynthetic program during wood formation. PLoS One 8 (7):e69219. doi:10.1371/journal.pone.0069219

Zuo J, Niu QW, Chua NH (2000) Technical advance: An estrogen receptor-based transactivator XVE mediates highly inducible gene expression in transgenic plants. Plant J 24 (2):265-273. doi:tpj868 [pii]

Table 2S.1. **Primer Table**

Upstream Prom	Potri ID	Primer 5' to 3'
Pal3s	Potri.010G22410	GGTACCTACCATGCACTCGCAATGAA
Pal3as	Potri.010G22410	ACTAGTCGTGAATCTTGACAAAATTCCT
CaCOs2	Potri.009G099800	GGTACCGCTTACTTAGTTAGCATACGAATCTAGAG
CaCOas	Potri.009G099800	ACTAGTGACCTCAATTTTGGGATCTATG
HCTS	Potri.003G183900	GGTACCCACTCATTCATGAATATATGGGCTC
HCTAS	Potri.003G183900	ACTAGTCTCCTTCACGTTGATTATCAAC
Revs	Potri.004G211300	GGTACCGAAGCGTACTATCTAGAAGACGAG
RevAS	Potri.004G211300	ACTAGTTCTGCTGTGTACCGAACATACTTC
Ark2s	Potri.002G113300	GGTACCGAAGTTAACGACCATGTTAGCCTC
Ark2as	Potri.002G113300	ACTAGTCACTCATTTGATTGTTGTCCTCC
PtrXCP2s	Potri.002G005700	GGGGACAACTTTGTATAGAAAAGTTGTGTCAGTGACTGTGAGTGCACTCC
PtrXCP2as	Potri.002G005700	GGGGACTGCTTTTTTGTACAAACTTGAATTGGCGAAGAATGAGATG
amRADP1	Potri.002G260000	CCTCTGGTCAGTGTAGTTGGGCAGTTGTGGCTCTTCCTTTTC
amRADP2	Potri.002G260000	AACTGCCCAACTACACTAGCAGAGGGTAGAGCCAAAACAAG
amRADP3	Potri.002G260000	AACTACCCAACTACAGTAGCAGTGGATGGAGCTACTAACAG
amRADP4	Potri.002G260000	CCACTGCTACTGTAGTTGGGTAGTTCATCTGTCTCTGCTCC
amDRIFPP1	Potri.007G132700	CCTTGCTTCATTAGTTCTGGCACTTGTGGCTCTTCCTTTTC
amDRIFPP2	Potri.007G132700	AAGTGCCAGAACTAATGAAGCAAGGGTAGAGCCAAAACAAG
amDRIFPP3	Potri.007G132700	AAGTACCAGAACTAAAGAAGCATGGATGGAGCTACTAACAG
amDRIFPP4	Potri.007G132700	CCATGCTTCTTTAGTTCTGGTACTTCATCTGTCTCTGCTCC
amPB23P1	Potri.014G066200	CCTTGAAATTGATGGAACTTGGCTTGTGGCTCTTCCTTTTC
amPB23P2	Potri.014G066	AAGCCAAGTTCCATCAATTTCAAGGGTAGAGCCA

	200	AAACAAG
amPB23P3	Potri.014G066200	AAGCAAAGTTCCATCTATTTCATGGATGGAGCTACTAACAG
amPB23P4	Potri.014G066200	CCATGAAATAGATGGAACTTTGCTTCATCTGTCTCTGCTCC
LMX5s	Potri.002G101200	AAGCTTGATGCAAAAGCTGGAATGAG
LMX5as	Potri.002G101200	TTAATTAAAGAAGAAGGTGTTTGGGTTGC
LMX5 494SRDX s	Potri.009G042600	CCTAGGATGAAGTGGGAAACGGAAATC
LMX5 494SRDX as	Potri.009G042600	GAGCTCTTAAGCGAAACCCAAACGGAGTTCTAGATCCAGATCTAGCCCGGGTCCATGAGG
Pal3s/G	Potri.010G22410	CACCTACCATGCACTCGCAATGAA
Pal3as/G	Potri.010G22410	CGTGAATCTTGACAAAATTCCT
CaCOs/G	Potri.009G099800	CACCGCTTACTTAGTTAGCATACGAATCTAGAG
CaCOas/G	Potri.009G099800	GACCTCAATTTTGGGATCTATG
HCTS/G	Potri.003G183900	CACCCACTCATTCATGAATATATGGGCTC
HCTAs/G	Potri.003G183900	CTCCTTCACGTTGATTATCAAC
PtrXCP2s/G	Potri.002G005700	CACCTGTCAGTGACTGTGAGTGCACTCC
PtrXCP2as/G	Potri.002G005700	ATTGGCGAAGAATGAGATG

Chapter 3

DIVARICATA AND RADIALIS INTERACTING FACTOR (DRIF) also interacts with WOX, and KNOX proteins associated with wood formation in *Populus trichocarpa*

Abstract

DIVARICATA AND RADIALIS INTERACTING FACTOR (DRIF) from snapdragon (*Antirrhinum majus*) is a MYB/SANT protein that interacts with related MYB/SANT proteins, RADIALIS and DIVARICATA, through its N-terminal MYB/SANT domain. In addition to the MYB/SANT domain, DRIF contains a C-terminal Domain of Unknown Function (DUF3755). Here we describe novel protein-protein interactions involving a poplar (*Populus trichocarpa*) homolog of DRIF, PtrDRIF1. In addition to interacting with poplar homologs of RADIALIS (PtrRAD1) and DIVARICATA (PtrDIV4), PtrDRIF1 interacted with members of other families within the homeodomain-like superfamily, including PtrWOX13c, a WUSCHEL-RELATED HOMEOBOX protein, and PtrKNAT7, a KNOTTED1-LIKE HOMEOBOX protein. PtrRAD1 and PtrDIV4 interacted with the MYB/SANT-containing N-terminal portion PtrDRIF1, while DUF3755 was both necessary and sufficient for interactions with PtrWOX13c and PtrKNAT7. Of the two MYB/SANT domains present in PtrDIV4, only the N-terminal MYB/SANT domain interacted with PtrDRIF1. GFP-PtrDRIF1 expressed alone or with PtrRAD1 localized to the cytoplasm, while co-expression of GFP-PtrDRIF1 with PtrDIV4, PtrWOX13c, or PtrKNAT7 resulted in nuclear localization of GFP-PtrDRIF1. Modified yeast two-hybrid and BiFC experiments using PtrDRIF1 as a bridge protein revealed that PtrDRIF1 simultaneously interacted with PtrRAD1 and PtrWOX13c but could not form a heterotrimeric complex when PtrKNAT7 was substituted for PtrWOX13c or when PtrDIV4 was substituted for PtrRAD1. The discovery of an additional protein-protein interaction domain in DRIF proteins, DUF3755, and its ability to form heterodimers and heterotrimers involving MYB/SANT and wood-associated homeodomain proteins implicates DRIF proteins as mediators of a broader array of processes than previously reported.

Introduction

Plant organ polarity and morphology depend on the interactions of a variety of transcription factors (TFs). For example, the bilateral symmetry of snapdragon (*Antirrhinum majus*) flowers is regulated by five TFs: *CYCLOIDEA* (*CYC*), *DICHOTAMA* (*DICH), RADIALIS* (Liu et al.), *DIVARICATA* (*DIV*) and *DIVARICATA and RADIALIS INTERACTING FACTOR* (*DRIF*). CYC and DICH are two partially redundant TFs belonging to the TCP family. CYC and DICH promote the expression of *RAD*, and together these three genes specify dorsal identity, while DIV promotes ventral identity in snapdragon flowers (Luo et al. 1999; Luo et al. 1996; Corley et al. 2005; Almeida et al. 1997; Galego and Almeida 2007; Hileman 2014). Although expression of *RAD* is limited to the dorsal region, *DIV* is expressed in both dorsal and ventral regions of the flower (Raimundo et al. 2013). However, as proposed by Raimondo et al. (2013), RAD protein prevents DIV from promoting ventral identity in the dorsal region by competing with DIV for interaction with DRIF. As a result of this competition, transcriptional activation mediated by the DIV-DRIF heterodimer occurs only in the ventral region, while DRIF protein is sequestered in a transcriptionally inactive RAD-DRIF heterodimer in the dorsal region.

RAD possesses a single MYB/SANT domain and no other known conserved domains. DRIF proteins contain a single MYB/SANT domain located in the N-terminal half and a DUF3755 domain near the C-terminus. DIV includes two MYB/SANT domains, with the N-terminal MYB/SANT domain sharing a higher degree of similarity with the single MYB/SANT domain of RAD and DRIF, while the second MYB-like domain in DIV corresponds to the SHAQKY class of MYB/SANT domain proteins (Rose et al. 1999). MYB family TFs are known to form dimers (Lu et al. 2002). Work with snapdragon RAD, DIV, and DRIF and homologous proteins from tomato (FSM1, MYBI and FSB1, respectively) has shown that the single MYB/SANT domain in RAD and DRIF and the N-terminal MYB/SANT domain in DIV antagonistically mediate formation of the RAD-DRIF and DIV-DRIF heterodimers, while the second MYB/SANT domain in DIV binds to I-box consensus DNA sequences to activate target genes. (Machemer et al. 2011; Raimundo et al. 2013; Rose et al. 1999).

Although current understanding of RAD and DIV functions are derived mainly from investigations of floral bilateral symmetry in snapdragon, divergent roles for RAD homologs

have come to light from work with Arabidopsis and tomato. Overexpression of the Arabidopsis *RAD* homolog *RSM1* resulted in defects in gravitropism and altered morphology of dark-grown seedlings, including failure to form the apical hook and reduction in hypocotyl length, phenotypes similar to those of the *HOOKLESS1* loss-of-function mutant, *hls1-1* (Hamaguchi et al. 2008). Overexpression of the tomato *RAD* homolog *FSM1* led to a loss of apical dominance and growth retardation in tomato and Arabidopsis (Barg et al. 2005). Overexpression of *FSM1* also reduced tomato fruit size through suppression of cell expansion in the pericarp, potentially due to competition between FSM1 and the tomato DIV homolog, MYBI, for binding to the tomato DRIF homolog, FSB1 (Machemer et al., 2011). Considered together, the work with snapdragon, tomato, and Arabidopsis implicates antagonistic RAD-DRIF and DIV-DRIF dimer formation in the control of plant growth and morphology, potentially through regulation of differential cell growth.

As part of our ongoing efforts to identify and characterize novel protein-protein interactions among regulatory proteins associated with wood formation in poplar, we used the yeast two-hybrid (Y2H) system to screen a poplar xylem cDNA library for proteins that interact with PtrRAD1, a poplar homolog of RAD that is upregulated in xylem (Rodgers-Melnick et al. 2012a). Consistent with previous investigations involving RAD, PtrRAD1 interacted with a poplar homolog of DRIF (PtrDRIF1) and PtrDRIF1 interacted with multiple poplar homologs of DIV. Surprisingly, PtrDRIF1 also interacted with additional homoeodomain (HD)-like superfamily members, PtrWOX13c and PtrKNAT7, not previously identified as DRIF interactors. Functions for *PtrWOX13c* have not been reported, although it is known to be highly upregulated in poplar xylem relative to other tissues (Rogers-Melnick et al. 2012). *PtrKNAT7* is likewise highly upregulated in xylem and appears to be functionally equivalent to the Arabidopsis *KNAT7* gene (Li et al. 2012a). Arabidopsis KNAT7 is a transcriptional repressor involved in negative regulation of secondary cell wall formation in xylem (Liu et al. 2014a). KNAT7 functions are partly dependent on its heterodimerization with the BELL1-LIKE HOMEODOMAIN protein BLH6. Here we show that these newly identified DRIF-binding proteins (PtrWOX13c and PtrKNAT7) interact with DUF3755 within the C-terminal portion of PtrDRIF1. DUF3755 was not previously known as a protein-protein interaction domain. Additionally, we demonstrate that PtrDRIF1 can form a heterotrimer with PtrRAD1 and

PtrWOX13c, but not with other combinations of DRIF interactors tested here. These findings expand the possibilities for DRIF-mediated regulation of gene expression beyond those previously reported for snapdragon and tomato DRIF proteins that form heterodimers with RAD or DIV.

Materials and Methods

Cloning

Cloning and sequencing of constructs was done in pENTR^{TM}/D-TOPO as per instructions in the manual (Invitrogen, Carlsbad, CA), LR Clonase was used as per directions in the insert (Invitrogen) into recipient AD-Dest, or DB-Dest vectors, destination vectors were also sequenced.

For subcellular localization the ORFs of *PotriRAD*, *PotriDIV1*, *PotriDIV4*, *PotriDIV5*, *PotriDIV6*, *PotriWOX13c*, and *PotriKNAT7* were cloned using Gateway technology (Invitrogen) into binary vector pK7WG2 (Karimi et al. 2005) for ectopic expression. Primers are listed in **Table 3.S3.**

Yeast two-hybrid assay

Preparation of competent yeast (*Saccharomyces cerevisiae*) strain Y8800 MTAa or MV203α cells by LiAc method and yeast transformation was carried out according to Yeast Protocols Handbook (BD Biosciences). After 2-3 days, transformed yeast cells were harvested and washed three times in sterile water. Five µl of yeast cells (OD_{600} = 1, 0.1, or 0.01) were spotted on synthetic dropout medium lacking tryptophan and leucine (SD -Trp –Leu), or tryptophan, leucine, and histidine (SD -Trp –Leu -His), or tryptophan, leucine, and adenine (SD -Trp –Leu -Ade) for yeast two-hybrid assays. All proteins cloned in DB-DEST vectors (Walhout and Vidal 2001) were tested for autoactivation on SD -Trp –Leu -His media. Autoactivators were used either exclusively as clones in AD-DEST vectors or, in cases of minimal autoactivation, background yeast growth on SD -Trp –Leu -His media was suppressed through addition of 3-Amino-1,2,4-triazole (3AT) at levels indicated in figure legends, DB-PotriDRIF1 required 20mM 3-AT routinely. Repeatability of protein-protein interactions and deletion analyses were verified through two or more replicated assays.

Modified 3-way Yeast two-hybrid experiments and competition assay

The protocol of Walhout and Vidal (2001) was followed as in our Y2H protocol, strain Y8800 MTAa was used. A three vector system was utilized using the same DB-Dest vector as previously in our Y2H. The second vector was constructed by changing pAD-Dest vector for kanMX resistance by deletion of the Trp resistance cassette and insertion of the kanMX resistance cassette by homologous recombination to create Vector pAD-kanMX. The kanMX cassette was amplified from pUG6 (Guldener et al. 1996); (GenBank: AF298793.1; a gift from Dr. Pilot) using iProof high-fidelity DNA polymerase (Bio-Rad, Hercules, CA) with primers KanMXs and KanMXas, each comprised of ~20 nt partition homologous to the kanMX module and of ~40 nt partition homologous to the upstream or downstream of the coding region of Trp in pAD. Purified PCR products were co-transformed with purified Bsu36 I-linearized pAD vector into yeast strain AH109 for gap repair. Yeast colonies were selected on YPD plates containing 200 mg/L G418. Yeast plasmid DNA was isolated by using Zymoprep™ Yeast Plasmid Miniprep II (Zymo Research, Irvine, CA) and transformed in E. coli (One Shot ccdB survival competent cells, Invitrogen, Carlsbad, CA). Colonies were selected on LB plates containing 100 mg/L ampicillin. Plasmid DNA from E. coli was isolated by using GenCatch ^{TM} Plasmid DNA Mini-Prep Kit (Epoch, Sugar Land, TX). AD-PtrWOX13C used this vector in the Y2H bridge.

A similar strategy was used to construct the third vector pΔAD-Dest. The gateway cassette of pAD-Dest was amplified by PCR with primers using primers Yeast3_s and Yeast3_as. Purified PCR products were co-transformed into yeast AH109 with purified Afe I/Sma I-linearized pAD-Dest vector. Yeast colonies were selected on SD/-Trp plates. The following steps were the same as the construction of pAD-kanMX (replacing Trp).

The NLS was amplified from the AD-Dest vector then cloned into pENTR^{TM}/D-TOPO using LR clonase into recipient vector pΔAD-Dest to create NLS-vector for the negative control. The (pΔAD-Dest) NLS:PotriKNAT7 and (pΔAD-Dest) NLS:PotriDRIF vectors were cloned using the primers listed in **Table 3.S4**. All vectors and inserts were sequenced. The Y2H bridge experiment results were verified > 3 times.

Subcellular localization experiments

Subcellular localization was performed by transient expression in the leaves of 2-4 week old *N.benthamiana* using *Agrobacterium tumafaciens* strain GV3101. Plants were inoculated with either GFP::PotriDRIF plus vector alone (negative control) or a combination of GFP::PotriDRIF plus effector protein. A minimum of three independent replicates were performed for all combinations. Leaves were analyzed for subcellular localization 48-72 hours post inoculation.

Expression, purification of recombinant proteins

For expression in *E. coli* as GST-tagged proteins, ORFs for *PotriDRIF1*, *PotriWOX13c*, and *PotriKNAT7* were cloned into pGEM-T Easy (Promega, Madison, WI), inserts were released by digestion with BamH I and Xma I and ligated into PGEX 4T-1 (GE Healthcare, Buckinghamshire, UK). GST fusions were purified using GST SpinTrap™ columns according to the manufacturers' instructions in the product booklet (28-09523-59, GE Healthcare). Equal concentrations as measured using the BCA Protein assay kit (23250, Pierce) of fusion proteins and GST controls were bound to the columns for pull-down assays.

Pull-downs of GFP-tagged proteins

The constructs for GFP::PotriDRIF and GFP::PotriRAD were cloned into vector pK7WGF2 as N-terminal GFP fusions (Karimi et al. 2005). Infiltrated leaves of *N. benthamiana* were checked by fluorescence microscopy for GFP 3 days post-inoculation. Protein was extracted from GFP-positive leaves by homogenizing 0.1 g leaf tissue in 1 mL of freshly prepared IP buffer (50 mM Tris-HCl, pH 7.5, 150 mM NaCl, 0.5% (v/v) NP-40, 5mM β-Mercaptoethanol, 1% (v/v) Halt protease cocktail (Thermo Scientific). The homogenate was centrifuged at 10,000 x g for 15 minutes at 4° C. Clarified supernatant (500 µL) was added to SpinTrap™ columns pre-loaded with either GST-fusion protein or GST only (negative control). Columns were rotated for 2 hours at 4° C, washed with 15 bed volumes of buffer TBST (25mM Tris-HCL, pH 7.5, 5mM B-ME, 150mM NaCl, 0.5% (v/v) Tween-20, 1% (v/v) Halt protease cocktail (Thermo Scientific). A 10 µL slurry of GST-beads, representing 5% of the beads, was boiled in SDS-PAGE sample buffer and analyzed by Western Blot using anti-GFP primary antibody (A11122 Invitrogen, Carlsbad, CA), and secondary antibody IgG-HRP (4054-05, Southern Biotech, Birmingham, AL). Western Blots were developed using ECL™ Prime Western Blotting Detection Reagents (RPN2232, GE Healthcare) according to manufacturer's instructions prior to chemiluminescence detection on ChemiDoc™ plus XRS system (Bio-Rad, Hercules, CA)

Bimolecular fluorescence complementation bridge experiments

To clone vectors pFGC5941_35S-NYFP and pFGC5941_35S-CYFP used for BiFC bridge (BiFCB) assays, the N-terminal and C-terminal portions of YFP were amplified from pSPYNE-35S and pSPYCE-35S, a gift from Klaus Harter (Walte et al., 2004), using primers P501 N-YFPs, P502 N-YFPas, P503 C-YFPs, P504 C-YFPas (Table S4). PCR products were cloned into pGEM-T Easy. NYFP and CYFP were then subcloned into pFGC5941 by digesting pGEM-NYFP or pGEM-CYFP with Sac I, blunting the resulting 5' overhang with klenow treatment, followed by digestion with Xma I, and ligation into pFGC5941, providing multiple cloning sites Xho I, BamH I, and Sma I upstream of the first ATG of NYFP or CYFP and generating pFGC5941_35S-NYFP and pFGC5941_35S-CYFP. The ORF of *PotriRAD* was cloned upstream of NYFP using the Xho I and BamH I restriction sites, the ORF of *PotriWOX13c* was cloned upstream of CYFP using the Xho I and BamH I restriction sites in pFGC5941_35S-CYFP, primers are listed in Table S3. PotriDRIF1 bridge protein was cloned into binary vector pK7WG2, empty pK7WG2 vector was used as a control. The BiFCB assays were first visualized under a light microscope using excitation and the appropriate filters compared to negative controls. Three separate biological replicates were compared to confirm results prior to capturing images by confocal microscopy. Transient expression in *N. bethamiana* for BiFC experiments was as described previously for GFP-fusion proteins.

Bimolecular fluorescence complementation experiments

The protocol of (Gookin and Assmann 2014) Gookin and Assman (2014) was followed for BiFC to show interactions occurring between PotriWOX13c, PotriKNAT7, and DUF3755. The vector used was pDOE-01, which contains the *35s* promoter in front of N and C-terminal Venus 210 fusion proteins allowing single vector construction of X::NmVenus210--X::CVenus210 . Cloning was done using the In-Fusion® HD Cloning Kit (Clontech, Mountain View, CA) utilizing the primers listed in Table S3 directly into vector CD3- 1901 as per the protocol in the In-Fusion manual (Clontech) . DUF3755 was inserted in-frame into the vector CD3-1901 to create the parent vector DUFD::NmVenus210--X::CVenus210. In-frame C-terminal constructs were made for the ORFS of *PotriWOX13c*, *PotriKNAT7*, and *PotriDIV4*, primers are listed in Table S3, these constructs were all made in parent vector DUFD::NmVenus210--X::CVenus210. Full-length PotriDRIF::NmVenus210—X::CVenus210 parent vector was constructed by the same method and the ORF of *PotriDIV4* was inserted into the parent vector as a C-terminal in-

frame fusion. *A. tumafaciens* GV3101 cultures containing constructs were inoculated at OD 0.100 except for DUFD::NmVenus210—PotriDIV4::CVenus210 was inoculated at OD 0.150. Three separate biological replicates were compared to confirm results prior to capturing images by confocal microscopy. Transient expression in *N. bethamiana* for BiFC experiments were as described previously for subcellular localization.

RNA seq data analysis

STAR mapped read files from Immanen et al., (2016) were obtained from the Array Express database under the accession number E-MTAB-4631. RNAseq data was processed and samples were labelled according to Petzold and Rigoulot et al., (2017). As per that manuscript the section order became "Phloem 1 (P1),Phloem 2 (P2), Phloem/Cambium (PC), Cambial Zone 1 (CZ1), Cambial Zone 2 (CZ2), Cambium/Xylem (CZ), Young Xylem 1 (YX1), Young Xylem 1 (YX2), Transition Xylem (TX), Mature Xylem 1 (MX1), Mature Xylem 2 (MX2) and Mature Xylem 3 (MX3)". FPKM (average) and replicate FPKM values for genes relevant to DRIF experimentation, used to generate Figure 1, were obtained from cummeRbund analysis software.

Phylogenetic analyses

DRIF, RAD/DIV, KNOX and BELL family sequences were obtained from predicted proteome or protein databases by BLASTP, querying with representative family members. For each family, protein sequences were aligned using MUSCLE (Edgar 2004). For the RAD/DIV group, a maximum likelihood phylogenetic analysis was performed on the sequence alignment using the JTT model, a site coverage cutoff of 90% for alignment gaps/missing data and 500 bootstraps for branch support testing with the program MEGA6 (Tamura et al. 2013). All other trees were inferred using the neighbor-joining method and complete deletion of gaps/missing data.

Results

MYB/SANT and HD family proteins interact with PtrDRIF1

The potential for RAD-DRIF and DIV-DRIF heterodimers to regulate cell expansion, a critical component of wood quality, together with the observation that *PtrRAD1* is upregulated in xylem prompted us to perform an Y2H screen for PtrRAD1-interacting proteins in a poplar xylem cDNA library. Consistent with previous reports for homologous proteins from tomato and snapdragon (Machemer et al. 2011; Raimundo et al. 2013), this Y2H screen identified PtrDRIF1 as a PtrRAD1 interactor (**Table 3.S1; Fig. 3.S1**). To determine whether PtrDRIF1 interacted with DIV homologs, we performed a second round of Y2H screening using PtrDRIF1 as bait and recovered a clone for *PtrDIV4* (**Table 3.S1; Fig. 3.1**). Additional PtrDIV homologs, PtrDIV1, PtrDIV5, and PtrDIV6 were tested by binary Y2H assays, and all interacted with PtrDRIF1 (**Figs. 3.S1** and **3.S2**; **Table 3.S2**). In addition to confirming the previously reported RAD-DRIF and DIV-DRIF interactions, the Y2H xylem cDNA library screens yielded clones for two HD family proteins belonging to the ancient clade of *WUSCHEL-RELATED HOMEOBOX* (*WOX*) genes, *PtrWOX13c* and *PtrWOX13a* (**Fig. 3.1b**; **Table 3.S1**; **Fig. 3.S1**) (Liu et al. 2014a). *PtrWOX13c* is highly upregulated in poplar xylem (Rodgers-Melnick et al. 2012a), although its function is currently unknown. To explore the potential diversity of interactions between PtrDRIF1 and HD proteins, several additional HD proteins were tested in binary Y2H assays for interaction with PtrDRIF1. These included representatives of the ancient, intermediate and modern WOX proteins, TALE protein family members from classes I and II KNOTTED1-LIKE HOMEOBOX (KNOX) and BEL1-LIKE HD (BLH) proteins, and class III HD-ZIP proteins (**Fig. 3.S1**; **Table 3.S2**). Of these, only the remaining ancient WOX protein, PtrWOX13b, PtrKNAT7, and an additional member of the class II KNOX proteins (PtrKNAT3a) interacted with PtrDRIF1 (**Figs. 3.1**; **3.S1**; **Table 3.S2**). Analysis of spatially detailed expression data from across the poplar secondary stem (Immanen et al. 2016) revealed that genes encoding PtrDRIF1 interactors were upregulated in developing xylem (**Fig.3.1a**; **Table 3.S3**). In contrast, *PtrDRIF1* was expressed at a similar level across the stem.

The newly discovered DRIF-HD protein interactions were independently tested using GST- and GFP-fusion proteins for pull-downs. As a positive control, we confirmed the previously reported DRIF-RAD interaction using GST-PtrDRIF1 and GFP-PtrRAD1 (**Fig. 3.2a**). In contrast to our

experience with GFP-PtrRAD1, we found that PtrWOX13c and PtrKNAT7 were produced more efficiently as GST fusions than GFP fusions. Hence, GST-PtrWOX13c and GST-PtrKNAT7 were bound to glutathione beads and used to show that GFP-PtrDRIF1 specifically bound to both HD proteins (**Fig. 3.2b** and **c**). Despite the use of protease inhibitors in tobacco leaf extracts, GFP-PtrDRIF1 breakdown products were routinely detected in input lanes, and these varied in abundance and profile among biological replicates of GFP-PtrDRIF1 expression. Notably, however, PtrWOX13c or PtrKNAT7 bound selectively to full-length PtrDRIF1, not the breakdown products thereof.

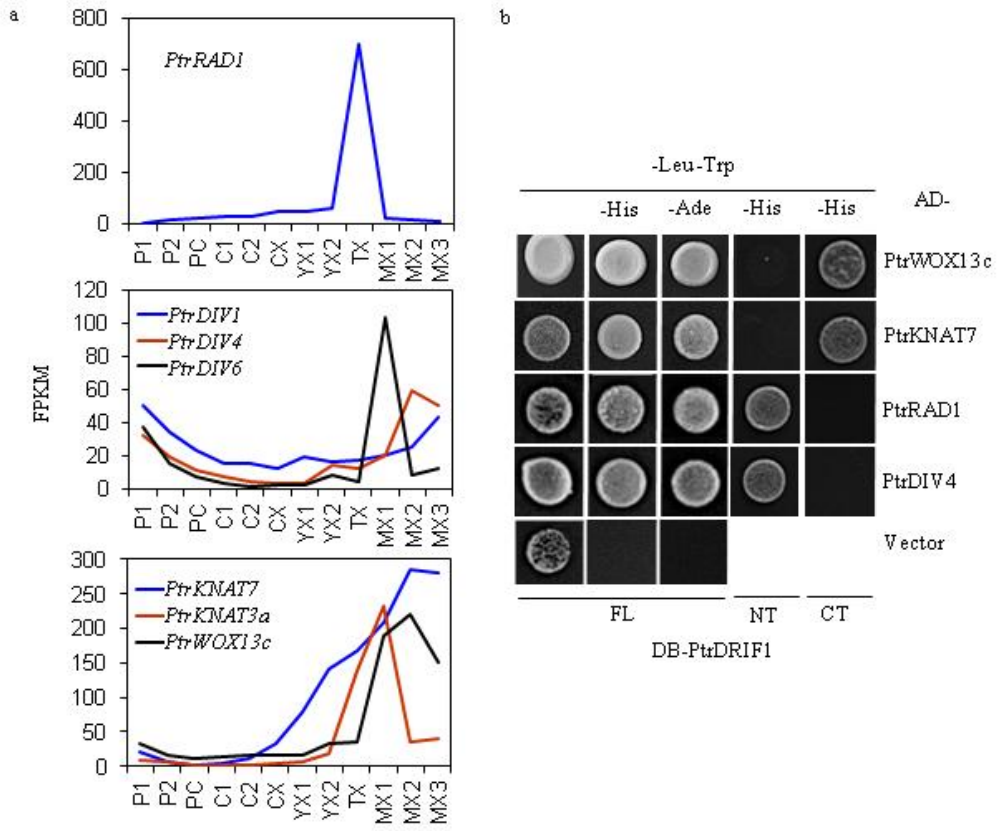

Figure 3.1. PtrDRIF1 interacts with proteins from wood up-regulated genes, *PtrRAD1*, *PtrDIV4*, *PtrWOX13c*, and *PtrKNAT7*.

(a) Gene expression patterns for PtrDRIF1 interactors in phloem, cambium, and xylem are represented as fragments per kilobase of transcript per million mapped reads (FPKM) in all three panels. P1, phloem 1; P2, phloem 2; PC, phloem/cambium; CZ1, cambial zone 1; CZ2, cambial zone 2; CX, cambium/xylem; YX1, young xylem 1; YX2, young xylem 2; TX, transition xylem; MX1, mature xylem 1; MX2, mature xylem 2; MX3, mature xylem 3. (b) DB-PtrDRIF1 interactors were evaluated by yeast two-hybrid assays in synthetic dropout media (−His or –Ade). AD fusion proteins tested are listed at right. NT, the N-terminal MYB/SANT domain of PtrDRIF1 (PtrDRIF1$^{1\text{-}100}$); CT, the C-terminal DUF3755-containing domain of PtrDRIF1 (PtrDRIF1$^{101\text{-}238}$). The PtrDRIF1 NT and CT assays yielded yeast growth on both –His and –Ade; however, for simplicity, only –His results are shown. All –His assays included 20 mM 3-AT.

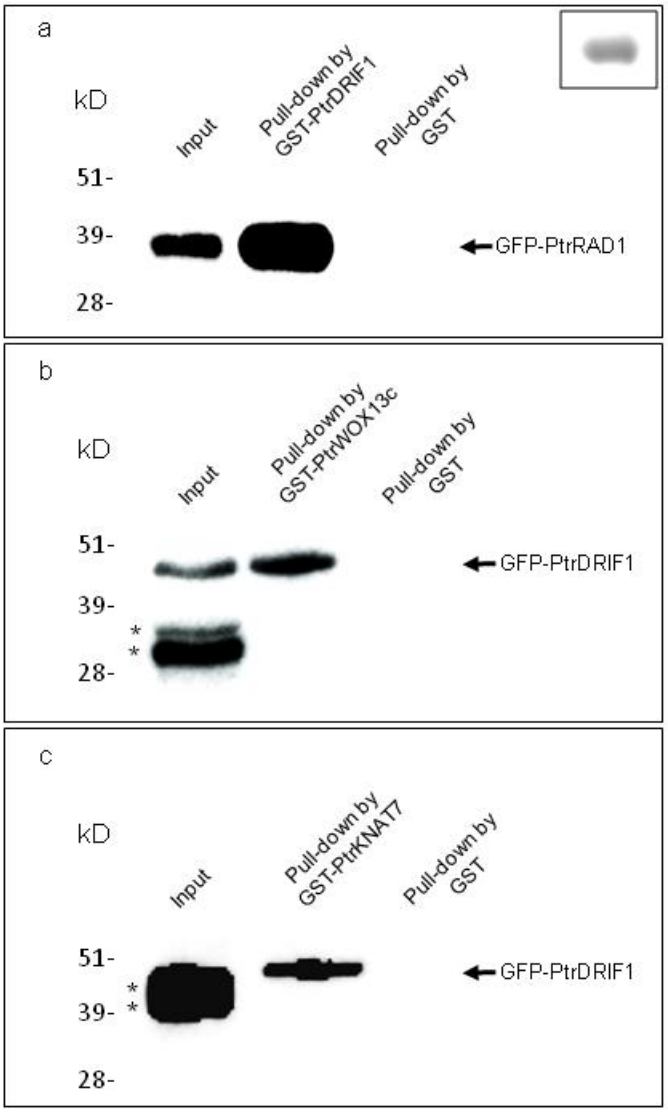

Figure 3.2. GST-fusion protein pull-down assays for PtrDRIF1 interactions with PtrRAD1, PtrWOX13c and PtrKNAT7

(a) GFP-PtrRAD1 bound specifically to GST-PotriDRIF1, not to GST alone. Inset in (a) shows Coomassie-stained GST bound to glutathione beads, representing aliquots used for GST controls in all panels. (b, c) GFP-PtrDRIF1 bound specifically to GST-PtrWOX13c (b) or GST-PotriKNAT7 (c). Lower molecular mass immunoreactive bands (asterisks in b, c) are partial GFP-PtrDRIF1 proteins. Full-length GFP-PtrDRIF1 bound to GST-PtrWOX13c (b) or GST-PtrKNAT7 (c). Input lanes contained 0.5% of total plant extract incubated with glutathione beads. For all GST-fusion proteins and GST-only lanes, 5% of total glutathione bead bed volume was loaded. GFP fusion proteins were detected with anti-GFP antibody for all panels.

Figure 3.3 shows domain organization for PtrDRIF1, PtrRAD1, PtrDIV4, PtrWOX13c, and PtrKNAT7. Interestingly, neither PtrWOX13c nor PtrKNAT7 contains the MYB/SANT domain known to mediate FSM1-FSB1 and MYBI-FSB1 interactions (Machemer et al. 2011). To identify the PtrDRIF1 domain that mediates interactions with PtrWOX13c and PtrKNAT7 we performed Y2H assays with truncated versions of PtrDRIF1 designed to separate the MYB/SANT domain from the DUF3755-containing C-terminal region. We found that the MYB/SANT-containing PtrRAD1 and PtrDIV4 proteins interacted with the MYB/SANT-containing N-terminus of PtrDRIF1 (PtrDRIF1$^{1-100}$) but not with the DUF3755-containing C-terminus (PtrDRIF1$^{101-238}$), consistent with previous work using homologous tomato proteins (Machemer et al. 2011). In contrast, both PtrWOX13c and PtrKNAT7 required the C-terminal portion of PtrDRIF1 for interaction (**Fig. 3.1b**).

To determine whether DUF3755 played a role in the observed interactions between the C-terminal portion of PtrDRIF1 and PtrKNAT7 or PtrWOX13c, additional deletions of DB-PtrDRIF1 were tested by Y2H (**Fig. 3.4a**). Extending the aforementioned N-terminal deletion (PtrDRIF1$^{101-238}$, **Fig. 1**) to eliminate all but DUF3755 and the remaining C-terminal amino acids (PtrDRIF1$^{178-238}$) revealed that these 61 amino acids were sufficient for interaction with PtrWOX13c and PtrKNAT7. However, deletion of just 11 additional amino acids (PtrDRIF1$^{189-238}$), eliminating one of two highly conserved Asn residues in DUF3755 (**Fig. 3.S3**), abolished yeast growth in interaction tests with PtrWOX13c and PtrKNAT7. DUF3755 alone (PtrDRIF$^{178-213}$) was sufficient for interaction with both PtrWOX13c and PtrKNAT7, although growth was observed on –His selection only for PtrKNAT7 (**Fig. 3.4**). Together, the Y2H results for PtrDRIF1 deletions indicate that DUF3755 is both necessary and sufficient for interactions with PtrWOX13c and PtrKNAT7, although the DUF3755 interaction with the latter appears weakened in the absence of the C-terminus of PtrDRIF1.

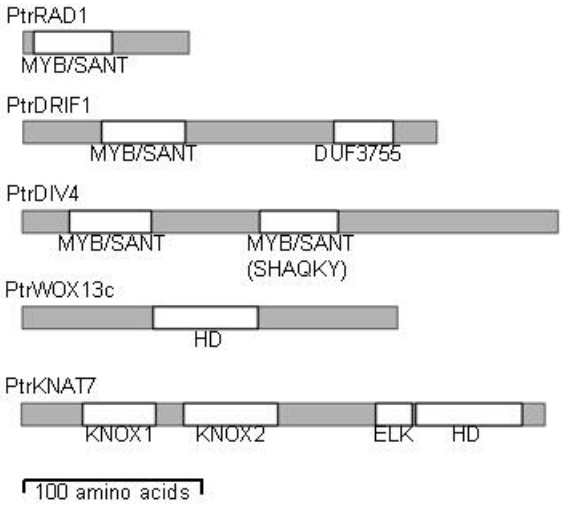

Figure 3.3. Schematic diagram of the conserved domains in PtrDRIF1 and interacting homeodomain-like superfamily proteins

Interacting proteins include MYB/SANT (PtrRAD1, PtrDRIF1, and PtrDIV4), WOX (PtrWOX13c), and KNOX (PtrKNAT7). All protein and domain sizes are drawn to scale.

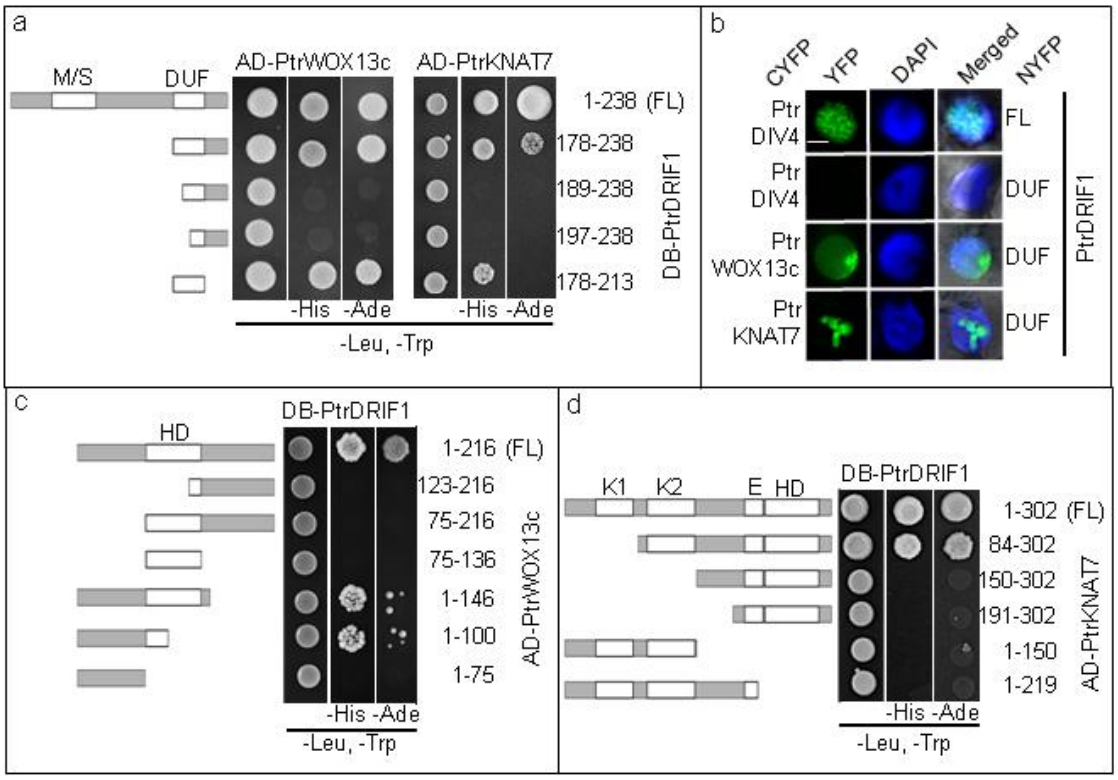

Figure 3.4. Deletion analyses of PtrDRIF1 and its interacting homeodomain proteins PtrWOX13c and PtrKNAT7

(a) Combinations of AD-PtrWOX13c or AD-PtrKNAT7 with DB-PtrDRIF1 deletions were evaluated by yeast two-hybrid assays in synthetic dropout media (−His or –Ade). (b) Confocal microscopy images show interactions between full-length PtrDRIF1 and PtrDIV4 and between DUF3755 and PtrWOX13c and PtrKNAT7 transiently co-expressed in tobacco leaves and detected as reconstituted YFP in the nucleus, as determined by co-localization with DAPI stain. PtrDIV4 with DUF3755 is the negative control. Merged images show YFP, DAPI and transmitted light. Full-length PtrDRIF1 and DUF3755 were fused to the N-terminal portion of YFP (NYFP). PtrDIV4, PtrWOX13c, and PtrKNAT7 were fused to the C-terminal portion of YFP (CYFP). Bar in top left panel is 5 mm for all panels. (c) Analysis of the yeast two-hybrid interaction between full-length DB-PtrDRIF1 and AD-PtrWOX13c deletions. (d) Analysis of the yeast two-hybrid interaction between full-length DB-PtrDRIF1 and AD-PtrKNAT7 deletions. (a, c, d) Deletions are shown schematically (left of panels) and by amino acid positions (right of panels). DUF, DUF3755; E, ELK; FL, full-length protein; HD, homeodomain; K1, KNOX1; K2, KNOX2; M/S, MYB/SANT. All –His assays included 3-AT.

Bimolecular fluorescence complementation (BiFC) was also used to test the ability of the DUF3755 to interact with PtrWOX13c and PtrKNAT7 during transient co-expression in tobacco. Expression of either *DUF3755*::*NmVenus210-PtrWOX13c*::*CVenus210* or *DUF3755*::*NmVenus210-PtrKNAT7*::*CVenus210* resulted in nuclear YFP signal. The negative control vector containing *DUF3755*::*NmVenus210-PtrDIV4*::*CVenus210* lacked the PtrDRIF1 MYB/SANT domain necessary for the PtrDRIF1-PtrDIV4 interaction, and, as expected, did not reconstitute detectable YFP (**Fig 3.4b**). Substitution of full-length PtrDRIF1 for the lone DUF3755 domain in this same vector yielded nuclear YFP signal, demonstrating that while PtrDIV4 is functional in this BiFC assay it does not interact with DUF3755, as indicated in **Figure 1b**. Overall, these BiFC results indicate that DUF3755 is sufficient for interactions with the HD proteins PtrWOX13c and PtrKNAT7, but not the interaction with PtrDIV4, consistent with Y2H results in **Figures 3.1b** and **3.4a**.

Both PtrWOX13c and PtrKNAT7 were tested by deletion analyses in Y2H assays for interaction with full-length PtrDRIF1. The only known conserved domain within PtrWOX13c is the HD (**Fig. 3.3**). The PtrWOX13c HD alone was not sufficient for interaction with PtrDRIF1 (PtrWOX13c$^{75\text{-}136}$). Instead, approximately half of the HD plus the N-terminal region of PtrWOX13c were necessary and sufficient for yeast growth (compare PtrWOX13c$^{1\text{-}100}$ to PtrWOX13c$^{1\text{-}75}$) (**Fig. 3.4c**). PtrKNAT7 is a multi-domain protein comprised of KNOX1 and KNOX2 (both within the MEINOX domain) in its N-terminal half and ELK and HD domains it its C-terminal half (**Fig. 3.3**). **Figure 3.4d** shows that only full-length PtrKNAT7$^{1\text{-}302}$ and PtrKNAT7$^{84\text{-}302}$ (lacking KNOX1) were sufficient for growth on –His and –Ade selection when co-expressed with PtrDRIF1. The KNOX2 domain was necessary (PtrKNAT7$^{150\text{-}302}$) but not sufficient (PtrKNAT7$^{1\text{-}150}$). Eliminating the HD (PtrKNAT7$^{1\text{-}219}$) abolished yeast growth on selection media, while the ELK plus HD together (PtrKNAT7$^{191\text{-}302}$) were not sufficient. In summary, only KNOX1 was expendable, and it appears that KNOX2, HD, and possibly ELK domains together are necessary for interaction with PtrDRIF1. The results for Y2H analyses of deletions of PtrWOX13C and PtrKNAT7 were similar in that co-expression of the HD with PtrDRIF1 was not sufficient to allow yeast growth on selection media. Instead, an N-terminal flanking region combined with at least a portion of the HD was both necessary and sufficient for interaction with PtrDRIF1.

Co-expression of PtrDRIF1 with its interactors alters PtrDRIF1 subcellular localization

Work by Raimundo et al. (2013) indicated that the snapdragon RAD-DRIF1 interaction led to sequestration of DRIF1 in the cytosol, whereas DRIF1 localized to the nucleus upon interaction with DIV. Using transient expression in tobacco, we studied the effects PtrRAD1, PtrDIV homologs, PtrWOX13c, and PtrKNAT7 on GFP-PtrDRIF1 localization. GFP-PtrDRIF1 alone localized mainly to the cytosol, but was also detectable at low levels in the nucleus of a small proportion of cells (**Fig. 3.5a**). Co-expression of *PtrRAD1* with *GFP-PtrDRIF1* resulted in a shift of GFP-PtrDRIF1 from its mainly cytosolic localization pattern to numerous vesicles of various sizes. In contrast, co-expression of *GFP-PtrDRIF1* and any of the four PtrDIV homologs resulted in a near complete shift of the GFP signal from the cytosol to the nucleus (**Figs. 3.5a** and **3.S4**), consistent with previous work with snapdragon DIV and DRIF1 or DRIF2 (Raimundo et al., 2013). PtrWOX13c and PtrKNAT7 were also able to shift GFP-PtrDRIF1 localization to the nucleus (**Fig. 3.5a**). Together, the results from pull-down (**Fig. 3.2**), BiFC (**Fig. 3.4**), and re-localization of GFP-PtrDRIF1 (**Fig. 3.5**) experiments indicate that PtrDRIF1 can interact with PtrRAD1, PtrDIV homologs, PtrWOX13c, and PtrKNAT7 in plant cells. Moreover, the distinct re-localization patterns observed for the PtrRAD1/GFP-PtrDRIF1 combination compared to all other combinations suggests that PtrRAD1 has the potential to mediate availability of PtrDRIF1 not only for interactions with PtrDIV proteins, as reported for homologous snapdragon proteins, but also for interactions with PtrWOX13c and PtrKNAT7.

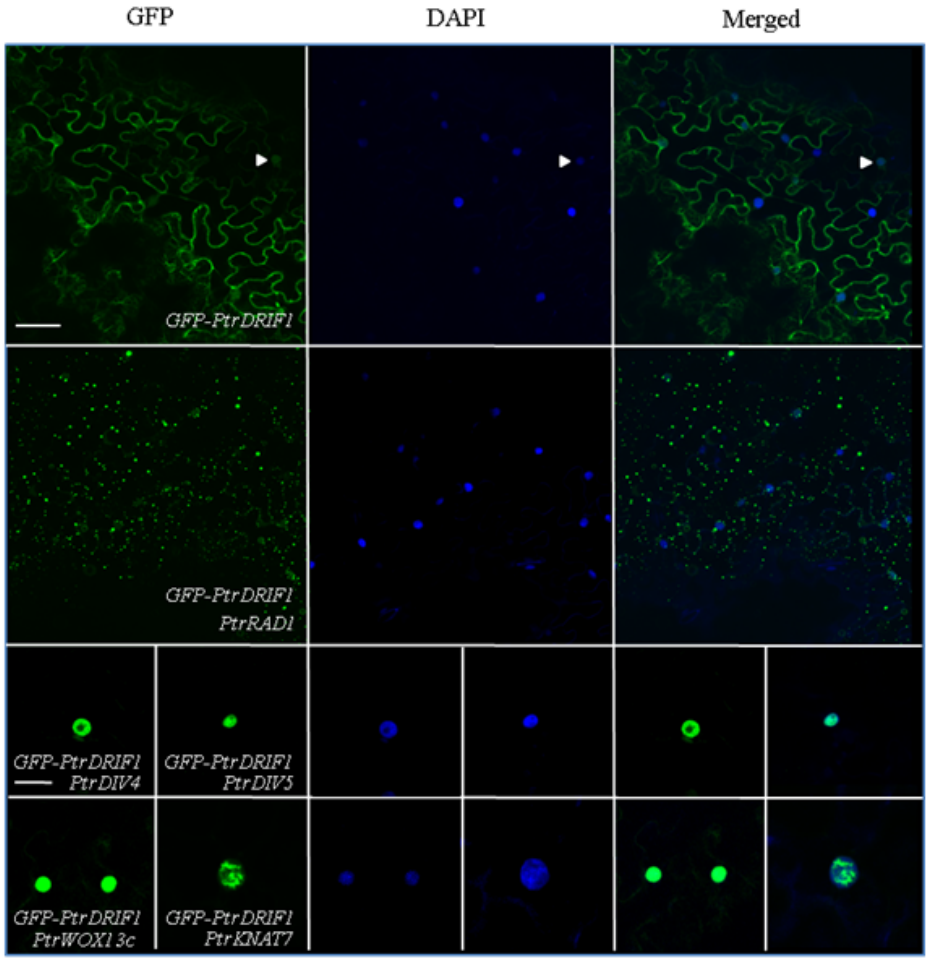

Figure 3.5. GFP-PtrDRIF1 subcellular localization is altered by co-expression with interacting proteins.

Images from confocal microscopy show GFP-PtrDRIF1 (left column), DAPI-stained nuclei (center column) and merger of these images (right column). Tobacco leaf cells were transformed with *GFP-PtrDRIF1* alone (top row) or *GFP-PtrDRIF1* combined with plasmids encoding PtrDRIF1 interactors as indicated (left colum). The 35S promoter was used in all cases. When expressed alone, GFP-PtrDRIF1 localized to the cytosol and at low levels in nuclei (e.g., at arrowhead). Co-expression of *GFP-PtriDRIF1* with *PtrRAD1* shifted localization of GFP-PtrDRIF1 from the cytosol to numerous vesicles. Co-expression of *GFP-PtrDRIF1* with *PtrDIVs*, *PtrWOX13c* or *PtrKNAT7* resulted in nuclear localization of GFP-PtrDRIF1. Bar in upper left panel is 50 mm for all panels in upper two rows. Bar in left panel, third row, is 20 mm for all panels in lower two rows.

PtrDRIF1 forms a heterotrimer with PtrRAD1 and PtrWOX13

DIV and RAD proteins compete for the same MYB/SANT domain when binding to DRIF proteins (Machemer et al., 2011; Raimundo et al., 2013). However, as the HD proteins PtrWOX13c and PtrKNAT7 bind to the DUF3755, it is possible that PtrWOX13c or PtrKNAT7 could bind to PtrDRIF1 simultaneously with PtrRAD1 or PtrDIV proteins, forming heterotrimers. We tested for heterotrimers consisting of PtrRAD1 and PtrWOX13c (the two smallest PtrDRIF1-binding proteins; **Fig. 3.3**) with PtrDRIF1 using a modified Y2H-bridge (Y2HB) assay wherein PtrRAD1 and PtrWOX13c, were fused to the GAL4 DB and AD domains, respectively, and PtrDRIF1 was fused to a nuclear localization sequence (NLS) only (**Fig. 3.6**). The combination of DB-PtrRAD1 and AD-PtrWOX13c in the presence of the empty NLS vector did not activate *His* or *Ade* reporters, indicating that PtrRAD1 and PtrWOX13c do not interact. NLS-PtrDRIF1 and DB-PtrRAD1 in the presence of empty AD vector also failed to activate reporters, confirming that NLS-PtrDRIF1 is not an autoactivator. Only when yeast was co-transformed with DB-PtrRAD1, AD-PtrWOX13c and NLS-PtrDRIF1 were reporters activated, indicating that PtrDRIF1 interacted with PtrRAD1 and PtrWOX13c simultaneously, thereby serving as a bridge between these two non-interacting proteins. In contrast, when heterotrimer formation was tested using DB-PtrDIV5 substituted for DB-PtrRAD1, yeast growth was not observed (**Fig. 3.6a**). However, when PtrDIV5 was truncated to eliminate the C-terminal MYB/SANT domain, yeast growth in the presence of all three proteins (NLS-PtrDRIF1, DB-PtrDIV5$^{1\text{-}97}$, and AD-PtrWOX1c) was observed. PtrDIV5 possessing only the C-terminal MYB/SANT domain (DB-DIV5$^{97\text{-}199}$) did not support yeast growth in the presence of NLS-PtrDRIF and AD-PtrWOX13c (**Fig. 3.6a**). We performed a similar test for heterotrimer formation involving DB-PtrRAD1, AD-PtrKNAT7 and NLS-PtrDRIF1 and did not detect yeast growth (data not shown). Formation of the PtrDRIF1-PtrRAD1-PtrWOX13c heterotrimer was also observed in tobacco cells, using PtrDRIF1 in a modified BiFC bridge assay (BiFCB). YFP was detected only when PtrDRIF1 was co-expressed with PtrRAD1-CYFP and PtrWOX13c-NYFP (**Figs. 3.6b** and **3.S4**). YFP was localized to nuclei consistent with the ability of PtrWOX13c to sequester PtrDRIF1 in the nucleus (**Fig. 3.5**).

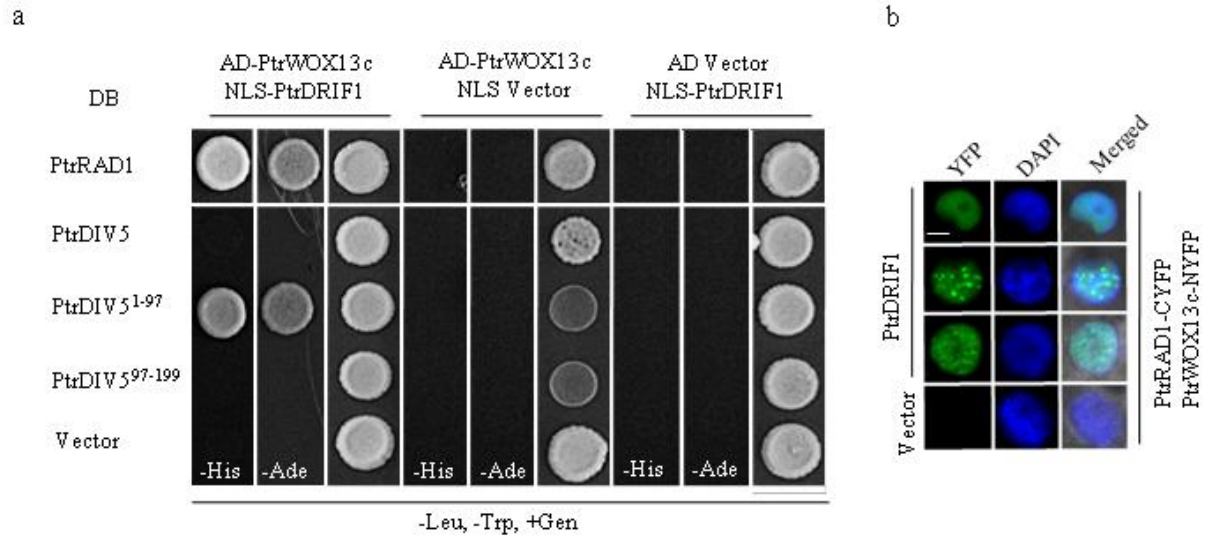

Figure 3.6. Formation of a heterotrimer comprised of PtrDRIF1, PtrRAD1, and PtrWOX13c

(a) A modified yeast two-hybrid assay tested the ability of PtrDRIF1 to function as a bridge protein. DB fusions tested are indicated at left. Columns labeled –His or –Ade show activity of yeast two-hybrid reporters for three distinct combinations of AD and nuclear localization signal (NLS) fusions and vector only controls, shown at top. +Gen, plus geneticin (KanMX) selection for AD vector, -Leu for DB, and –Trp for NLS vector. (b) Confocal microscopy images of bimolecular fluorescence complementation-based detection of PtrDRIF1-PtrRAD1-PtrWOX13c heterotrimer formation. Non-interacting negative control proteins PtrRAD1 and PtrWOX13c fused to the C-terminal (CYFP) and the N-terminal portion (NYFP) of YFP, respectively, and co-expressed without PtrDRIF1 (vector only) are shown in bottom row. Co-expression of PtrDRIF1 with PtrRAD1-CYFP and PtrWOX13c-NYFP resulted in reconstitution of YFP co-localized with DAPI staining, consistent with the ability of PtrWOX13c to target PtrDRIF1 to the nucleus (Fig. 5). Examples from three replicates of transient co-expression experiments in tobacco leaves, show distinct YFP patterns. Merged images show YFP, DAPI and transmitted light. Additional negative controls are shown in Fig. S4. Bar in top panel of YFP column is 5 mm for all panels.

PtrKNAT7 disrupts PtrRAD1-PtrDRIF1 interaction

PtrDIV proteins and PtrKNAT7 are substantially larger than their PtrDRIF1-binding counterparts, PtrRAD1 and PtrWOX13c (**Fig. 3.3**), suggesting that steric hindrance prevented formation of PtrDIV5-PtrDRIF1-PtrWOX13c (**Fig. 3.6**) and PtrRAD1-PtrDRIF1-PtrKNAT7 (data not shown) heterotrimers in Y2HB assays. This hypothesis is consistent with the finding that Y2HB assays using the smaller RAD-like N-terminal domain of PtrDIV5 (DB-PtrDIV5$^{1-97}$) supported heterotrimer formation, while full-length PtrDIV5 did not. To further explore the influence of PtrKNAT7 on interactions between PtrDRIF1 and PtrRAD1, a Y2H competition assay was performed. The two interacting proteins, PtrRAD1 and PtrDRIF1, were fused to GAL4 DB and AD domains, respectively, while PtrKNAT7 was fused to NLS or AD. The combination of DB-PtrRAD1, AD-PtrDRIF1, and NLS-PtrKNAT7 showed a marked decrease in yeast growth for both reporters when compared to the NLS vector control (**Fig. 3.7**). In a similar Y2H competition assay substituting AD-PtrKNAT7 for NLS-PtrKNAT7, yeast growth was inhibited in the presence of AD-PtrKNAT7, DB-PtrRAD, and AD-PtrDRIF1 compared to DB-PtrRAD, AD-PtrDRIF1, and AD vector control (**Fig. 3.S6**). The decrease in PtrRAD1-PtrDRIF1-mediated yeast growth in the presence of PtrKNAT7 (**Figs. 3.7 and 3.S5**), despite the fact that PtrRAD1 and PtrKNAT7 bind to distinct regions of PtrDRIF1 (**Fig. 3.1**), indicates that PtrKNAT7 inhibits the interaction between PtrRAD1 and PtrDRIF1 through steric hindrance or other currently unknown mechanism rather than competitive binding.

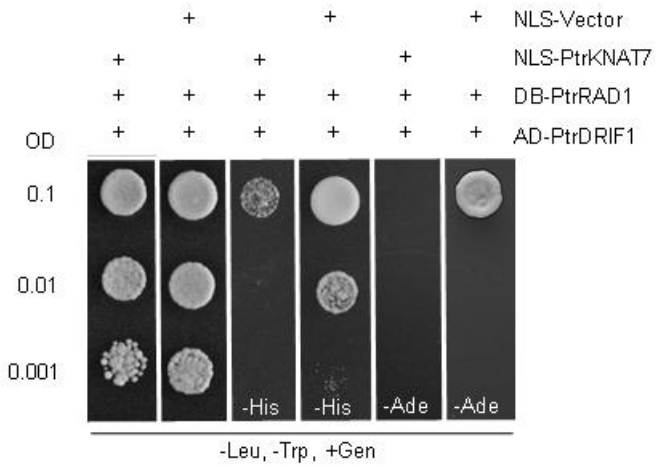

Figure 3.7. Negative impact of PtrKNAT7 on the PtrRAD1-PtrDRIF1 interaction

Combinations of AD-PtrDRIF1 and DB-PtrRAD1 with NLS-PtrKNAT7 or NLS-Vector control were evaluated by yeast two-hybrid assays in synthetic dropout media (−His or –Ade). Vector combinations used for yeast transformation are indicated above columns. NLS, nuclear localization signal; +Gen, plus geneticin (KanMX) selection for the AD vector, -Leu for DB vector, and –Trp for NLS vector; OD, optical density (A_{600}) of yeast cells spotted on plates.

Discussion

The relative abundance of RAD and RAD-DRIF heterodimers as antagonists of DIV-DRIF heterodimer formation and activity is likely to play an important role in the regulation of asymmetric floral development and tomato fruit cell expansion (Machemer et al. 2011; Raimundo et al. 2013). Asymmetric development and cell expansion are also important to the production of secondary xylem and phloem. *PtrRAD1* is expressed at a higher level in xylem relative to other poplar tissues examined by Rogers-Melnick et al. (2012). Hence, we investigated whether protein-protein interactions involving poplar homologs of RAD, DIV, and DRIF were conserved and might therefore be logical subjects for future functional analyses in the context of wood formation. As was the case for homologous proteins from tomato and snapdragon, PtrRAD1 interacted with PtrDRIF1, which also interacted with several PtrDIV homologs (Table 3.S2). These interactions were mediated through their shared MYB/SANT domain, as shown previously for homologous proteins from tomato and snapdragon (Machemer et al. 2011; Raimundo et al. 2013). Surprisingly, in addition to its interactions with PtrRAD1 and PtrDIVs, PtrDRIF1 interacted with HD proteins from the WOX and KNOX families. Although we did not comprehensively test all WOX and KNOX proteins from poplar for interactions with PtrDRIF1, Y2H screens of representatives of ancient, intermediate, and modern WOX, Classes I and II KNOX, BLH, and Class II HD-ZIP proteins indicated that PtrDRIF1 interactions with HD proteins were limited to members of the ancient WOX and Class II KNOX clades (Table 3.S2). Using PtrWOX13c and PtrKNAT7 as representatives of these clades, we performed in vitro pull-down and BiFC assays and independently confirmed their interactions with PtrDRIF1 (**Figs. 3.2 and 3.4**).

A deletion analysis by Y2H partly resolved the necessary and sufficient domains in both PtrDRIF1 and its newly discovered interactors, PtrWOX13c and PtrKNAT7 (**Figs. 3.1 and 3.4**). Importantly, it was shown that DUF3755 was sufficient for the interactions with PtrWOX13c and PtrKNAT7 and that these HD proteins did not interact with the MYB/SANT-containing N-terminal 100-amino acid portion of PtrDRIF1 that was, on the other hand, sufficient for interaction with PtrRAD1 and PtrDIV4. DUF3755 was not previously known to mediate protein-protein interactions. Additionally, PtrWOX13c and PtrKNAT7 both required at least part of their HD and flanking N-terminal amino acids for interaction with PtrDRIF1. The HD

forms a characteristic structure of three alpha helices for DNA-binding. Hence it may not be directly engaged in protein-protein interactions. Rather the HD may influence folding of adjacent domains or improve protein stability, thereby indirectly favoring protein-protein interactions mediated through other motifs within the N-terminal flank of the HD.

Discovery of the second protein-protein interaction domain in PtrDRIF1 raised the possibility that PtrDRIF1 could serve as a scaffold for transcription factor complexes involving MYB/SANT and HD proteins that do not directly interact. Y2HB, BiFCB, and Y2H competition assays were used to test various combinations of MYB/SANT, HD proteins, and PtrDRIF1for heterotrimerization. We determined that PtrDRIF1 was able to bind PtrRAD1 and PtrWOX13c simultaneously but could not bind other tested combinations of proteins, i.e., PtrRAD with PtrKNAT7 or PtrDIV5 with PtrWOX13c. However, removal of the C-terminal MYB/SANT domain of PtrDIV5, creating PrtDIV5$^{1\text{-}97}$, allowed both PrtDIV5$^{1\text{-}97}$ and PtrWOX13c to bind to PtrDRIF1 in heterotrimer formation in Y2HB assays (**Figs. 3.6**). Steric hindrance may have prevented the larger PtrDIV5 and PtrKNAT7 proteins from forming heterotrimers with PtrDRIF1 bound to PtrWOX13c or PtrDIVs, respectively. The discovery that PtrWOX13c and PtrDIV proteins do not simultaneously bind to PtrDRIF1 suggests that PtrWOX13c, similar to RAD, can antagonize DIV-DRIF dimerization. However, distinct from the proposed RAD-based antagonism of DIV-DRIF dimerization, which includes sequestration of a large proportion of cytosolic RAD-DRIF from nuclear DIV, the PtrWOX13c-PtrDRIF1 interaction was linked with nuclear localization, not retention in the cytosol (**Fig. 3.5**).

PtrKNAT7 is implicated in control of wood formation by both its relatively high level of expression in that tissue (Rogers-Melnick et al., 2012; **Fig. 1a**) and the observation that overexpression of *PtrKNAT7* in Arabidopsis rescued loss-of-function *irregular xylem11*/*knat7-1* mutants (Brown et al. 2005; Li et al. 2012a). KNAT7 has been described as a transcriptional repressor that negatively regulates cell wall biosynthesis in xylem and the seed coat. Transcriptional repression by KNAT7 is enhanced by its interaction with a diverse set of transcriptional regulators including Ovate Family Protein 4 (OFP4), MYB75, and BEL6 (Bhargava et al. 2013; Li et al. 2012a; Liu et al. 2014b). The MEINOX domain, in particular the included KNOX2 domain, was necessary and in some cases sufficient for interactions between

KNAT7 and its partners. In the case of OFP4, the HD was also sufficient to support interaction (Li et al., 2011). These findings for KNAT7 are partly in agreement with those reported here for PtrKNAT7 in that the combined KNOX2 and HD regions were necessary for the PtrDRIF1-PtrKNAT7 interaction (**Fig. 3.3**). In contrast to results for KNAT7 deletions, neither the MEINOX nor the HD from PtrKNAT7 was sufficient by itself to support the interaction with PtrDRIF1 (**Fig. 3.3**). PtrDRIF1 is an interesting addition to the growing list of proteins that interact with KNAT7. Moreover, that co-expression of PtrKNAT7 was linked with the movement of GFP-PtrDRIF1 from the cytosol to the nucleus during transient expression in tobacco indicates that the PtrKNAT7-PtrDRIF1 heterodimer may influence PtrKNAT7 function as a transcriptional regulator (**Fig. 3.5**).

WOX genes participate in a diverse array of processes ranging from embryogenesis and meristem maintenance to floral organ formation and lateral organ development (reviewed by (van der Graaff et al. 2009)). *PtrWOX13c* is predicted to be involved in secondary cell wall formation by virtue of its relatively high level of expression in poplar wood-forming tissue (Roger-Melnick et al., 2012; **Fig. 3.1a**) and the reported functions of Arabidopsis *WOX13* (AT4G35550, **Fig. 3.S1**). *WOX13* is expressed in the replum, a meristematic tissue in Arabidopsis fruits (siliques). Lignification of silique valve margins, which facilitate detachment of valves from the replum and thus silique dehiscence, decreased in *35S:WOX13* plants and increased in *wox13* loss-of-function plants. Replums were enlarged in *35S:WOX13* transgenics, possibly due to increased cell proliferation induced by *WOX13* overexpression (Romera-Branchat et al. 2013). Among the modern, intermediate and ancient WOX proteins tested by Y2H for this report, only the latter interacted with PtrDRIF1 in Y2H. Ancient WOX proteins lack the conserved repressor domain (WUS box) found in members of the modern clade (Lin et al. 2013). Therefore, WOX13 may function as a transcriptional activator that negatively regulates differentiation (including lignification) indirectly thorough positive regulation of proliferation (Deveaux et al. 2008; Romera-Branchat et al. 2013).

Proliferation of vascular cambium cells is a critical factor affecting wood quantity, while expansion of vessel elements derived from cambium cells is a determinant of wood density and hydraulic conductivity. The extent of xylem vessel expansion is partly determined by the timing

of the onset of deposition of the secondary cell wall, which prevents further cell expansion due largely to extensive lignin cross-linking. The regulatory mechanisms controlling the transition from vascular cambium cell division to vessel element expansion to lignocellulose deposition are the subjects of intensive investigation in Arabidopsis (Etchells and Turner 2010; Hirakawa et al. 2010; Hirakawa et al. 2008; Ji et al. 2010; Kondo et al. 2014; Suer et al. 2011; Whitford et al. 2008). However, the existence of major distinctions in secondary xylem phenology in trees versus herbaceous plants warrants continued research with additional models for wood formation. Although a role for *WOX13* in secondary xylem has not been reported, its action in the replum provides clues to the potential function of *PtrWOX13c* in wood formation. Specifically, putative functional conservation with *WOX13* combined with wood-associated expression implicates *PtrWOX13c* as a positive regulator of vascular cambium proliferation and negative regulator of lignification of xylem cells. The antagonistic RAD-DRIF/DIV-DRIF regulatory system is implicated in the control of expansion of cells in tomato fruit (Machemer et al. 2011), and the poplar orthologs of these proteins may perform similar roles in the context of wood formation. It will be interesting to determine in future studies whether the newly discovered PtrDRIF1 interactors, PtrWOX13c and PtrKNAT7, are components of a PtrDRIF1-mediated xylem regulatory module for integrating cambium cell proliferation versus commitment to differentiation (PtrWOX13c) with the extent of vessel expansion (PtrRAD1 and PtrDIV) regulated by timing of lignification (PtrKNAT7).

References

Aida M, Ishida T, Fukaki H, Fujisawa H, Tasaka M (1997) Genes involved in organ separation in Arabidopsis: an analysis of the cup-shaped cotyledon mutant. Plant Cell 9 (6):841-857. doi:10.1105/tpc.9.6.8419/6/841 [pii]Almeida J, Rocheta M, Galego L (1997) Genetic control of flower shape in Antirrhinum majus. Development 124 (7):1387-1392Arabidopsis Genome I (2000) Analysis of the genome sequence of the flowering plant Arabidopsis thaliana. Nature 408 (6814):796-815. doi:10.1038/35048692

Avci U, Petzold HE, Ismail IO, Beers EP, Haigler CH (2008) Cysteine proteases XCP1 and XCP2 aid micro-autolysis within the intact central vacuole during xylogenesis in Arabidopsis roots. Plant J 56 (2):303-315. doi:10.1111/j.1365-313X.2008.03592.x

Barg R, Sobolev I, Eilon T, Gur A, Chmelnitsky I, Shabtai S, Grotewold E, Salts Y (2005) The tomato early fruit specific gene Lefsm1 defines a novel class of plant-specific SANT/MYB domain proteins. Planta 221 (2):197-211. doi:10.1007/s00425-004-1433-0

Baxter CE, Costa MM, Coen ES (2007) Diversification and co-option of RAD-like genes in the evolution of floral asymmetry. Plant J 52 (1):105-113. doi:10.1111/j.1365-313X.2007.03222.x

Bhargava A, Ahad A, Wang S, Mansfield SD, Haughn GW, Douglas CJ, Ellis BE (2013) The interacting MYB75 and KNAT7 transcription factors modulate secondary cell wall deposition both in stems and seed coat in Arabidopsis. Planta 237 (5):1199-1211. doi:10.1007/s00425-012-1821-9

Bonan GB (2008) Forests and climate change: forcings, feedbacks, and the climate benefits of forests. Science 320 (5882):1444-1449. doi:10.1126/science.1155121

Brady SM, Zhang L, Megraw M, Martinez NJ, Jiang E, Yi CS, Liu W, Zeng A, Taylor-Teeples M, Kim D, Ahnert S, Ohler U, Ware D, Walhout AJ, Benfey PN (2011) A stele-enriched gene regulatory network in the Arabidopsis root. Mol Syst Biol 7:459. doi:10.1038/msb.2010.114

Brown DM, Zeef LA, Ellis J, Goodacre R, Turner SR (2005) Identification of novel genes in Arabidopsis involved in secondary cell wall formation using expression profiling and reverse genetics. Plant Cell 17 (8):2281-2295. doi:10.1105/tpc.105.031542

Brunner AM, Yakovlev IA, Strauss SH (2004) Validating internal controls for quantitative plant gene expression studies. BMC Plant Biol 4:14. doi:10.1186/1471-2229-4-14

Cassan-Wang H, Goue N, Saidi MN, Legay S, Sivadon P, Goffner D, Grima-Pettenati J (2014) Identification of novel transcription factors regulating secondary cell wall formation in Arabidopsis (vol 4, 189, 2013). Front Plant Sci 5. doi:ARTN 24610.3389/fpls.2014.00246

Chaffey N, Cholewa E, Regan S, Sundberg B (2002) Secondary xylem development in Arabidopsis: a model for wood formation. Physiol Plant 114 (4):594-600

Clough SJ, Bent AF (1998) Floral dip: a simplified method for Agrobacterium-mediated transformation of Arabidopsis thaliana. Plant Journal 16 (6):735-743. doi:DOI 10.1046/j.1365-313x.1998.00343.x

Corley SB, Carpenter R, Copsey L, Coen E (2005) Floral asymmetry involves an interplay between TCP and MYB transcription factors in Antirrhinum. Proceedings of the National Academy of Sciences of the United States of America 102 (14):5068-5073. doi:0501340102 [pii] 10.1073/pnas.0501340102

Demura T, Fukuda H (2007) Transcriptional regulation in wood formation. Trends in plant science 12 (2):64-70. doi:10.1016/j.tplants.2006.12.006

Demura T, Tashiro G, Horiguchi G, Kishimoto N, Kubo M, Matsuoka N, Minami A, Nagata-Hiwatashi M, Nakamura K, Okamura Y, Sassa N, Suzuki S, Yazaki J, Kikuchi S, Fukuda H (2002) Visualization by comprehensive microarray analysis of gene expression programs during transdifferentiation of mesophyll cells into xylem cells. Proc Natl Acad Sci U S A 99 (24):15794-15799. doi:10.1073/pnas.232590499

Deplancke B, Mukhopadhyay A, Ao W, Elewa AM, Grove CA, Martinez NJ, Sequerra R, Doucette-Stamm L, Reece-Hoyes JS, Hope IA, Tissenbaum HA, Mango SE, Walhout AJ (2006a) A gene-centered C. elegans protein-DNA interaction network. Cell 125 (6):1193-1205. doi:10.1016/j.cell.2006.04.038

Deplancke B, Vermeirssen V, Arda HE, Martinez NJ, Walhout AJ (2006b) Gateway-compatible yeast one-hybrid screens. CSH Protoc 2006 (5). doi:10.1101/pdb.prot4590

Deveaux Y, Toffano-Nioche C, Claisse G, Thareau V, Morin H, Laufs P, Moreau H, Kreis M, Lecharny A (2008) Genes of the most conserved WOX clade in plants affect root and flower development in Arabidopsis. BMC Evol Biol 8:291. doi:10.1186/1471-2148-8-291

Dharmawardhana P, Brunner AM, Strauss SH (2010) Genome-wide transcriptome analysis of the transition from primary to secondary stem development in Populus trichocarpa. Bmc Genomics 11. doi:Artn 150 10.1186/1471-2164-11-150

Dortay H, Gruhn N, Pfeifer A, Schwerdtner M, Schmulling T, Heyl A (2008) Toward an interaction map of the two-component signaling pathway of Arabidopsis thaliana. J Proteome Res 7 (9):3649-3660. doi:10.1021/pr0703831

Du J, Groover A (2010) Transcriptional regulation of secondary growth and wood formation. J Integr Plant Biol 52 (1):17-27. doi:10.1111/j.1744-7909.2010.00901.x

Du J, Mansfield SD, Groover AT (2009) The Populus homeobox gene ARBORKNOX2 regulates cell differentiation during secondary growth. Plant J 60 (6):1000-1014. doi:10.1111/j.1365-313X.2009.04017.x

Du J, Miura E, Robischon M, Martinez C, Groover A (2011) The Populus Class III HD ZIP transcription factor POPCORONA affects cell differentiation during secondary growth of woody stems. PLoS One 6 (2):e17458. doi:10.1371/journal.pone.0017458

Du Q, Wang H (2015) The role of HD-ZIP III transcription factors and miR165/166 in vascular development and secondary cell wall formation. Plant Signal Behav 10 (10):e1078955. doi:10.1080/15592324.2015.1078955

Edgar RC (2004) MUSCLE: a multiple sequence alignment method with reduced time and space complexity. BMC Bioinformatics 5:113. doi:10.1186/1471-2105-5-113

Etchells JP, Turner SR (2010) The PXY-CLE41 receptor ligand pair defines a multifunctional pathway that controls the rate and orientation of vascular cell division. Development 137 (5):767-774. doi:10.1242/dev.044941

Fields S, Song O (1989) A novel genetic system to detect protein-protein interactions. Nature 340 (6230):245-246. doi:10.1038/340245a0

Fornale S, Shi X, Chai C, Encina A, Irar S, Capellades M, Fuguet E, Torres JL, Rovira P, Puigdomenech P, Rigau J, Grotewold E, Gray J, Caparros-Ruiz D (2010) ZmMYB31 directly represses maize lignin genes and redirects the phenylpropanoid metabolic flux. Plant J 64 (4):633-644. doi:10.1111/j.1365-313X.2010.04363.x

Fukuda H (1996) Xylogenesis: Initiation, Progression, and Cell Death. Annu Rev Plant Physiol Plant Mol Biol 47:299-325. doi:10.1146/annurev.arplant.47.1.299
Fukuda H, Watanabe Y, Kuriyama H, Aoyagi S, Sugiyama M, Yamamoto R, Demura T, Minami A (1998) Programming of cell death during xylogenesis. J Plant Res 111 (1102):253-256. doi:Doi 10.1007/Bf02512179
Galego L, Almeida J (2007) Molecular genetic basis of flower colour variegation in Linaria. Genet Res 89 (3):129-134. doi:10.1017/S0016672307008786
Goicoechea M, Lacombe E, Legay S, Mihaljevic S, Rech P, Jauneau A, Lapierre C, Pollet B, Verhaegen D, Chaubet-Gigot N, Grima-Pettenati J (2005) EgMYB2, a new transcriptional activator from Eucalyptus xylem, regulates secondary cell wall formation and lignin biosynthesis. Plant J 43 (4):553-567. doi:TPJ2480 [pii]10.1111/j.1365-313X.2005.02480.x
Gookin TE, Assmann SM (2014) Significant reduction of BiFC non-specific assembly facilitates in planta assessment of heterotrimeric G-protein interactors. Plant J 80 (3):553-567. doi:10.1111/tpj.12639
Grant EH, Fujino T, Beers EP, Brunner AM (2010) Characterization of NAC domain transcription factors implicated in control of vascular cell differentiation in Arabidopsis and Populus. Planta 232 (2):337-352. doi:10.1007/s00425-010-1181-2
Groover AT, Mansfield SD, DiFazio SP, Dupper G, Fontana JR, Millar R, Wang Y (2006) The Populus homeobox gene ARBORKNOX1 reveals overlapping mechanisms regulating the shoot apical meristem and the vascular cambium. Plant Mol Biol 61 (6):917-932. doi:10.1007/s11103-006-0059-y
Guldener U, Heck S, Fielder T, Beinhauer J, Hegemann JH (1996) A new efficient gene disruption cassette for repeated use in budding yeast. Nucleic Acids Res 24 (13):2519-2524
Hamaguchi A, Yamashino T, Koizumi N, Kiba T, Kojima M, Sakakibara H, Mizuno T (2008) A small subfamily of Arabidopsis RADIALIS-LIKE SANT/MYB genes: a link to HOOKLESS1-mediated signal transduction during early morphogenesis. Biosci Biotechnol Biochem 72 (10):2687-2696. doi:JST.JSTAGE/bbb/80348 [pii]
Hileman LC (2014) Bilateral flower symmetry--how, when and why? Current opinion in plant biology 17:146-152. doi:10.1016/j.pbi.2013.12.002
Hirakawa Y, Kondo Y, Fukuda H (2010) Regulation of vascular development by CLE peptide-receptor systems. Journal of integrative plant biology 52 (1):8-16. doi:10.1111/j.1744-7909.2010.00904.x
Hirakawa Y, Shinohara H, Kondo Y, Inoue A, Nakanomyo I, Ogawa M, Sawa S, Ohashi-Ito K, Matsubayashi Y, Fukuda H (2008) Non-cell-autonomous control of vascular stem cell fate by a CLE peptide/receptor system. Proceedings of the National Academy of Sciences of the United States of America 105 (39):15208-15213. doi:10.1073/pnas.0808444105
Hiratsu K, Matsui K, Koyama T, Ohme-Takagi M (2003) Dominant repression of target genes by chimeric repressors that include the EAR motif, a repression domain, in Arabidopsis. Plant J 34 (5):733-739
Immanen J, Nieminen K, Smolander OP, Kojima M, Alonso Serra J, Koskinen P, Zhang J, Elo A, Mahonen AP, Street N, Bhalerao RP, Paulin L, Auvinen P, Sakakibara H, Helariutta Y (2016) Cytokinin and Auxin Display Distinct but Interconnected Distribution and Signaling Profiles to Stimulate Cambial Activity. Curr Biol 26 (15):1990-1997. doi:10.1016/j.cub.2016.05.053

Ji J, Strable J, Shimizu R, Koenig D, Sinha N, Scanlon MJ (2010) WOX4 promotes procambial development. Plant physiology 152 (3):1346-1356. doi:10.1104/pp.109.149641
Jin H, Cominelli E, Bailey P, Parr A, Mehrtens F, Jones J, Tonelli C, Weisshaar B, Martin C (2000) Transcriptional repression by AtMYB4 controls production of UV-protecting sunscreens in Arabidopsis. EMBO J 19 (22):6150-6161. doi:10.1093/emboj/19.22.6150
Kalay G, Lusk R, Dome M, Hens K, Deplancke B, Wittkopp PJ (2016) Potential Direct Regulators of the Drosophila yellow Gene Identified by Yeast One-Hybrid and RNAi Screens. G3 (Bethesda) 6 (10):3419-3430. doi:10.1534/g3.116.032607
Karimi M, De Meyer B, Hilson P (2005) Modular cloning in plant cells. Trends Plant Sci 10 (3):103-105. doi:10.1016/j.tplants.2005.01.008
Karpinska B, Karlsson M, Srivastava M, Stenberg A, Schrader J, Sterky F, Bhalerao R, Wingsle G (2004) MYB transcription factors are differentially expressed and regulated during secondary vascular tissue development in hybrid aspen. Plant Mol Biol 56 (2):255-270. doi:DO00003354 [pii] 10.1007/s11103-004-3354-5
Kim WC, Kim JY, Ko JH, Kang H, Han KH (2014) Identification of direct targets of transcription factor MYB46 provides insights into the transcriptional regulation of secondary wall biosynthesis. Plant Mol Biol 85 (6):589-599. doi:10.1007/s11103-014-0205-x
Ko JH, Jeon HW, Kim WC, Kim JY, Han KH (2014) The MYB46/MYB83-mediated transcriptional regulatory programme is a gatekeeper of secondary wall biosynthesis. Ann Bot 114 (6):1099-1107. doi:10.1093/aob/mcu126
Kondo Y, Ito T, Nakagami H, Hirakawa Y, Saito M, Tamaki T, Shirasu K, Fukuda H (2014) Plant GSK3 proteins regulate xylem cell differentiation downstream of TDIF-TDR signalling. Nature communications 5:3504. doi:10.1038/ncomms4504
Kubo M, Udagawa M, Nishikubo N, Horiguchi G, Yamaguchi M, Ito J, Mimura T, Fukuda H, Demura T (2005) Transcription switches for protoxylem and metaxylem vessel formation. Genes Dev 19 (16):1855-1860. doi:19/16/1855 [pii]10.1101/gad.1331305
Kumar M, Campbell L, Turner S (2016) Secondary cell walls: biosynthesis and manipulation. J Exp Bot 67 (2):515-531. doi:10.1093/jxb/erv533
Legay S, Sivadon P, Blervacq AS, Pavy N, Baghdady A, Tremblay L, Levasseur C, Ladouce N, Lapierre C, Seguin A, Hawkins S, Mackay J, Grima-Pettenati J (2010) EgMYB1, an R2R3 MYB transcription factor from eucalyptus negatively regulates secondary cell wall formation in Arabidopsis and poplar. New Phytol 188 (3):774-786. doi:10.1111/j.1469-8137.2010.03432.x
Levyadun S (1994) Induction of Sclereid Differentiation in the Pith of Arabidopsis-Thaliana (L) Heynh. J Exp Bot 45 (281):1845-1849. doi:DOI 10.1093/jxb/45.12.1845
Li C, Wang X, Ran L, Tian Q, Fan D, Luo K (2015) PtoMYB92 is a Transcriptional Activator of the Lignin Biosynthetic Pathway During Secondary Cell Wall Formation in Populus tomentosa. Plant Cell Physiol 56 (12):2436-2446. doi:10.1093/pcp/pcv157
Li E, Bhargava A, Qiang W, Friedmann MC, Forneris N, Savidge RA, Johnson LA, Mansfield SD, Ellis BE, Douglas CJ (2012a) The Class II KNOX gene KNAT7 negatively regulates secondary wall formation in Arabidopsis and is functionally conserved in Populus. The New phytologist 194 (1):102-115. doi:10.1111/j.1469-8137.2011.04016.x
Li EY, Bhargava A, Qiang WY, Friedmann MC, Forneris N, Savidge RA, Johnson LA, Mansfield SD, Ellis BE, Douglas CJ (2012b) The Class II KNOX gene KNAT7 negatively regulates secondary wall formation in Arabidopsis and is functionally

conserved in Populus. New Phytologist 194 (1):102-115. doi:10.1111/j.1469-8137.2011.04016.x
Li L, Zhou Y, Cheng X, Sun J, Marita JM, Ralph J, Chiang VL (2003) Combinatorial modification of multiple lignin traits in trees through multigene cotransformation. Proc Natl Acad Sci U S A 100 (8):4939-4944. doi:10.1073/pnas.0831166100
Li S, Armstrong CM, Bertin N, Ge H, Milstein S, Boxem M, Vidalain PO, Han JD, Chesneau A, Hao T, Goldberg DS, Li N, Martinez M, Rual JF, Lamesch P, Xu L, Tewari M, Wong SL, Zhang LV, Berriz GF, Jacotot L, Vaglio P, Reboul J, Hirozane-Kishikawa T, Li Q, Gabel HW, Elewa A, Baumgartner B, Rose DJ, Yu H, Bosak S, Sequerra R, Fraser A, Mango SE, Saxton WM, Strome S, Van Den Heuvel S, Piano F, Vandenhaute J, Sardet C, Gerstein M, Doucette-Stamm L, Gunsalus KC, Harper JW, Cusick ME, Roth FP, Hill DE, Vidal M (2004) A map of the interactome network of the metazoan C. elegans. Science 303 (5657):540-543. doi:10.1126/science.1091403
Lin H, Niu L, McHale NA, Ohme-Takagi M, Mysore KS, Tadege M (2013) Evolutionarily conserved repressive activity of WOX proteins mediates leaf blade outgrowth and floral organ development in plants. Proc Natl Acad Sci U S A 110 (1):366-371. doi:10.1073/pnas.1215376110
Lipsick JS (1996) One billion years of Myb. Oncogene 13 (2):223-235
Liu B, Wang L, Zhang J, Li J, Zheng H, Chen J, Lu M (2014a) WUSCHEL-related Homeobox genes in Populus tomentosa: diversified expression patterns and a functional similarity in adventitious root formation. BMC genomics 15:296. doi:10.1186/1471-2164-15-296
Liu Y, You S, Taylor-Teeples M, Li WL, Schuetz M, Brady SM, Douglas CJ (2014b) BEL1-LIKE HOMEODOMAIN6 and KNOTTED ARABIDOPSIS THALIANA7 interact and regulate secondary cell wall formation via repression of REVOLUTA. Plant Cell 26 (12):4843-4861. doi:10.1105/tpc.114.128322
Lu CA, Ho TH, Ho SL, Yu SM (2002) Three novel MYB proteins with one DNA binding repeat mediate sugar and hormone regulation of alpha-amylase gene expression. The Plant cell 14 (8):1963-1980
Lu S, Sun YH, Shi R, Clark C, Li L, Chiang VL (2005) Novel and mechanical stress-responsive MicroRNAs in Populus trichocarpa that are absent from Arabidopsis. Plant Cell 17 (8):2186-2203. doi:10.1105/tpc.105.033456
Luo D, Carpenter R, Copsey L, Vincent C, Clark J, Coen E (1999) Control of organ asymmetry in flowers of Antirrhinum. Cell 99 (4):367-376. doi:S0092-8674(00)81523-8 [pii]
Luo D, Carpenter R, Vincent C, Copsey L, Coen E (1996) Origin of floral asymmetry in Antirrhinum. Nature 383 (6603):794-799. doi:10.1038/383794a0
Machemer K, Shaiman O, Salts Y, Shabtai S, Sobolev I, Belausov E, Grotewold E, Barg R (2011) Interplay of MYB factors in differential cell expansion, and consequences for tomato fruit development. Plant J 68 (2):337-350. doi:10.1111/j.1365-313X.2011.04690.x
Mauseth J (1988) Plant Anatomy. The Benjamin/Cummings Publish Company Menlo Park, CA
McCarthy RL, Zhong R, Fowler S, Lyskowski D, Piyasena H, Carleton K, Spicer C, Ye ZH (2010) The poplar MYB transcription factors, PtrMYB3 and PtrMYB20, are involved in the regulation of secondary wall biosynthesis. Plant Cell Physiol 51 (6):1084-1090. doi:10.1093/pcp/pcq064

McCarthy RL, Zhong R, Ye ZH (2009) MYB83 is a direct target of SND1 and acts redundantly with MYB46 in the regulation of secondary cell wall biosynthesis in Arabidopsis. Plant & cell physiology 50 (11):1950-1964. doi:10.1093/pcp/pcp139
Meilan R, Ma C (2006) Poplar (Populus spp.). Methods Mol Biol 344:143-151. doi:10.1385/1-59745-131-2:143
Meyerowitz EM (2001) Prehistory and history of Arabidopsis research. Plant physiology 125 (1):15-19
Mitsuda N, Iwase A, Yamamoto H, Yoshida M, Seki M, Shinozaki K, Ohme-Takagi M (2007) NAC transcription factors, NST1 and NST3, are key regulators of the formation of secondary walls in woody tissues of Arabidopsis. Plant Cell 19 (1):270-280. doi:10.1105/tpc.106.047043
Mitsuda N, Seki M, Shinozaki K, Ohme-Takagi M (2005) The NAC transcription factors NST1 and NST2 of Arabidopsis regulate secondary wall thickenings and are required for anther dehiscence. Plant Cell 17 (11):2993-3006. doi:10.1105/tpc.105.036004
Nakano Y, Yamaguchi M, Endo H, Rejab NA, Ohtani M (2015) NAC-MYB-based transcriptional regulation of secondary cell wall biosynthesis in land plants. Front Plant Sci 6:288. doi:10.3389/fpls.2015.00288
Nieminen KM, Kauppinen L, Helariutta Y (2004) A weed for wood? Arabidopsis as a genetic model for xylem development. Plant physiology 135 (2):653-659. doi:10.1104/pp.104.040212
Novaes E, Kirst M, Chiang V, Winter-Sederoff H, Sederoff R (2010) Lignin and biomass: a negative correlation for wood formation and lignin content in trees. Plant Physiol 154 (2):555-561. doi:10.1104/pp.110.161281
Ohashi-Ito K, Bergmann DC (2007) Regulation of the Arabidopsis root vascular initial population by LONESOME HIGHWAY. Development 134 (16):2959-2968. doi:10.1242/dev.006296
Ohashi-Ito K, Matsukawa M, Fukuda H (2013) An atypical bHLH transcription factor regulates early xylem development downstream of auxin. Plant Cell Physiol 54 (3):398-405. doi:10.1093/pcp/pct013
Ohman D, Demedts B, Kumar M, Gerber L, Gorzsas A, Goeminne G, Hedenstrom M, Ellis B, Boerjan W, Sundberg B (2013) MYB103 is required for FERULATE-5-HYDROXYLASE expression and syringyl lignin biosynthesis in Arabidopsis stems. Plant Journal 73 (1):63-76. doi:10.1111/tpj.12018
Oono Y, Chen QG, Overvoorde PJ, Kohler C, Theologis A (1998) age Mutants of Arabidopsis exhibit altered auxin-regulated gene expression. The Plant cell 10 (10):1649-1662
Patzlaff A, McInnis S, Courtenay A, Surman C, Newman LJ, Smith C, Bevan MW, Mansfield S, Whetten RW, Sederoff RR, Campbell MM (2003a) Characterisation of a pine MYB that regulates lignification. Plant J 36 (6):743-754. doi:1916 [pii]
Patzlaff A, Newman LJ, Dubos C, Whetten RW, Smith C, McInnis S, Bevan MW, Sederoff RR, Campbell MM (2003b) Characterisation of Pt MYB1, an R2R3-MYB from pine xylem. Plant Mol Biol 53 (4):597-608. doi:10.1023/B:PLAN.0000019066.07933.d6 5255410 [pii]
Plomion C, Leprovost G, Stokes A (2001) Wood formation in trees. Plant Physiol 127 (4):1513-1523
Raimundo J, Sobral R, Bailey P, Azevedo H, Galego L, Almeida J, Coen E, Costa MM (2013) A subcellular tug of war involving three MYB-like proteins underlies a molecular

antagonism in Antirrhinum flower asymmetry. Plant J 75 (4):527-538. doi:10.1111/tpj.12225
Riechmann JL, Heard J, Martin G, Reuber L, Jiang C, Keddie J, Adam L, Pineda O, Ratcliffe OJ, Samaha RR, Creelman R, Pilgrim M, Broun P, Zhang JZ, Ghandehari D, Sherman BK, Yu G (2000) Arabidopsis transcription factors: genome-wide comparative analysis among eukaryotes. Science 290 (5499):2105-2110
Roberts K, McCann MC (2000) Xylogenesis: the birth of a corpse. Curr Opin Plant Biol 3 (6):517-522
Robischon M, Du J, Miura E, Groover A (2011a) The Populus class III HD ZIP, popREVOLUTA, influences cambium initiation and patterning of woody stems. Plant physiology 155 (3):1214-1225. doi:10.1104/pp.110.167007
Robischon M, Du JA, Miura E, Groover A (2011b) The Populus Class III HD ZIP, popREVOLUTA, Influences Cambium Initiation and Patterning of Woody Stems. Plant Physiol 155 (3):1214-1225. doi:10.1104/pp.110.167007
Rodgers-Melnick E, Mane SP, Dharmawardhana P, Slavov GT, Crasta OR, Strauss SH, Brunner AM, DiFazio SP (2012a) Contrasting patterns of evolution following whole genome versus tandem duplication events in Populus. Genome Res 22 (1):95-105. doi:10.1101/gr.125146.111
Rodgers-Melnick E, Mane SP, Dharmawardhana P, Slavov GT, Crasta OR, Strauss SH, Brunner AM, Difazio SP (2012b) Contrasting patterns of evolution following whole genome versus tandem duplication events in Populus. Genome research 22 (1):95-105. doi:10.1101/gr.125146.111
Romera-Branchat M, Ripoll JJ, Yanofsky MF, Pelaz S (2013) The WOX13 homeobox gene promotes replum formation in the Arabidopsis thaliana fruit. Plant J 73 (1):37-49. doi:10.1111/tpj.12010
Rose A, Meier I, Wienand U (1999) The tomato I-box binding factor LeMYBI is a member of a novel class of myb-like proteins. Plant J 20 (6):641-652. doi:tpj638 [pii]
Rual JF, Venkatesan K, Hao T, Hirozane-Kishikawa T, Dricot A, Li N, Berriz GF, Gibbons FD, Dreze M, Ayivi-Guedehoussou N, Klitgord N, Simon C, Boxem M, Milstein S, Rosenberg J, Goldberg DS, Zhang LV, Wong SL, Franklin G, Li S, Albala JS, Lim J, Fraughton C, Llamosas E, Cevik S, Bex C, Lamesch P, Sikorski RS, Vandenhaute J, Zoghbi HY, Smolyar A, Bosak S, Sequerra R, Doucette-Stamm L, Cusick ME, Hill DE, Roth FP, Vidal M (2005) Towards a proteome-scale map of the human protein-protein interaction network. Nature 437 (7062):1173-1178. doi:10.1038/nature04209
Shi R, Sun YH, Li Q, Heber S, Sederoff R, Chiang VL (2010) Towards a systems approach for lignin biosynthesis in Populus trichocarpa: transcript abundance and specificity of the monolignol biosynthetic genes. Plant Cell Physiol 51 (1):144-163. doi:pcp175 [pii]10.1093/pcp/pcp175
Sterky F, Regan S, Karlsson J, Hertzberg M, Rohde A, Holmberg A, Amini B, Bhalerao R, Larsson M, Villarroel R, Van Montagu M, Sandberg G, Olsson O, Teeri TT, Boerjan W, Gustafsson P, Uhlen M, Sundberg B, Lundeberg J (1998) Gene discovery in the wood-forming tissues of poplar: Analysis of 5,692 expressed sequence tags. P Natl Acad Sci USA 95 (22):13330-13335. doi:DOI 10.1073/pnas.95.22.13330
Stewart JJ, Akiyama T, Chapple C, Ralph J, Mansfield SD (2009) The effects on lignin structure of overexpression of ferulate 5-hydroxylase in hybrid poplar. Plant physiology 150 (2):621-635. doi:10.1104/pp.109.137059

Stracke R, Ishihara H, Huep G, Barsch A, Mehrtens F, Niehaus K, Weisshaar B (2007) Differential regulation of closely related R2R3-MYB transcription factors controls flavonol accumulation in different parts of the Arabidopsis thaliana seedling. Plant J 50 (4):660-677. doi:TPJ3078 [pii] 10.1111/j.1365-313X.2007.03078.x

Stracke R, Werber M, Weisshaar B (2001) The R2R3-MYB gene family in Arabidopsis thaliana. Curr Opin Plant Biol 4 (5):447-456. doi:S1369-5266(00)00199-0 [pii]

Suer S, Agusti J, Sanchez P, Schwarz M, Greb T (2011) WOX4 imparts auxin responsiveness to cambium cells in Arabidopsis. The Plant cell 23 (9):3247-3259. doi:10.1105/tpc.111.087874

Tamura K, Stecher G, Peterson D, Filipski A, Kumar S (2013) MEGA6: Molecular Evolutionary Genetics Analysis version 6.0. Mol Biol Evol 30 (12):2725-2729. doi:10.1093/molbev/mst197

Taylor-Teeples M, Lin L, de Lucas M, Turco G, Toal TW, Gaudinier A, Young NF, Trabucco GM, Veling MT, Lamothe R, Handakumbura PP, Xiong G, Wang C, Corwin J, Tsoukalas A, Zhang L, Ware D, Pauly M, Kliebenstein DJ, Dehesh K, Tagkopoulos I, Breton G, Pruneda-Paz JL, Ahnert SE, Kay SA, Hazen SP, Brady SM (2015) An Arabidopsis gene regulatory network for secondary cell wall synthesis. Nature 517 (7536):571-575. doi:10.1038/nature14099

Teng S, Keurentjes J, Bentsink L, Koornneef M, Smeekens S (2005) Sucrose-specific induction of anthocyanin biosynthesis in Arabidopsis requires the MYB75/PAP1 gene. Plant Physiol 139 (4):1840-1852. doi:pp.105.066688 [pii] 10.1104/pp.105.066688

Ter-Mikaelian MT, Colombo SJ, Lovekin D, McKechnie J, Reynolds R, Titus B, Laurin E, Chapman AM, Chen JX, MacLean HL (2015) Carbon debt repayment or carbon sequestration parity? Lessons from a forest bioenergy case study in Ontario, Canada. Gcb Bioenergy 7 (4):704-716. doi:10.1111/gcbb.12198

Tuskan GA, Difazio S, Jansson S, Bohlmann J, Grigoriev I, Hellsten U, Putnam N, Ralph S, Rombauts S, Salamov A, Schein J, Sterck L, Aerts A, Bhalerao RR, Bhalerao RP, Blaudez D, Boerjan W, Brun A, Brunner A, Busov V, Campbell M, Carlson J, Chalot M, Chapman J, Chen GL, Cooper D, Coutinho PM, Couturier J, Covert S, Cronk Q, Cunningham R, Davis J, Degroeve S, Dejardin A, Depamphilis C, Detter J, Dirks B, Dubchak I, Duplessis S, Ehlting J, Ellis B, Gendler K, Goodstein D, Gribskov M, Grimwood J, Groover A, Gunter L, Hamberger B, Heinze B, Helariutta Y, Henrissat B, Holligan D, Holt R, Huang W, Islam-Faridi N, Jones S, Jones-Rhoades M, Jorgensen R, Joshi C, Kangasjarvi J, Karlsson J, Kelleher C, Kirkpatrick R, Kirst M, Kohler A, Kalluri U, Larimer F, Leebens-Mack J, Leple JC, Locascio P, Lou Y, Lucas S, Martin F, Montanini B, Napoli C, Nelson DR, Nelson C, Nieminen K, Nilsson O, Pereda V, Peter G, Philippe R, Pilate G, Poliakov A, Razumovskaya J, Richardson P, Rinaldi C, Ritland K, Rouze P, Ryaboy D, Schmutz J, Schrader J, Segerman B, Shin H, Siddiqui A, Sterky F, Terry A, Tsai CJ, Uberbacher E, Unneberg P, Vahala J, Wall K, Wessler S, Yang G, Yin T, Douglas C, Marra M, Sandberg G, Van de Peer Y, Rokhsar D (2006) The genome of black cottonwood, Populus trichocarpa (Torr. & Gray). Science 313 (5793):1596-1604. doi:10.1126/science.1128691

van der Graaff E, Laux T, Rensing SA (2009) The WUS homeobox-containing (WOX) protein family. Genome Biol 10 (12):248. doi:10.1186/gb-2009-10-12-248

Vermaas JV, Petridis L, Qi XH, Schulz R, Lindner B, Smith JC (2015) Mechanism of lignin inhibition of enzymatic biomass deconstruction. Biotechnol Biofuels 8. doi:ARTN 217 10.1186/s13068-015-0379-8

Vermeirssen V, Barrasa MI, Hidalgo CA, Babon JA, Sequerra R, Doucette-Stamm L, Barabasi AL, Walhout AJ (2007) Transcription factor modularity in a gene-centered C. elegans core neuronal protein-DNA interaction network. Genome research 17 (7):1061-1071. doi:10.1101/gr.6148107

Walhout AJ, Vidal M (2001) High-throughput yeast two-hybrid assays for large-scale protein interaction mapping. Methods 24 (3):297-306. doi:10.1006/meth.2001.1190

Whitford R, Fernandez A, De Groodt R, Ortega E, Hilson P (2008) Plant CLE peptides from two distinct functional classes synergistically induce division of vascular cells. Proceedings of the National Academy of Sciences of the United States of America 105 (47):18625-18630. doi:10.1073/pnas.0809395105

Wilkins O, Nahal H, Foong J, Provart NJ, Campbell MM (2009) Expansion and diversification of the Populus R2R3-MYB family of transcription factors. Plant physiology 149 (2):981-993. doi:10.1104/pp.108.132795

Yamaguchi M, Mitsuda N, Ohtani M, Ohme-Takagi M, Kato K, Demura T (2011) VASCULAR-RELATED NAC-DOMAIN7 directly regulates the expression of a broad range of genes for xylem vessel formation. Plant J 66 (4):579-590. doi:10.1111/j.1365-313X.2011.04514.x

Yang L, Zhao X, Yang F, Fan D, Jiang Y, Luo K (2016) PtrWRKY19, a novel WRKY transcription factor, contributes to the regulation of pith secondary wall formation in Populus trichocarpa. Sci Rep 6:18643. doi:10.1038/srep18643

Yang Y, Li R, Qi M (2000) In vivo analysis of plant promoters and transcription factors by agroinfiltration of tobacco leaves. Plant J 22 (6):543-551. doi:tpj760 [pii]

Zhang J, Elo A, Helariutta Y (2011) Arabidopsis as a model for wood formation. Curr Opin Biotechnol 22 (2):293-299. doi:10.1016/j.copbio.2010.11.008

Zhao C, Avci U, Grant EH, Haigler CH, Beers EP (2008) XND1, a member of the NAC domain family in Arabidopsis thaliana, negatively regulates lignocellulose synthesis and programmed cell death in xylem. Plant J 53 (3):425-436. doi:TPJ3350 [pii] 10.1111/j.1365-313X.2007.03350.x

Zhao C, Craig JC, Petzold HE, Dickerman AW, Beers EP (2005a) The xylem and phloem transcriptomes from secondary tissues of the Arabidopsis root-hypocotyl. Plant Physiol 138 (2):803-818. doi:pp.105.060202 [pii] 10.1104/pp.105.060202

Zhao CS, Craig JC, Petzold HE, Dickerman AW, Beers EP (2005b) The xylem and phloem transcriptomes from secondary tissues of the Arabidopsis root-hypocotyl. Plant Physiol 138 (2):803-818. doi:10.1104/pp.105.060202

Zhong R, Lee C, Ye ZH (2010) Functional characterization of poplar wood-associated NAC domain transcription factors. Plant physiology 152 (2):1044-1055. doi:10.1104/pp.109.148270

Zhong R, Lee C, Zhou J, McCarthy RL, Ye ZH (2008) A battery of transcription factors involved in the regulation of secondary cell wall biosynthesis in Arabidopsis. Plant Cell 20 (10):2763-2782. doi:10.1105/tpc.108.061325

Zhong R, McCarthy RL, Haghighat M, Ye ZH (2013) The poplar MYB master switches bind to the SMRE site and activate the secondary wall biosynthetic program during wood formation. PLoS One 8 (7):e69219. doi:10.1371/journal.pone.0069219

Zhong R, Richardson EA, Ye ZH (2007a) The MYB46 transcription factor is a direct target of SND1 and regulates secondary wall biosynthesis in Arabidopsis. The Plant cell 19 (9):2776-2792. doi:10.1105/tpc.107.053678

Zhong R, Richardson EA, Ye ZH (2007b) Two NAC domain transcription factors, SND1 and NST1, function redundantly in regulation of secondary wall synthesis in fibers of Arabidopsis. Planta 225 (6):1603-1611. doi:10.1007/s00425-007-0498-y

Zhong R, Ye ZH (2007) Regulation of HD-ZIP III Genes by MicroRNA 165. Plant Signal Behav 2 (5):351-353

Zuo J, Niu QW, Chua NH (2000) Technical advance: An estrogen receptor-based transactivator XVE mediates highly inducible gene expression in transgenic plants. Plant J 24 (2):265-273. doi:tpj868 [pii]

A

RAD

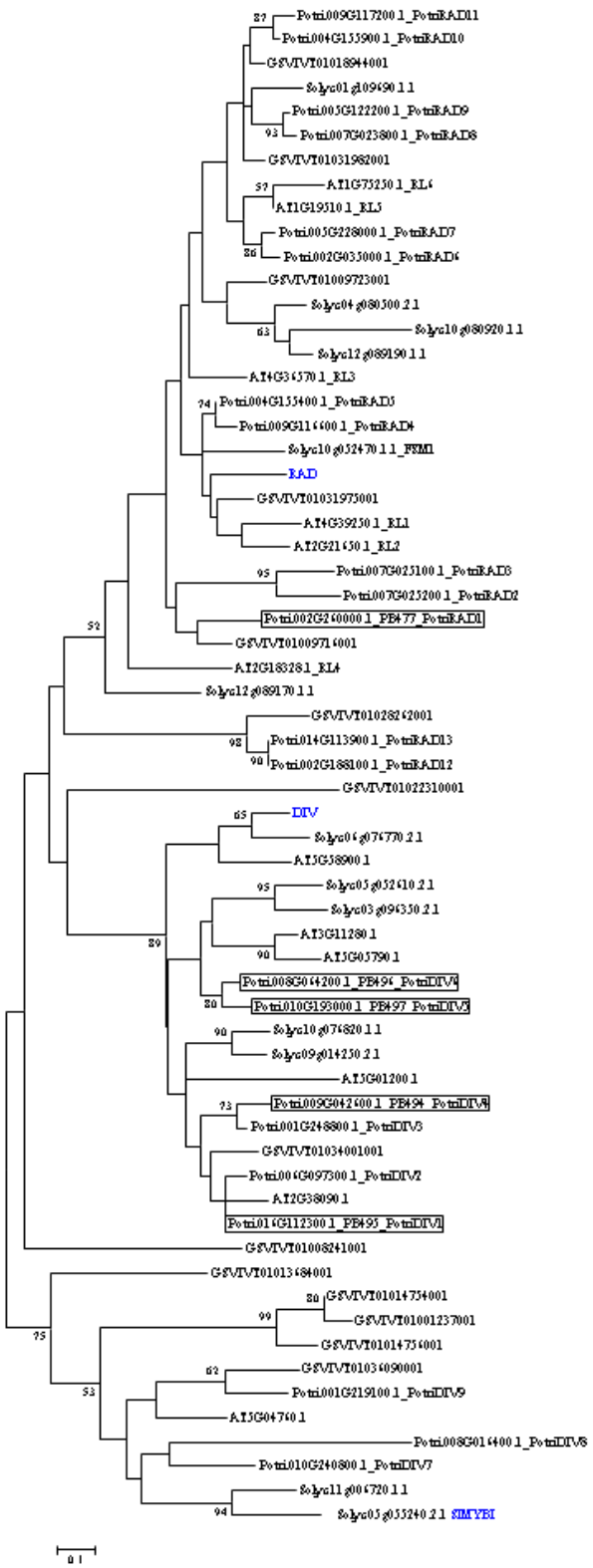
Potri.009G117200.1_PotriRAD11
Potri.004G155900.1_PotriRAD10
GSVIVT01018944001
Solyc01g109490.1.1
Potri.005G122200.1_PotriRAD9
Potri.007G023800.1_PotriRAD8
GSVIVT01031982001
AT1G75250.1_RL6
AT1G19510.1_RL5
Potri.005G228000.1_PotriRAD7
Potri.002G035000.1_PotriRAD6
GSVIVT01009723001
Solyc04g080500.2.1
Solyc10g080920.1.1
Solyc12g089190.1.1
AT4G34570.1_RL3
Potri.004G155400.1_PotriRAD5
Potri.009G116400.1_PotriRAD4
Solyc10g052470.1.1_FSM1
RAD
GSVIVT01031975001
AT4G39250.1_RL1
AT2G21430.1_RL2
Potri.007G025100.1_PotriRAD3
Potri.007G025200.1_PotriRAD2
Potri.002G240000.1_PB477_PotriRAD1
GSVIVT01009714001
AT2G18328.1_RL4
Solyc12g089170.1.1
GSVIVT01028242001
Potri.014G113900.1_PotriRAD13
Potri.002G188100.1_PotriRAD12
GSVIVT01022310001
DIV
Solyc04g074770.2.1
AT3G58900.1
Solyc05g052410.2.1
Solyc03g094350.2.1
AT3G11280.1
AT5G03790.1
Potri.008G044200.1_PB494_PotriDIV4
Potri.010G193000.1_PB497_PotriDIV5
Solyc10g074820.1.1
Solyc09g014250.2.1
AT5G01200.1
Potri.009G042400.1_PB494_PotriDIV6
Potri.001G248800.1_PotriDIV3
GSVIVT01034001001
Potri.004G097300.1_PotriDIV2
AT2G38090.1
Potri.014G112300.1_PB495_PotriDIV1
GSVIVT01008241001
GSVIVT01013484001
GSVIVT01014754001
GSVIVT01001237001
GSVIVT01014754001
GSVIVT01034090001
Potri.001G219100.1_PotriDIV9
AT5G04740.1
Potri.008G016400.1_PotriDIV8
Potri.010G240800.1_PotriDIV7
Solyc11g004720.1.1
Solyc05g055240.2.1 SlMYB1
0.1

B

DRIF

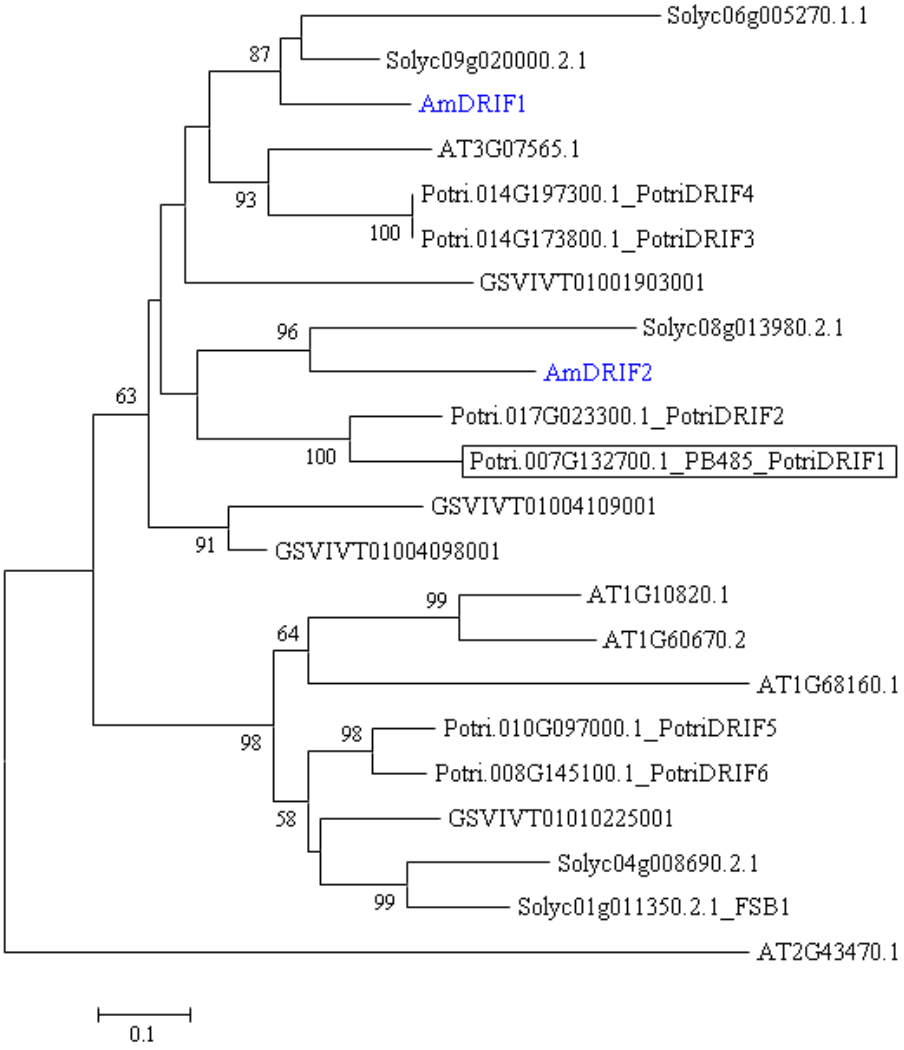
Solyc06g005270.1.1
87
Solyc09g020000.2.1
AmDRIF1
AT3G07565.1
93
Potri.014G197300.1_PotriDRIF4
100
Potri.014G173800.1_PotriDRIF3
GSVIVT01001903001
96
Solyc08g013980.2.1
AmDRIF2
63
Potri.017G023300.1_PotriDRIF2
100
Potri.007G132700.1_PB485_PotriDRIF1
GSVIVT01004109001
91
GSVIVT01004098001
99
AT1G10820.1
64
AT1G60670.2
AT1G68160.1
98
98
Potri.010G097000.1_PotriDRIF5
Potri.008G145100.1_PotriDRIF6
58
GSVIVT01010225001
Solyc04g008690.2.1
99
Solyc01g011350.2.1_FSB1
AT2G43470.1
0.1

C

KNOX

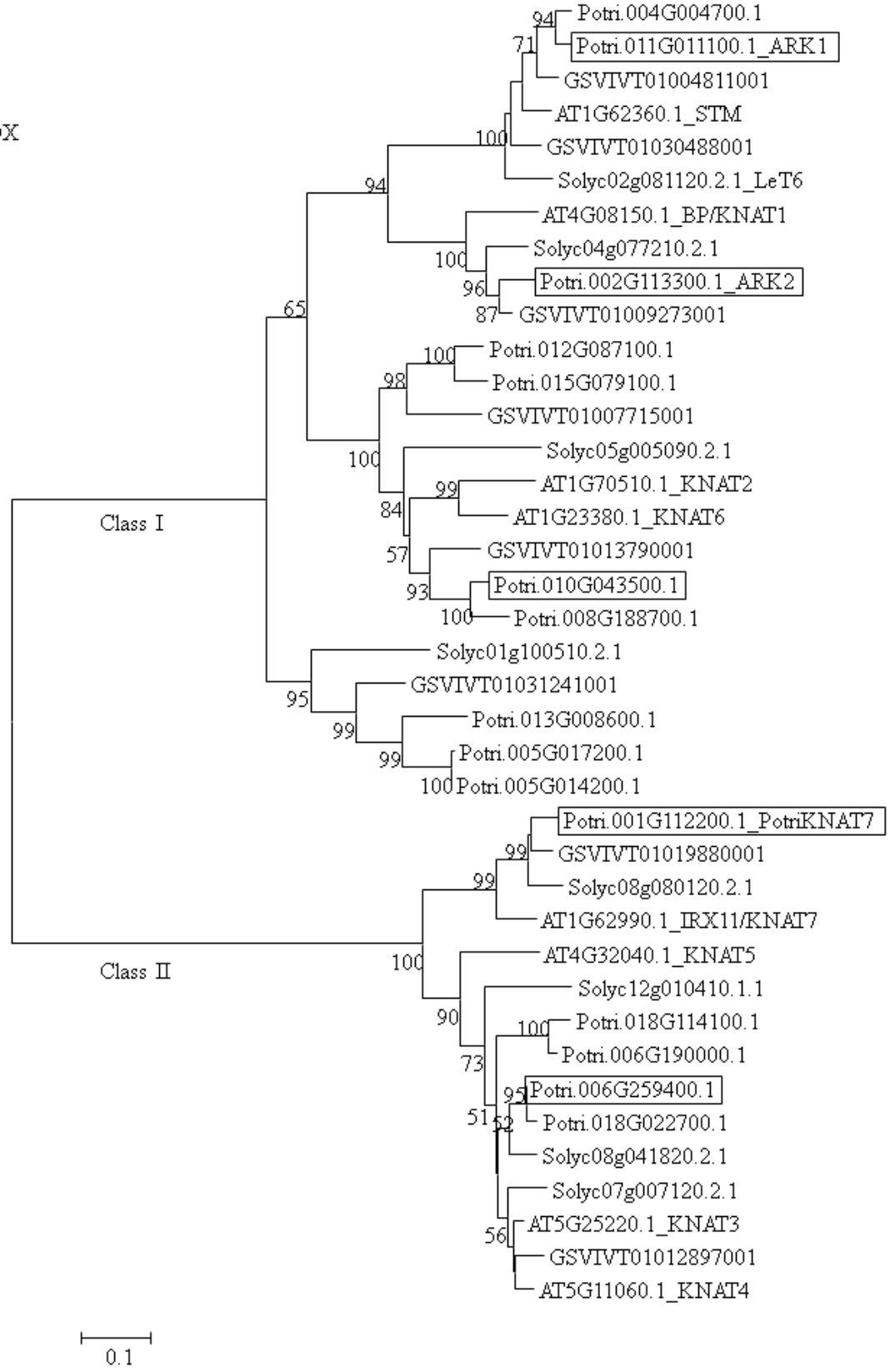
Potri.004G004700.1
Potri.011G011100.1_ARK1
GSVIVT01004811001
AT1G62360.1_STM
GSVIVT01030488001
Solyc02g081120.2.1_LeT6
AT4G08150.1_BP/KNAT1
Solyc04g077210.2.1
Potri.002G113300.1_ARK2
GSVIVT01009273001
Potri.012G087100.1
Potri.015G079100.1
GSVIVT01007715001
Solyc05g005090.2.1
AT1G70510.1_KNAT2
AT1G23380.1_KNAT6
GSVIVT01013790001
Potri.010G043500.1
Potri.008G188700.1
Solyc01g100510.2.1
GSVIVT01031241001
Potri.013G008600.1
Potri.005G017200.1
Potri.005G014200.1
Potri.001G112200.1_PotriKNAT7
GSVIVT01019880001
Solyc08g080120.2.1
AT1G62990.1_IRX11/KNAT7
AT4G32040.1_KNAT5
Solyc12g010410.1.1
Potri.018G114100.1
Potri.006G190000.1
Potri.006G259400.1
Potri.018G022700.1
Solyc08g041820.2.1
Solyc07g007120.2.1
AT5G25220.1_KNAT3
GSVIVT01012897001
AT5G11060.1_KNAT4
Class I
Class II
0.1

D

BELL

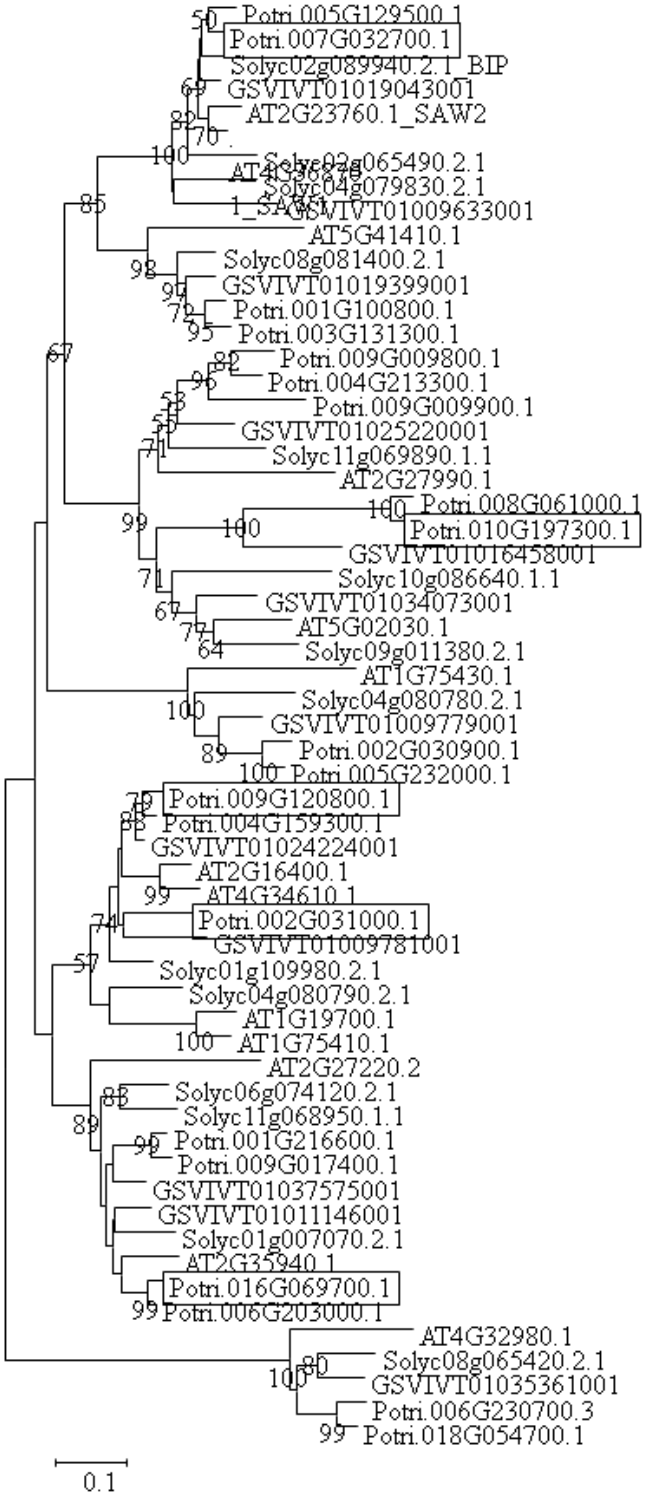
Potri.005G129500.1
Potri.007G032700.1
Solyc02g089940.2.1_BIP
GSVIVT01019043001
AT2G23760.1_SAW2
Solyc02g065490.2.1
Solyc04g079830.2.1
GSVIVT01009633001
AT5G41410.1
Solyc08g081400.2.1
GSVIVT01019399001
Potri.001G100800.1
Potri.003G131300.1
Potri.009G009800.1
Potri.004G213300.1
Potri.009G009900.1
GSVIVT01025220001
Solyc11g069890.1.1
AT2G27990.1
Potri.008G061000.1
Potri.010G197300.1
GSVIVT01016458001
Solyc10g086640.1.1
GSVIVT01034073001
AT5G02030.1
Solyc09g011380.2.1
AT1G75430.1
Solyc04g080780.2.1
GSVIVT01009779001
Potri.002G030900.1
Potri.005G232000.1
Potri.009G120800.1
Potri.004G159300.1
GSVIVT01024224001
AT2G16400.1
AT4G34610.1
Potri.002G031000.1
GSVIVT01009781001
Solyc01g109980.2.1
Solyc04g080790.2.1
AT1G19700.1
AT1G75410.1
AT2G27220.2
Solyc06g074120.2.1
Solyc11g068950.1.1
Potri.001G216600.1
Potri.009G017400.1
GSVIVT01037575001
GSVIVT01011146001
Solyc01g007070.2.1
AT2G35940.1
Potri.016G069700.1
Potri.006G203000.1
AT4G32980.1
Solyc08g065420.2.1
GSVIVT01035361001
Potri.006G230700.3
Potri.018G054700.1
0.1

E

WOX

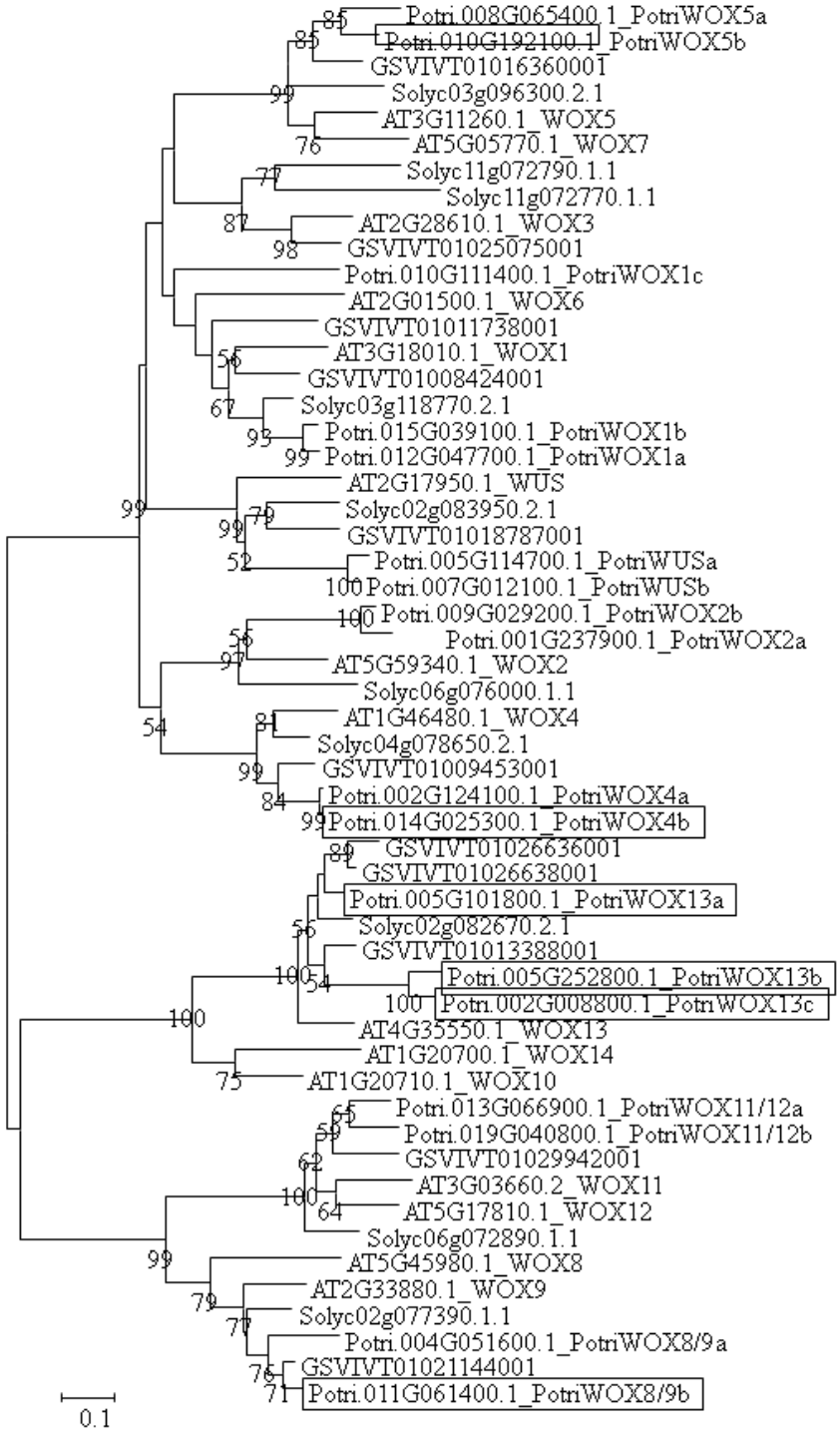
Potri.008G065400.1_PotriWOX5a
Potri.010G192100.1_PotriWOX5b
GSVIVT01016360001
Solyc03g096300.2.1
AT3G11260.1_WOX5
AT5G05770.1_WOX7
Solyc11g072790.1.1
Solyc11g072770.1.1
AT2G28610.1_WOX3
GSVIVT01025075001
Potri.010G111400.1_PotriWOX1c
AT2G01500.1_WOX6
GSVIVT01011738001
AT3G18010.1_WOX1
GSVIVT01008424001
Solyc03g118770.2.1
Potri.015G039100.1_PotriWOX1b
Potri.012G047700.1_PotriWOX1a
AT2G17950.1_WUS
Solyc02g083950.2.1
GSVIVT01018787001
Potri.005G114700.1_PotriWUSa
Potri.007G012100.1_PotriWUSb
Potri.009G029200.1_PotriWOX2b
Potri.001G237900.1_PotriWOX2a
AT5G59340.1_WOX2
Solyc06g076000.1.1
AT1G46480.1_WOX4
Solyc04g078650.2.1
GSVIVT01009453001
Potri.002G124100.1_PotriWOX4a
Potri.014G025300.1_PotriWOX4b
GSVIVT01026636001
GSVIVT01026638001
Potri.005G101800.1_PotriWOX13a
Solyc02g082670.2.1
GSVIVT01013388001
Potri.005G252800.1_PotriWOX13b
Potri.002G008800.1_PotriWOX13c
AT4G35550.1_WOX13
AT1G20700.1_WOX14
AT1G20710.1_WOX10
Potri.013G066900.1_PotriWOX11/12a
Potri.019G040800.1_PotriWOX11/12b
GSVIVT01029942001
AT3G03660.2_WOX11
AT5G17810.1_WOX12
Solyc06g072890.1.1
AT5G45980.1_WOX8
AT2G33880.1_WOX9
Solyc02g077390.1.1
Potri.004G051600.1_PotriWOX8/9a
GSVIVT01021144001
Potri.011G061400.1_PotriWOX8/9b
0.1

Figure 3.S1. Phylogenetic trees showing RADIALIS , DIVARICATA, DRIF, WOX, KNOX and BELL proteins.

Proteins investigated for this report are boxed. See Table S2 for summary of Y2H results for boxed proteins. A) RADIALIS, ML tree, JT model, uniform rates, partial deletion (90% cutoff), NNI method 1,000 bootstraps; B) DRIF, NJ tree, default settings (JTT, uniform rates, complete deletion); C) KNOX, NJ tree (JTT, uniform rates); D) WOX, NJ tree (JTT, uniform rates); E) BELL, NJ tree (JTT, uniform rates).

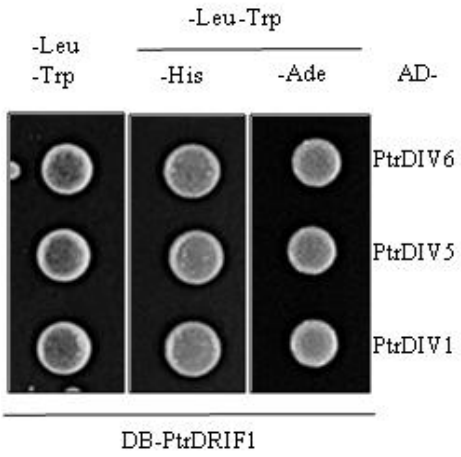

Figure 3.S2. PtrDRIF1 interacts with multiple PtrDIV homologs.

Columns labeled -His and –Ade show activity of yeast two-hybrid reporters for combinations of DB-PtrDRIF1 with AD fusion proteins as indicated at right. See Figure 1 for vector only controls. All assays included 20 mM 3-AT.

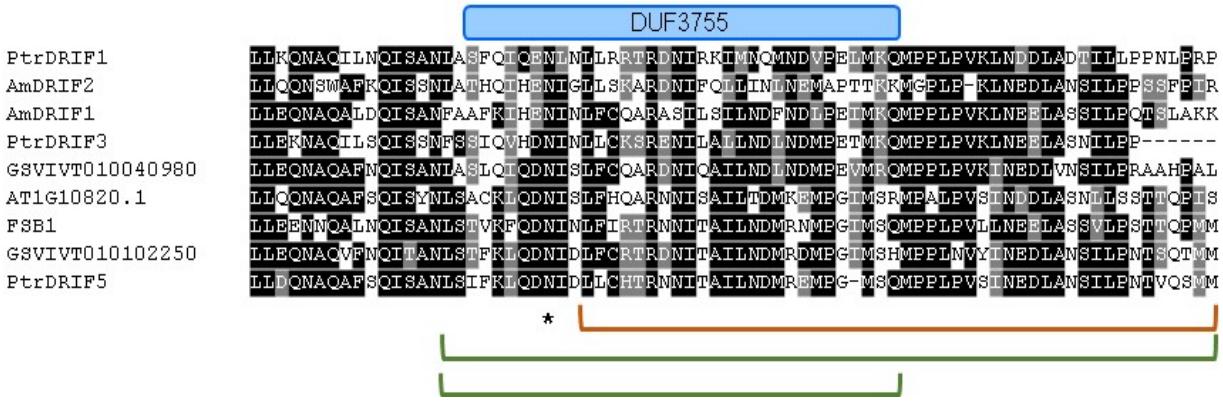

Figure 3.S3. Alignment of the C-terminal region of PtrDRIF1 with additional selected DRIF homologs (see Figure S1).

DUF3755 domain is marked by the blue rectangle. Peptides sufficient for protein-protein interactions with PtrWOX13c and PtrKNAT7 are indicated by green brackets. The peptide marked by the orange bracket was not sufficient for protein-protein interactions with PtrWOX13c and PtrKNAT7. *, conserved Asn residue of unknown function. See Figure 4 for relevant Y2H and BiFC results.

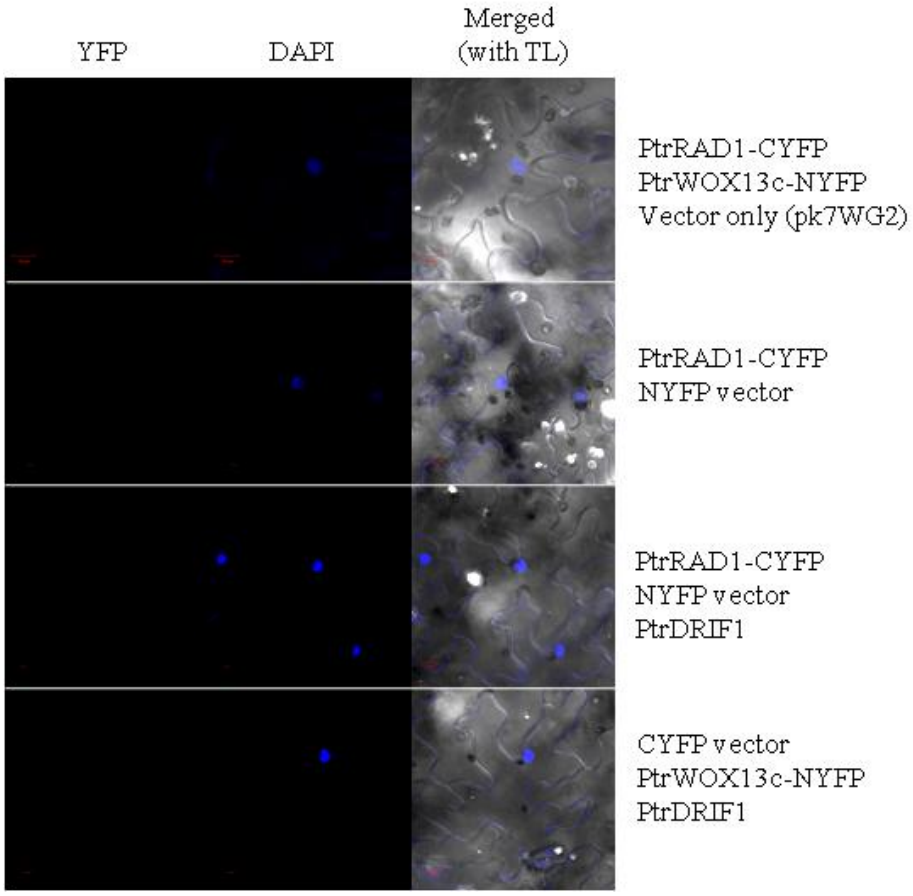

Figure 3.S4. Negative controls for the BiFC assay forformation of the PtrDRIF1-PtrRAD1-PtrWOX13c heterotrimer.

Images from laser scanning confocal microscopy show absence of YFP fluorescence (left column) in DAPI-stained nuclei (center column) and merger of these images with the transmitted light (TL) images (right column) for tobacco leaves transformed with vectors shown at right.

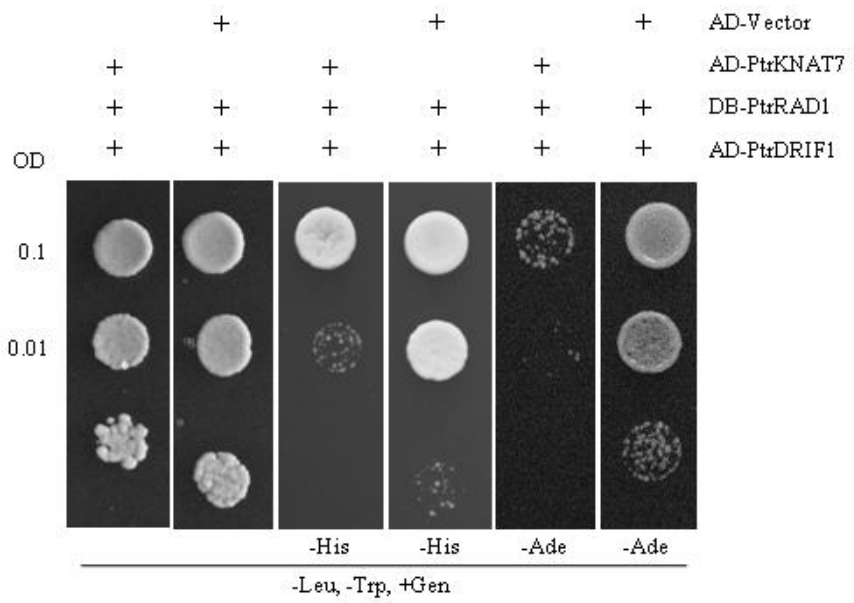

Figure 3.S5. PtrKNAT7 disrupts PtrRAD1-PtrDRIF1 interactions

(a) Yeast growth dependent on the interaction of DB-PtrRAD1 and AD-PtrDRIF1 is reduced in the presence of AD-PtrKNAT7 compared to the AD vector control. +Gen, plus geneticin (KanMX) selection for AD-PtrDRIF1 vector, -Trp for AD-PtrKNAT7, and –Leu for DB-PtrRAD1.

Table 3.S1. Identity of clones recovered from Y2H screen of poplar xylem cDNA library using PotriDRIF1 (Potri.007G132700) as bait.

P. trichocarpa locus	Best match *A. thaliana* locus	Annotation	Comment*
Potri.002G260000	AT1G75250 *ATRL6*	MYB/SANT domain	***PotriRAD1***
Potri.009G042600	AT5G58900	Duplicated homeodomain	***PotriDIV4***
Potri.002G008800	AT4G35550 *WOX13*	WOX homeodomain	***PotriWOX13c***
Potri.005G101800	AT4G35550 *WOX13*	WOX homeodomain	***PotriWOX13a***
Potri.017G054800	AT4G13640 *PHL3*/*UNE16*	Myb-like DNA-binding, SHAQKYF class	
Potri.001G314800	AT4G13640 *PHL3*/*UNE16*	Myb-like DNA-binding, SHAQKYF class	
Potri.001G208700	AT3G54630	Ncd80 domain	
Potri.002G091700	AT1G22060	F-box-containing Leu-rich repeat	
Potri.004G087600	AT5G16720 *MYOB3*	DUF593	
Potri.006G194900	AT3G12020	Kinesin motor domain	
Potri.010G219700	AT5G50840	Taxilin domain-containing	
Potri.012G055100	AT3G18290 *BTS*	Zinc-finger, E3 ligase	
Potri.012G119200	AT5G45100 *BRG1*	Zinc-finger, RING-type	
Potri.014G055800	AT2G44950 *HUB1*	Zinc-finger, RING-type	
Potri.018G026000	AT4G32160	Phox domain	
Potri.014G097800	AT2G46420	Unknown	
Potri.014G139000	AT1G03290	Unknown	
Potri.008G048100	AT5G13560	Unknown	

* Genes in bold (and selected homologs) were investigated for this report.

Table 3.S2. Result of Y2H binary screens for interactions of PotriDRIF1 with PotriDRIF1, RADIALIS, DIVARICATA, WOX, KNOX, BELL, or additional selected homeodomain proteins.

JGI ID	Gene name	Y2H result
Potri.007G132700.1	PotriDRIF1	Negative
Potri.002G260000.1	PotriRAD1	Positive
Potri.008G064200.1	PotriDIV6	Positive
Potri.010G193000.1	PotriDIV5	Positive
Potri.009G042600.1	PotriDIV4	Positive
Potri.016g112300.1	PotriDIV1	Positive
Potri.005G101800.1	PotriWOX13A (Ancient)	Positive
Potri.005G252800.1	PotriWOX13B (Ancient)	Positive
Potri.002G008800.1	PotriWOX13C (Ancient)	Positive
Potri.001G112200.1	PotriKNAT7 (Class II KNOX)	Positive
Potri.006G259400.1	Class II KNOX	Positive
Potri.011G061400.1	PotriWOX8/9B (Intermediate)	Negative
Potri.014G025300.1	PotriWOX4B (Modern)	Negative
Potri.010G192100.1	PotriWOX5B (Modern)	Negative
Potri.011G011100.1	ARK1 (Class I KNOX)	Negative
Potri.002G113300.1	ARK2 (Class I KNOX)	Negative
Potri.010G043500.1	Class I KNOX	Negative
Potri.007G032700.1	BLH	Negative
Potri.016G069700.5	BLH	Negative
Potri.002G031000.1	BEL1-LIKE HD 6-RELATED	Negative
Potri.009G120800.1	BEL1-LIKE HD 6-RELATED	Negative
Potri.010G197300.1	BEL1-LIKE HD 8-RELATED	Negative
Potri.001G188800.1	Class III HD-ZIP*	Negative
Potri.001G188800.4	Class III HD-ZIP (CORONA-like)*	Negative
Potri.004G211300.1	Class III HD-ZIP*	Negative
Potri.017G082900.1	ZINC-FINGER HD PROTEIN*	Negative
*Homeodomain proteins not shown in phylogenetic trees in Figure S1.		

Table 3.S3. Primers

Primer Name	Potri ID	Primer sequence
PtrRAD s	Potri.002G260000.1	CACCATGGCTTCAGGTTCTAGTAAT
Ptr RAD as	Potri.002G260000.1	TCAGTTGAGATTAAGATTCTT
PtrDIV I s	Potri.016G112300.1	CACCATGAATCGGGGCATTGGAATG
PtrDIV I as	Potri.016G112300.1	TTAGTGATGTTGCATTGATTG
PtrDIV 4 s	Potri.009G042600.1	CACCATGAAGTGGGAAACGGAAATC
PtrDIV 4 as	Potri.009G042600.1	TCATCCATGAGGGTAGTGTTG
PtrDIV 5 s	Potri.010G193000.1	CACCATGGAAACTCTGAATCCATCT
PtrDIV 5 as	Potri.010G193000.1	CTAATATTGAATTTGAAATCTTGG
PtrDIV 6 s	Potri.008G064200.1	CACCATGGAAACTCTATATTCATCT
PtrDIV 6 as	Potri.008G064200.1	TCAATGAATTTGAAATCTTGG
PtrDRIFs	Potri.007G132700	CACCATGGCAAACCCATCTGGGACA
PtrDRIFas	Potri.007G132700	TTATGGCCTAGGAAGGTTTGG
PtrWOX13C	Potri.002G008800.1	CACCATGGAGGAGGGGAGGTTTCAG
PtrWOX13C	Potri.002G008800.1	TCATCCAAACAAGTCATATTG
PtrKNAT7 s	Potri.001G112200.1	CACCATGCAAGAACCAAACTTGGGC
PtrKNAT7 as	Potri.001G112200.1	CTACCTTTTGCGCTTGGACTT
PtrKNAT3-like s	Potri.006G259400.1	CACCATGGCCTTTCACCATAACTTG
PtrKNAT3-like as	Potri.006G259400.1	TTACACAAATCGATCGCCATT
PtrKNAT6-like s	Potri.010G043500.1	CACCATGGACGGAACGTACGGTCTG
PtrKNAT6-like as	Potri.010G043500.1	TCAGTCGTCTTCTGTAAAGAACTG
PtrWOX8/9 s	Potri.011G061400.1	CACCATGGCTTCATCAAACAGACAC
PtrWOX8/9 a s	Potri.011G061400.2	CTATATATGTTCACTAATGGA
PtrWOX4Bs	Potri.014G025300.1	CACCATGGGAAGCATGAAGGTGCAT
PtrWOX4B as	Potri.014G025300.2	TCATCTTCCTTCCGGGTGCAA
PtrWOX5B s	Potri.010G192100.1	CACCATGGAAGAGAGAATGTCAGGC
PtrWOX5B as	Potri.010G192100.1	CTACACAAAGCTTAATCGCAG
PtrARK1 s	Potri.011G011100.1	CACCATGGAGGGTGGTGGTGGTGAT
PtrARK1 as	Potri.011G011100.1	TCAAAGCAGTGTGGGAGAGAT
PtrARK2 s	Potri.002G113300.1	CACCATGGAGGACTACAATCAAATG
PtrARK2 as	Potri.002G113300.1	TCATGGACCGAGCCGATAATG
PtrBLH1 s	Potri.007G032700.1	CACCATGGGAATAGCTACAACACCT
PtrBLH1 as	Potri.007G032700.1	TCAACAGCCCCCAAAATCTCT
PtrBLH2 s	Potri.016G069700.5	CACCATGGCGACATACTTTCATGGG
PtrBLH2 as	Potri.016G069700.5	TCAGGCCACAAAGTCTGGCAA
PtrBLHD6A s	Potri.002G031000.1	CACCATGGCTACCTATTACCCAACT
PtrBLHD6A as	Potri.002G031000.1	TTAAACCACAAAATCATGTAA
PtrBLHD6 B as	Potri.009G120800.1	CACCATGGCTACCTATTACACTAGT
PtrBLHD6 B s	Potri.009G120800.1	TCAAGCAACGAAATCATGAAA

PtrBLHD8 s	Potri.010G197300.1	CACCATGGCACAAAACTTTGAACCC
PtrBLHD8 as	Potri.010G197300.1	TTACTCTTTCCCAAAATGCTG
Class3HDZipA s	Potri.001G188800.1	CACCATGATGGCAATGTCCTGCAAG
Class3HDZipA as	Potri.001G188800.1	TCAAACAAAAGACCAGTTTAT
Class3HDZipB as	Potri.001G188800.4	CACCATGCCACCAGTGCAGCATTTT
Class3HDZipB s	Potri.001G188800.4	TCAAACAAAAGACCAGTTTAT
Class3HDZipC s	Potri.004G211300.1	CACCATGGCCATGGAAGTGGCCCCT
Class3HDZipC as	Potri.004G211300.1	TCACAAAAAAGACCAGTTTAC
ZFHD 1 s	Potri.017G082900.1	CACCATGGACATGACAACAACAACA
ZFHD 1 as	Potri.017G082900.1	TTAAGAAGATGAGGAAGACCC
PtrDIV5(1-97) s	Potri.010G193000.1	CACCATGGAAACTCTGAATCCATCTT
PtrDIV5(1-97) as	Potri.010G193000.1	TCAGCTATTGCCAACCAACTGGAA
PtrDIV5(97-199) s	Potri.010G193000.1	CACCAGCAATTTTGATGCGTATAGG
PtrDIV5(97-199) as	Potri.010G193000.1	TCAATCTGACGGAGTAGTAGCATC
PtrKNAT7 Deletion Analysis		
KNAT7 Del 1S	Potri.001G112200.1	CACCATGCAAGAACCAAACTTGGGC
KNAT7 Del1AS	Potri.001G112200.1	CTACCTTTTGCGCTTGGACTT
KNAT7 De2S	Potri.001G112200.1	CACCTATGCTTCACAGCACAACCAA
KNAT7 Del2AS	Potri.001G112200.1	CTACCTTTTGCGCTTGGACTT
KNAT7 Del3S	Potri.001G112200.1	CACCCTAGGAGAAGGTACGGGTGCA
KNAT7 Del3AS	Potri.001G112200.1	CTACCTTTTGCGCTTGGACTT
KNAT7 Del4S	Potri.001G112200.1	CACCGAATCTGAAAGGTCTTTGATG
KNAT7 Del 4AS	Potri.001G112200.1	CTACCTTTTGCGCTTGGACTT
KNAT7 Del 5S	Potri.001G112200.1	CACCATGCAAGAACCAAACTTGGGC
KNAT7 Del5AS	Potri.001G112200.1	TCAAGTCACACCAGTGAGAGCCTG
KNAT7 ELKS	Potri.001G112200.1	CACCATGCAAGAACCAAACTTGGGC
KNAT7 ELKAS	Potri.001G112200.1	TCAGTAAGGCCACTTGGAGTGTTG
PtrWOX13C Deletion Analysis		
WOX13C 1S	Potri.002G008800.1	CACCATGGAGGAGGGGAGGTTTCAG
WOX13C 1AS	Potri.002G008800.1	TCACCCTATCTTGTGGACAGCAGA
WOX13C 2S	Potri.002G008800.1	CACCATGGAGGAGGGGAGGTTTCAG
WOX13C 2AS	Potri.002G008800.1	TGATTGCTTTCTTTTTGAACGAGC
WOX13C 3S	Potri.002G008800.1	CACCTCGAGGCAGCGGTGGACACCG
WOX13C 3AS	Potri.002G008800.1	TCATCCAAACAAGTCATATTG
WOX13C 4S	Potri.002G008800.1	CACCATGGAGGAGGGGAGGTTTCAG
WOX13C 4AS	Potri.002G008800.1	TCATGGAGTCGCATTGCATTGTTC
WOX13C 5S	Potri.002G008800.1	CACCCCAGGCAGGCAGAAGATCAAA
WOX13C 5AS	Potri.002G008800.1	TCATCCAAACAAGTCATATTG
WOX13C 6S	Potri.002G008800.1	CACCGTCTATAATTGGTTCCAAAAC

WOX13C 6AS	Potri.002G008800.1	TCATCCAAACAAGTCATATTG
WOX13C 7S	Potri.002G008800.1	CACCAGAGCTCGTTCAAAAAGAAAG
WOX13C 7AS	Potri.002G008800.1	TCATCCAAACAAGTCATATTG
WOX13C HDS	Potri.002G008800.1	CACCTCGAGGCAGCGGTGGACACCG
WOX13C HDAS	Potri.002G008800.1	TCATTGCTTTCTTTTTGAACGAGC
PtrDRIF Deletions		
DRIF Del 1S/FL	Potri.007G132700.1	CACCATGGCAAACCCATCTGGGACA
DRIF Del 1AS/FL	Potri.007G132700.1	TTATGGCCTAGGAAGGTTTGG
DRIF Del 2S/M2	Potri.007G132700.1	CACCATGGCAAACCCATCTGGGACA
DRIF Del 2AS	Potri.007G132700.1	CTATAGATTAATAGCTATCTTTGC
DRIF Del 3S/M3	Potri.007G132700.1	CACCATGGCAAACCCATCTGGGACA
DRIF Del 3AS	Potri.007G132700.1	TCACCATCTGCAACGCAAAGCAAC
DRIF Del 4SM/4	Potri.007G132700.1	CACCATGGCAAACCCATCTGGGACA
DRIF Del 4AS	Potri.007G132700.1	TCAACTTTCCAGTGGCAGCATTGG
DRIF Del 5S/M5	Potri.007G132700.1	CACCGGCATCTCATATGATGCAATT
DRIF Del 5AS	Potri.007G132700.1	TTATGGCCTAGGAAGGTTTGG
DRIF Del 6S	Potri.007G132700.1	CACCCTTGCAAGTTTTCAGATACAG
DRIF Del 6AS	Potri.007G132700.1	TTATGGCCTAGGAAGGTTTGG
DRIF Del 7S	Potri.007G132700.1	CACCCTTCTCCGCCGAACGCGTGAC
DRIF Del 7AS	Potri.007G132700.1	TTATGGCCTAGGAAGGTTTGG
DRIF Del 8S	Potri.007G132700.1	CACCATCCGCAAAATTATGAACCAG
DRIF Del 8AS	Potri.007G132700.1	TTATGGCCTAGGAAGGTTTGG
DRIF Del 9S	Potri.007G132700.1	CACCATGAATGATGTGCCAGAACTA
DRIF Del 9AS	Potri.007G132700.1	TTATGGCCTAGGAAGGTTTGG
DRIF Del 10S	Potri.007G132700.1	CACCGCAAGTTTTCAGATACAGGAG
DRIF Del 10AS	Potri.007G132700.1	TTACTGCTTCATTAGTTCTGGCAC
BiFC Bridge experiments		
RAD Bifc s	Potri.002G260000	CTCGAGATGGCTTCAGGTTCTAGTAAT
RAD Bifc as	Potri.002G260000	GGATCCTCAGTTGAGATTAAGATTCTT
WOX13c Bifc s	Potri.002G008800	CTCGAGATGGAGGAGGGGAGGTTTCAG
WOX13c Bifc as	Potri.002G008800	GGATCCTCATCCAAACAAGTCATATTG
PtrKNAT7	Potri.001G112200	CTCGAGATGCAAGAACCAAACTTGGGC
PtrKNAT7	Potri.001G112200	GGATCCCTACCTTTTGCGCTTGGACTT
GST/pGEX4T-1		
PtrRad/GST s	Potri.002G260000	GGATCCATGGCTTCAGGTTCTAGTAAT
PtrRad/GST s	Potri.002G260000	CCCGGGTCAGTTGAGATTAAGATTCTT
PtrWOX13C s	Potri.002G008800	GGATCCATGGAGGAGGGGAGGTTTCAG
PtrWOX13C as	Potri.002G008800	CCCGGGTCATCCAAACAAGTCATATTG

PtrKNAT7/GST s	Potri.001G112200	GGATCCATGCAAGAACCAAACTTGGGC
PtrKNAT7/GST as	Potri.001G112200	CCCGGGCTACCTTTTGCGCTTGGACTT
PtrDRIF/GST s	Potri.007G132700	GGATCCATGGCAAACCCATCTGGGACA
PtrDRIF/GST as	Potri.007G132700	CCCGGGTTATGGCCTAGGAAGGTTTGG

Table 3.S4. Primers for BiFC, and Y2H bridge assays

Primers	5' to 3'
Bifc vector pDOE-01	
DUF3755s/BiFC	CGCCCTAGGAACTAGTGCAAGTTTTCAGATACAGGAG
DUF3755as/BiFC	CGGATCCTCCACTAGTCTGCTTCATTAGTTCTGGCAC
DRIFFLs/BiFC	CGCCCTAGGAACTAGTATGGCAAACCCATCTGGGACAA
DRIFFLas/BiFC	CGGATCCTCCACTAGTTGGCCTAGGAAGGTTTGGAGG
WOX13cs/BiFC	CTACGTAGTCACGTGACGTCCATGGAGGAGGGGAGGTTTCAG
WOX13cas/BiFC	CACCAGAACCTCCGGACGTCCGTCCAAACAAGTCATATTGCTC
KNAT7s/BiFC	CTACGTAGTCACGTGACGTCCATGCAAGAACCAAACTTGGGC
KNAT7as/BiFC	CACCAGAACCTCCGGACGTCCGTCCATGAGGGTAGTGTTGCGC
DIV4s/BiFC	CTACGTAGTCACGTGACGTCCATGAAGTGGGAAACGGAAATC
DiV4as/BiFC	CACCAGAACCTCCGGACGTCCGTCCATGAGGGTAGTGTTGCGC
Vector preparation bridge assays	
KanMXs	TGAGTATACGTGATTAAGCACACAAA GGCAGCTTGGAGTCAGCTGAAGCTTCGTACGCT
KanMXas	GCACAAACAARACTTAAATAAATACT ACTCAGTAATAACCGCATAGGCCACTAGTGGAT
Yeast3_s	CACAATATTTCAAGCTATACCAAGCATACA ATCAACTCCCAAGTTTGTACAAAAAAGCTG
Yeast3_as	TGGAGACTTGACCAAACCTCTGGCGA AGAAGTCCAAAGCTCCACTTTGTACAAGAAAGCT
DRIFNLSs	CACCATGGATAAAGCGGAATTAATTCCCGAG CCTCCAAAAAAGAAGAGAAAGGTCGAA TTGGGTACCGCCATGGCAAACCCATCTGGGACA
DRIFNLS as	TCAATGAATTTGAAATCTTGG
NLSs	CACCATGGATAAAGCGGAATTAATT
NLSas	TCAGGCGGTACCCAATTCGAC
PotriKNAT7 NLS	CACCATGGATAAAGCGGAATTAATTCCCGAGCCTCCAA AAAAGAAGAGAAAGGTCGAATTGGGTACCGCC ATGCAAGAACCAAACTTGGGC
PotriKNAT7 NLS_as	CTACCTTTTGCGCTTGGACTT
501Y	CCCGGGATGGAGCAAAAGTT
502Y	GAGCTCTTAGGCCATGATATA
503Y	CCCGGGATGTACCCATACGA
504Y	GAGCTCTTACTTGTACAGCTC

Conclusion

In Chapter 2, the YIH assay was used to identify PDI involved in key aspects of wood development. The Y1H mini-library screens of 5 wood formation related promoters revealed PDI connections by network mapping. The *PtrXCP2* promoter Y1H library screen identified a PDI between a small MYB/SANT domain RADIALAS-like protein and the *XCP2* promoter. Based upon the aforementioned result, PtrRAD1 and 4 other MYB/SANT containing DIVARICATA-like proteins were cloned and added to other poplar TFs for use in targeted Y1H assays utilizing a xylem-biased mini-library. The results from the five mini-libraries Y1H screens were consistent with interactions previously identified from Arabidopsis research (Taylor-Teeples et al. 2015). Although, similarities were seen with the Arabidopsis data, differences existed that warranted further investigation by ectopic expression and gene silencing by amiRNA in a transgenic poplar field trial. Currently, transgenic trees are under investigation for changes in wood quality and biomass. The combination of xylem-biased expression profile, and PDIs of PtrRAD1 with several of the promoters screened by Y1H, led to the inclusion of PtrRAD1as a candidate protein for further characterization by Y2H screening. PtrRAD1 was used in an Y2H screen, leading to the identification of a PPI with PtrDRIF1. The RAD/DRIF interaction has been previously characterized in snapdragon (Raimundo et al. 2013) and tomato (Machemer et al. 2011). Subsequently, PtrDRIF1 was used in an Y2H screen that identified numerous interaction partners including members of MYB domain and HD TF families. PtrDRIF1 also formed interactions with cytoskeletal-related proteins and histone modifiers, suggesting PtrDRIF1 may function as a HUB protein involved in gene regulation.

In Chapter 3, the PPIs of PtrDRIF1 were further characterized by Y2H, pull-down assays, and BiFC. PtrDRIF1 contains two distinct domains, an N-terminal MYB/SANT like domain and a C-terminal DUF3755 domain. The N-terminal MYB/SANT domain of PtrDRIF1 interacted with the MYB/SANT containing PtrRAD1 and PtrDIV proteins. The C-terminal DUF3755 domain interacted with the HD containing ancient WOX clade and KNOX II clade of TFs. PtrDRIF1 was able to form a heterotrimer with PtrRAD1 and PtrWOX13c by BiFC bridge and Y2H bridge assays. Protein complexes involving different combinations of the larger PtrDIVs or PtrKNAT7

all inhibited formation of heterotrimers by BiFC or modified Y2H bridge assays. The higher molecular weight PPIs of PtrDIVs or PtrKNAT7 with PtrDRIF1, compared to PtrRAD1/WOX13c, may have contributed to the inability of heterotrimers to form. Interactions involving larger proteins may cause inaccessibility to binding sites due to steric hindrance. Arabidopsis *WOX13* is expressed in the replum, a meristematic tissue and ectopic expression and loss-of-function constructs resulted in altered lignification of the valve margin (Romera-Branchat et al. 2013). PtrKNAT7 is a functional homolog of KNAT7 from Arabidopsis and rescued loss-of-function *irregular xylem11/knat7-1* mutants. KNAT7 is generally considered to be a transcriptional repressor of lignification (Li et al. 2012b) and is highly expressed in the xylem of poplar (Rodgers-Melnick et al. 2012b). Although, the exact function of PtrDRIF1 is not currently known, the competition existing between interacting proteins and the ability of several TFs to localize PtrDRIF-GFP to the nucleus, suggest it may function in transcription, potentially as an enhancer. The interactions occurring with WOX, KNOX, and MYB/SANT proteins suggest that this interaction network may have been co-opted in trees to regulate cell expansion, proliferation, and potentially onset of lignification in wood-forming tissues.

The goal of this research was to identify novel regulators of wood-formation. Previous research from Arabidopsis and poplar concentrated primarily on MYB and NAC family TFs as regulators of wood-formation. In this study, a poplar xylem-biased transcription factor (TF) mini-library was used in Y1H experiments to identify TFs that regulate gene expression in wood formation. In Chapter 2, The Y1H assays identified several proteins not previously linked with wood formation, providing candidates for future characterization. Among these newly identified interactions were WOX13c, BEL1-like homeodomain (BLH), PtrRAD1, a B-Box microprotein (BBX), and two C2H2 type zinc-finger proteins. The potential exists for these novel interactions to lead to trees with increased biomass or decreased lignin. Currently, transgenic trees are being evaluated for wood quality, wood chemistry, and biomass production for several of the genes identified by Y1H. Further characterization of PtrRAD1 led to the identification of the PtrDRIF1 interaction module. In prior research the RAD-DRIF/DIV-DRIF regulatory system has been implicated in tomato fruit expansion (Machemer et al. 2011) and the poplar orthologs of these proteins may perform similar functions during wood formation. The newly discovered

PPIs between PtrDRIF1 and members of the ancient WOX and KNOX II clades of TFs provide interesting candidates for future research aimed at wood improvement.

References

Li EY, Bhargava A, Qiang WY, Friedmann MC, Forneris N, Savidge RA, Johnson LA, Mansfield SD, Ellis BE, Douglas CJ (2012) The Class II KNOX gene KNAT7 negatively regulates secondary wall formation in Arabidopsis and is functionally conserved in Populus. New Phytologist 194 (1):102-115. doi:10.1111/j.1469-8137.2011.04016.x

Machemer K, Shaiman O, Salts Y, Shabtai S, Sobolev I, Belausov E, Grotewold E, Barg R (2011) Interplay of MYB factors in differential cell expansion, and consequences for tomato fruit development. Plant J 68 (2):337-350. doi:10.1111/j.1365-313X.2011.04690.x

Raimundo J, Sobral R, Bailey P, Azevedo H, Galego L, Almeida J, Coen E, Costa MM (2013) A subcellular tug of war involving three MYB-like proteins underlies a molecular antagonism in Antirrhinum flower asymmetry. Plant J 75 (4):527-538. doi:10.1111/tpj.12225

Rodgers-Melnick E, Mane SP, Dharmawardhana P, Slavov GT, Crasta OR, Strauss SH, Brunner AM, Difazio SP (2012) Contrasting patterns of evolution following whole genome versus tandem duplication events in Populus. Genome research 22 (1):95-105. doi:10.1101/gr.125146.111

Romera-Branchat M, Ripoll JJ, Yanofsky MF, Pelaz S (2013) The WOX13 homeobox gene promotes replum formation in the Arabidopsis thaliana fruit. Plant J 73 (1):37-49. doi:10.1111/tpj.12010

Taylor-Teeples M, Lin L, de Lucas M, Turco G, Toal TW, Gaudinier A, Young NF, Trabucco GM, Veling MT, Lamothe R, Handakumbura PP, Xiong G, Wang C, Corwin J, Tsoukalas A, Zhang L, Ware D, Pauly M, Kliebenstein DJ, Dehesh K, Tagkopoulos I, Breton G, Pruneda-Paz JL, Ahnert SE, Kay SA, Hazen SP, Brady SM (2015) An Arabidopsis gene regulatory network for secondary cell wall synthesis. Nature 517 (7536):571-575. doi:10.1038/nature14099